SEISMIC SITE STUDIES IN PENDIK – TUZLA REGIONS IN ISTANBUL

by

Leyla Aslı Er

B.S., Geophysical Engineering, Kocaeli University, 2005

Submitted to the Kandilli Observatory and Earthquake Research Institute
in partial fulfillment of the requirements for the degree of
Master of Science

Graduate Program in Geophysical Department

Boğaziçi University

2010

ACKNOWLEDGEMENTS

I would like to express my sincere gratitude to my dear advisor, Prof. Dr. Cemil Gürbüz for his support, patience and encouragement throughout the preparation of this thesis. I also extend my sincere thanks to Esen Arpat for his valuable advices to my thesis.

Appreciation is extended to Necdet Özgül and members of OYO Company who spent their invaluable time and energy with me and I would like to thank Istanbul Metropolitan Municipality for permission to use the data.

I would like to thank my dear friends, Alper Denli and Esra Tekcan Sahin for their support and help for participating in my field studies.

I would also thank to my special colleques, Gülçin Güner and Zeynep Coşkun and all friends at Geophysics Department in Kandilli Observatory and Earthquake Research Institute.

Lastly, I want to thank my parents who have been most patient and supportive over the many years of schooling. I am also grateful to my husband for his encouragement and endless support during my thesis.

ABSTRACT

SEISMIC SITE STUDIES IN PENDIK – TUZLA REGIONS IN ISTANBUL

The objective of this study is to identify soil amplification and soil fundamental frequency in the area between Pendik and Tuzla, the southeast of Istanbul city, and showing how the values of soil amplification, dominant period and frequency will change according to layer thickness overlying the bedrock.

Pendik - Tuzla regions were selected according to variation of bedrock depth which changes from 65 to 150 meters and topographical changes from north to south representing a valley type structure.

According to geological formations, and topographic structure, 64 measurement points were selected for a horizontal/vertical spectral ratios method, (Nakamura's method) in Pendik–Tuzla area. In the same area, OYO Company collected data using Suspension Ps logging and Refraction Microtremor methods. I used these data to calculate amplification and dominant period using Shake 91 program for different 56 measurement points. Also, dominant periods were calculated using empirical formulas.

The results obtained from site measurements and model studies were correlated with each other and were displayed in contour maps and interpreted according to geology, topography and the geological distributions of bedrock depths and the formation types in the investigated area.

According to the H/V and model studies, amplifications on the three regions, Aydınlı, Orhanlı and south of the study areas were found much more bigger than surrounding stable areas. These three regions consist of approximately reaching up 120 m thickness of Cenozoic aged, Sultanbeyli and Kuşdili Formations, overlying the Paleozoic bedrocks. Besides, the highest fundamental soil period values calculating from both studies are estimated in these regions.

As a result through investigation and significant observation of both of these studies, thickness of sedimentary layers overlying bedrock and soil dynamic properties of these structure layers have a great effect on the evaluation of seismic site studies, soil transfer function and dominant period and frequencies.

ÖZET

PENDİK-TUZLA BÖLGELERİNDE ZEMİN ÖZELLİKLERİNİN BELİRLENMESİ ÇALIŞMASI

Bu çalışmanın amacı, İstanbul'un güney doğusunda Pendik - Tuzla ilçeleri arasında kalan bölgede, zemin büyütmesi, zemin hakim frekansı gibi sismik tehlikelerin dağılımını belirlemek ve anakaya üzerinde yer alan tabaka kalınlığına göre zemin büyütmesi, baskın frekans ve baskın period değerlerinin nasıl değişeceğini göstermektir.

Pendik –Tuzla bölgesini seçmemizdeki ana sebep; sediment tabakasının bazı yerlerde 65 dan 150 metre derinliğe ulaşan ve bölgeyi kuzeyden güneye kesen vadi görünümlü yapısıdır.

Çalışma bölgesinde topografya ve jeolojik formasyonların dağılımına göre "yatay/ düşey spektral oran" mikrotremor yöntemlerinden olan H/V Nakamura çalışması için 64 adet ölçüm noktası seçilmiştir. Aynı bölgede, daha önceden OYO firması tarafından İstanbul Büyükşehir Belediyesi mikrobölgeleme çalışması için kullanılmış kuyu logu, ReMi ve derinliğe göre formasyon dağılım verileri, 56 farklı nokta için Shake 91 programında kullanılarak modelleme yapılmıştır. Diğer taraftan, amprik bağıntılarla da bölgenin hakim periyot değerleri hesaplanmıştır.

Yapılan çalışmaların sonucunda, zemin büyütmesi, periyod ve frekans değerleri birbirleri ile karşılaştırılmış ve bölgenin jeolojisi, jeolojik formasyon yapısı, topografyası ve anakaya derinliği dikkate alınarak haritalanmış ve yorumlanmıştır.

H/V ve model çalışmasının sonuçlarına göre, zemin büyütmesi daha çok anakaya üzerinde yer alan kalın sediment tabakasının 70 ile 150 m arasında değiştiği yerlerde yüksek değerler almıştır. Bu yerler Aydınlı, Orhanlı ve çalışma bölgesinin güney kısmı olarak gösterilebilir. Bunun yanında, yüksek baskın periyot değerleri aynı yerlerde de yüksek değerler almıştır.

Bütün bu araştırmalar ve gözlemler dikkate alındığında, sismik zemin çalışmalarının değerlendirilmesinde anakaya üzerindeki sediman kalınlığının ve zemin tabakalarının dinamik özelliklerinin büyük bir öneme sahip olduğu görülmektedir.

TABLE OF CONTENTS

LIST OF FIGURES

LIST OF TABLES

LIST OF SYMBOLS / ABBREVIATIONS

ξ	Damping parameter
τ	Intercept time
d	Density
E_{RW}	Rayleigh wave
Vs	Shear wave
p	Ray Parameter
Z	Seismic impedance

ASCII	American Standard Code for Information Interchange
cm/s	centimeter per second
FFT	Fast fourier transform
Fk	Frequency–wavenumber spectrum
GCF	WinXComp Grouped Compressed File
GPS	Global Position System
H/V	Horizontal/Vertical spectral ratios
Hz	hertz
Kcf	kips Cubic Foot
m	meter
Ms	millisecond
N-S	North- South
p-f	slowness-frequency
ReMi	Refraction Microtremor
S	shear
SAC	Seismic Analysis Code
sec	second
SPAC	The Spatial Autocorrelation method
UTM	Universal Transverse Mercator
x-t	Distance and Time

1. INTRODUCTION

An increase in the level of ground shaking changes according to near-surface geological and topographical conditions. Assessments of local seismic hazards can be determined that depth of the bedrock and thickness of soil layers can generate significant amplification and spatial variations of the earthquake ground motion (Mirzaoğlu and Dikmen, 2003). The shape and the contents of amplitude and frequency of ground natural noise vary related to these soil structures. So that, the ground tremors magnify differently with respect to its features for each soil properties.

If the amplification is at low frequencies and high periods, this circumstance may be significant for most of the construction of structures because soft soil amplifies earthquake waves relative to stiff or hard soils and this situation plays an important role in damage occurred (Yalçınkaya, 2004). The knowledge of site effect, localized strong amplifications of seismic motion, is essential to build earthquake – resistant structures. How to design earthquake resistant building depends mainly on the physical properties of subsoil layers on which the structure rests. In general, damage is greater on soft and weak ground than it is on rigid ground. Therefore, the fact that how soft alluvial soil is affected by large earthquakes and which procedures notice to construction of building is very critical questions and become of main importance (Yalçınkaya, 2004). Besides, in order to decrease resonance effect between structure and soil, the dominant period values of structure and soil could not be done at same period values.

The best approach for analyzing ground conditions in order to reduce damages caused by the earthquakes is through direct observation of the seismic ground motion, but such studies are restricted to areas with relatively high seismicity. Besides, seismic explorations are economically and technically such as unavailability of transportations, high cultural noise difficult to carried out. However, microtremor is a very practical method to estimate the effect of surface geology on seismic motion without other geological information in the various places.

I have used Nakamura's method in my thesis. First chapter gives briefly information about site effect and it's importance on structures. The description of microtremor, soil transfer function and dominant period are explained in second chapter. Geological and topographical structure of study area are described in third part. Theoretical informations about microtremor and shear wave calculation methods are given in fourth and fifth parts, respectively. Field and model studies are explained in detailed in the sixth chapter of the thesis. Finally, the results, discussions and conclusions are given in last two chapters.

2. THE DEFINITIONS OF MICROTREMOR, SOIL AMPLIFICATION AND DOMINANT FREQUENCY

2.1. Microtremors

The surface of the Earth is always in motion at seismic frequencies, even without earthquakes. There are usually various vibrations, at small amplitude level of about several micrometers, which appear on surrounding ground surface. These constant vibrations of the Earth's surface are called microseisms or microtremors (Okada, 2003).

Microtremors are ground vibrations with displacement amplitude about 0.1-1. micron, and velocity amplitudes are 0.001-0.01cm/s. that can be detected by seismograph with high magnification (Mirzaoğlu and Dikmen, 2003). Although microtremors are very weak, they represent a source of noise to researchers of earthquake seismology; if amplifier gain is increased to record earthquake signals from a distant source, the amplitude of microtremors proportionally increases, and the desired earthquake signal is buried in the "noise" of microtremors. Elimination of this background noise is technically extremely difficult or impossible to achieve.Therefore earthquake researchers call microtremors "seismic noise" or, simply, "noise" (Okada, 2003).

There are two primary sources of microtremors. One is human activity such as traffic, train and factories. The others are natural sources such as the flow of water in rivers, rain, wind, variation of atmospheric pressure, and ocean waves. Both human activity and natural sources (such as climate and oceanic conditions) vary with time. Accordingly, microtremor activity varies over time. This variation is very complex and irregular, and not repeatable (Okada, 2003).

When microtremors are investigated simultaneously at several spatially separated stations, it is noted that these tremors are not completely random and that some coherent waves are contained in the records (Okada, 2003).

Moreover, microtremors can be classified into two types according to period range. One comprises short-period microtremors with periods less than 1. second, and is related to shallow subsurface structures several tens of meters thick. The other is long-period microtremors with periods longer than 1.second, which is related to deeper soil structure down to a depth of the hard rock with an S wave velocity of 3. km/s.

The microtremors originating from human activities are dominated by the components with periods shorter than one second, or higher than 1. Hz in frequency (Kulhanek, 1990 for example), and have clear diurnal variation in both amplitude and period.

On the other hand, due to natural phenomena such as climatic and oceanic condition the microtremors have fundamental periods greater than one second (frequency lower than 1 Hz), with associated amplitude and period variations corresponding to the vagaries of the respective natural phenomenon. A detailed analysis determines that microtremors vary depending upon location. The microtremor survey method has been devised to focus on this variation (Okada, 2003).

Measurements have to be carried out during midnight when the social activities stop almost completely in order to remove the effect of a tremor whose source can be identified, but this procedure will substantially detract the benefit of the microtremor such as readiness of measurement (Nakamura, 1989).

Microtremor methods include three methods: first is a horizontal /vertical spectral ratios (H/V methods), second is ReMi active method and third is Array passive methods. While horizontal/vertical spectral ratios methods supply with the estimation of soil amplification and dominant period, ReMi and Array methods including SPAC and F-K methods provide information about structure of shear wave velocity for a site.

2.2. Soil Amplification and Dominant Frequency

A survey on the earthquake damage shows that, considering seismic intensity equal, the influence on structures change considerably: some are free from damage almost completely while others suffer heavy damage. This phenomenon occurs due to difference in the seismic response characteristics of the structures. The surface layers carrying these structures also differ substantially in the effect of earthquake due to difference in their seismic response characteristics (Nakamura, 1989).

Soil layers play very important role in determining the structure of seismic motion. They can be seen as a filter for seismic waves because soil layers sometimes make seismic waves to damp or to amplify. If the amplification is at high frequencies, this may not be important for most of the engineering structures (Yalçınkaya, 2004). Soil amplification is known as soil transfer functions.

Some important factors that can take important role in soil amplification are given as below, respectively: impedance ratio and resonance effect, focusing effects of seismic waves with respect to topography, surface wave formations at the basin edges, nonlinear soil behavior and topographical effect (Yalçınkaya, 2004).

In the soft soil layers, the main cause of an increase in the amplification of earthquake motion is the difference in seismic impedance between soil and bedrock beneath it. Seismic impedance can be thought of a scale of environmental resistance across to particle motion (Aki and Richards, 1980). From (2.1), the seismic impedance for the propagation of vertical shear waves in the soil layer is obtained by multiplying the density and S wave velocity (Aki and Richards, 1980).

$$z = d * Vs \tag{2.1}$$

where d is density , Vs is shear wave velocity.

The difference in the impedance ratio between soil and its bedrock make seismic waves to be trapped within the layers. Interference of trapped waves cause increase of resonance frequency of resonance pick which has a relation between thickness of layers above the bedrock and S- wave velocity (Bard and Bouchon, 1985).

The amplitude of peak value of resonance is dependent mainly on seismic impedance difference between soil layer and its bedrock, damping ratio of soil layers, incoming wave properties such as wave type, incidence angle and geometry of structures (Yalçınkaya, 2004).

An increase in the thickness of soil layers makes its dominant frequency to decrease. The soil amplitude value is affected by the change of impedance ratio between soil and it's beneath, bedrock. Soil amplification is affected by any change in velocities in soil layers because of the change in impedance ratio. An increase in impedance ratio means of the increase in soil amplification.

According to engineering studies, the interval between the soil dominant frequency and the structure dominant frequency must be very long in order not to be resonance. Otherwise, an increase of load on the buildings can lead to destruction of these buildings during the earthquake.

Soil amplifications and resonance effect have played important role in the damages during the earthquakes. As a result, it is emphasized that depth of bedrock and S-wave velocity are very important for estimating soil transfer function (Yalçınkaya, 2004).

There are two different conclusions about the relationship of microtremor dominant frequency with local site conditions:

1. The microtremor dominant frequency is controlled by geological site conditions (Kanai and Tanaka, 1961; Kubotera and Otsuka, 1970).
2. It is primarily controlled by the microtremor source and propagation path (Udiwadia and Trifunac, 1973).

These inconsistent results explained that the influence on microtremors of geological site conditions, microtremor source, and propagation path change in observation sites. Therefore, the effects of the microtremor source and path must be eliminated to obtain accurate estimates of seismic site response characteristics (Horike *et al.*, 2001).

Direct computation of amplitude spectra, computation of spectral ratios relative to a firm soil, reference station and computation of spectral ratios between horizontal components of motion relative to the vertical are efficient microtremor methods in order to remove the effect of the microtremor source and path (Lermo and Chavez-Garcia, 1994).

3. GEOLOGY OF THE INVESTIGATION SITE

The general and local geology of the study area and the geological units at the site are described in this section.

3.1. The General Geology

The region of Istanbul lies over the geological units extending from Ordovisien series in early Paleozoic age to Quaternary in Cenozoic age. Istanbul city boundary is tectonically divided into two parts namely: Istranca Massif consists of metamorphosed stratified rock sequence and Istanbul Assemblage consists of unmetamorphosed stratified rock sequence (Özgül *et al.,* 2005).

Istranca massif consists of shale, quartzite, and magmatite takes places in the north of Trace peninsula, especially, in Tekirdag and Edirne. This metamorphic massif is located in the west and north of Catalca in Istanbul city boundary (Özgül *et al.,* 2005).

The Istanbul Unit consist of quaternary rock units that record major tectonic events over this long period which is being originated at Paleozoic and Mesozoic ages and extending great areas in the two side of the Bosporus and Kocaeli Peninsula. Figure 3.1 shows Paleozoic aged rock units for around Istanbul (Özgül *et al.,* 2005).

The Istanbul Assemblage is very distinctive from the Istranca massif in its stratigraphy, absence of metamorphism and lack of penetrative deformation. The Istanbul zone is described by a well developed, unmetamorphosed and slightly deformed Paleozoic sedimentary succession, extending from Ordovician to the Carboniferous which is overlain with a major unconformity by latest Permian to lowermost Triassic continental red beds (Okay, 1989).

The Istanbul Unit was located at the southern part of Laurussia throughout its early geological history and that the Late Silurian to Late Devonian interval is characterized in this unit by Atlantic-type continental margin sediments (Şengör *et al.*, 1984).

Kocatöngel and Kurtköy formations, the oldest rock formations in the Istanbul Unit, have terrigenous deposit and occurred in fluvial and lacustrine environments at Lower Ordovician. The marine transgression began with the feldspathic quartz-arenites and quartzites of the Kınalıada and Aydos formations, and stable and increasingly deeper marine conditions overlaid in the region throughout Silurian and Devonian. In this period the deposition continued with the Yayalar Formation (Lower Ordovician) of siltstone-sandstone, Pelitli Formation (Lower Ordovician-Silurian) characterized by shelf-type carbonates, Kartal Formation (Lower-Middle Devonian) of micaceous shales with rare limestone intercalations indicating low energy open shelf deposition, Denizli Village Formation (Upper Devonian-Lower Carboniferous) of nodular limestones deposited in an open shelf to slope setting. Magmatic intrusions, represented by the Sancaktepe Granite, were placed in the Carboniferous-Permian time and the region became a land area (Özgül, 2009).

The area was covered in thick Permian-Lower Triassic Continental deposits, later lagoonal-intertidal sediments (Erikli Formation, Demirciler Formation), shelf carbonates (Ballıkaya Formation) and slope deposits (Tepeköy Formation) followed the area in the Middle-Late Triassic time. The Triassic sequence displays a transgressive and increasingly marine character (Özgül, 2009). There is no data on the Jurassic-Lower Cretaceous rocks in the Istanbul region, this situation can be explained either by non-deposition or pre-Later Cretaceous erosion. Quaternary alluvium accumulated at a depositional low in the south-central portion on the Istanbul Unit, and natural continental and marine sediments line the coast above the bedrock (Özgül, 2009).

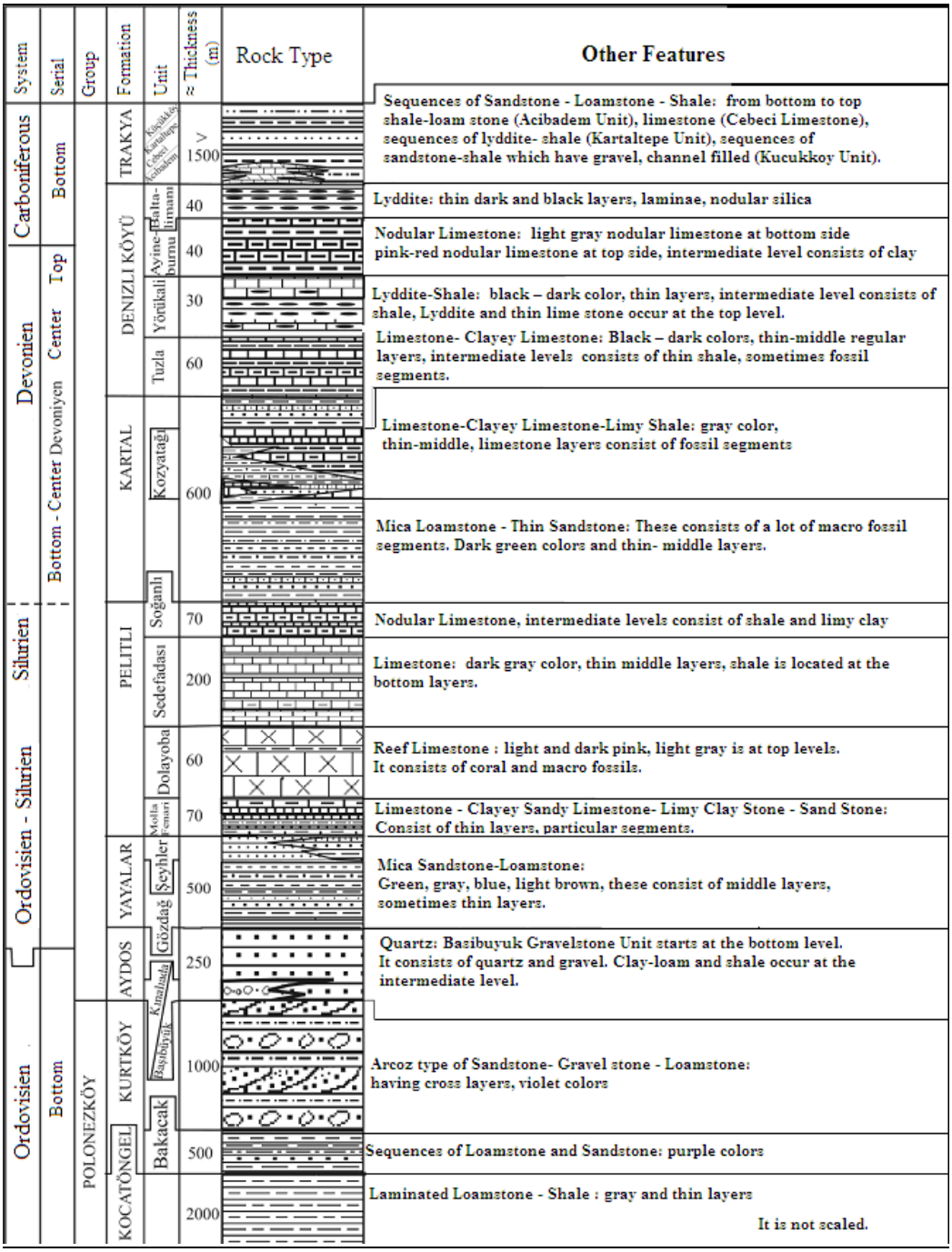

Figure 3.1. Generalized vertical section of Paleozoic aged rock stratigraphic units for around Istanbul (Özgül *et al.*, 2005)

3.2. The Local Geology

The study area is in the area between Tuzla and Pendik towns in the southeast of Istanbul city. Geology map of investigated area and legend of this map is shown in Figure 3.2.

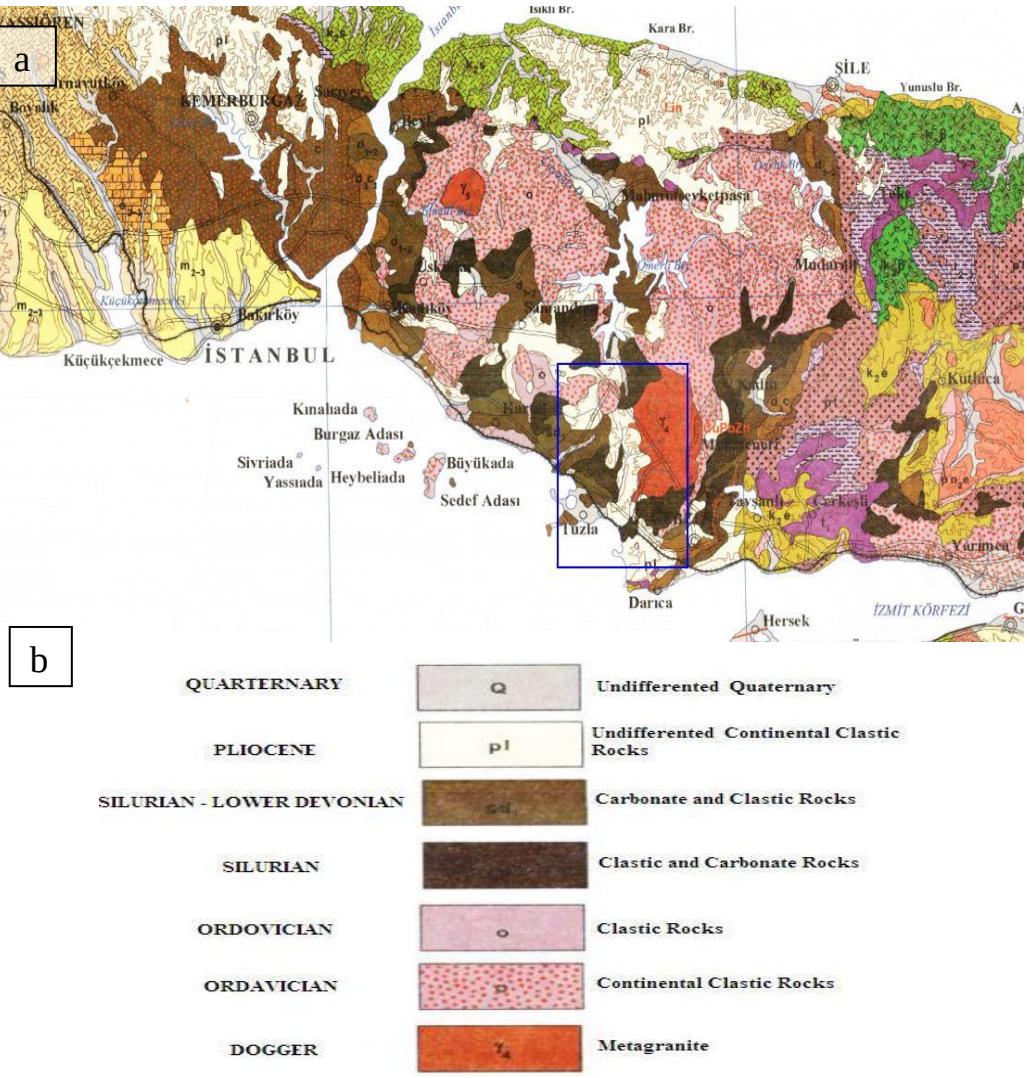

Figure 3.2. Geology map of study area. Blue rectangular shows the investigation area (a) Legend of above geology map (b) from General Directorate of Mineral Research - Exploration, 2001

The study area is analyzed in under four categories, Paleozoic aged, Cenozoic aged Mesozoic aged and Quaternary aged in order to provide easy comprehension of geological units.

3.2.1. Paleozoic Aged

3.2.1.1. Kurtköy Formation. Kurtköy Formation has the oldest rocks that lies over an age of Lower Paleozoic Age (Ordovician) and this formation made up of the most lower layers of the Istanbul stratigrafic sequence. Kurtköy Formation made up of violet, red and grey conglomerates, sandy conglomerates, arkoses, subarkoses, lithic arenites with subordinate pink and brick-red mudstones and shales. This arkose unit is defined as starting with lower conglomera zone and continue to arkose at the end of Silurien time (Paeckelmann, 1938). It was called that "Kurtköy Schichten" because of taking place in around Kurtköy (Haas, 1968). This formation represents Paleozoic sedimentary sequences (from Upper Ordovician to Silurian) in and its exposures around Kurtköy region, the west of Umraniye, the north of Maltepe, around Polonezköy-Cumhuriyet Villages, the north of Reşadiye village and Paşakoy - Omerli regions.

3.2.1.2. Aydos Formation. Aydos Formation like as Kurtköy Formation represents Paleozoic sedimentary sequences (from Upper Ordovician to Silurian) and this formation replaced around highest slopes in the Anatolian side of Istanbul. Aydos Formation is composed mainly of white, pale violet and grey quartz - arenites, quartzites, quartz conglomerates. The lower part contains thick - bedded conglomeratic interlayers with well-rounded quartz pebbles. The quartz - arenites include well - rounded and slightly deformed quartz grains, with rare white - mica flakes. They are silica cemented and comprise prismatic zircon grains. The violet quartzites are hematite-rich. The Aydos Formation displays well-developed cross-bedding and ripples. This formation takes place in Aydos Mountain, Kayisdağ, Alemdağ, Yakacik, Kurtköy, Beykoz, Dragos and Camlica Hill.

3.2.1.3. Yayalar Formation. Yayalar Formation is known as rock types that consist of siltstone-sandstone (psamit) from Lower Ordovician age. This formations has green, gray, blue and light brown color types and thin bedded laminated sandstones. The upper levels of this formation consist of feldispat quartzite. The area is classified in two parts: Gözdağ Formation and Aydınlı Formation (Önalan, 1981). Haas (1968) thought that Yayalar Formation can be seen clearly in a valley passing of north-east of Yayalar region and it exposures around the north of Pendik, Gözdağ hill and its south slope, between Gümüssuyu (Beykoz) and Zerzevatcı Village. This formation is investigated under three titles: Gözdağ Unit, Umurdere Unit and Seyhli Unit (Özgül, 2009).

3.2.1.4. Pelitli Formation. Pelitli Formation from Lower Ordovician-Silurian age characterized by shelf-type carbonates. Pelitli Formation mostly consists of limestone, but sometimes its different zones have thin interval layer clay and its upper level has noduler limestone and there is thin clay layers at different levels. The Pelitli Formation, introduced by Haas (1968), comprising a variety of carbonate rocks, ranging from boundstone to mudstone. The lower part of the unit is Dolayoba Limestone consists of massive reefal limestones rich in the late Silurian corals. This formation takes place in the north of Istanbul, Yakacik area, the valley of Büyükçeşme Deresi and Yumrukaya Deresi in the north of Gebze town, Kartal stone quarry the north of Ornek town.

3.2.1.5. Kartal Formation. Kartal Formation consists of sandy and silty shales The name Kartal Formation consist of the thick sequence of grey, variably calcareous mudrocks with intercalations of thin - bedded coquinite limestones and lithic sandstones (Kaya, 1973). Devonian aged Kartal Formation rock consists of coarse limestone, limy shale, greywacke and fossilious limestone with clay interlayer. In Istanbul, at its type locality, it corresponds to the lower clastic part of the old Lower Devonian classification (Paeckelmann, 1938).

3.2.1.6. Sancaktepe Granite. Sancaktepe Granite which is situated in Kocaeli Peninsula to the north of sea of Marmara is known geologically to be Silurian in age. Besides, Sancaktepe granite which is placed in the north and north-west of Gebze town, and Balcik, Sekerpinar and Cayirova Villages 100 m in length. In order to determine the absolute age of the massif, two methods Rb-Sr isochron method and K-A measurements are used. According to Yilmaz (1977), the age of the massif was found to be 255 million years by Rb-Sr isochron method. K-A measurements made on the biotites of the granite show that this massif is 254 million years old. On the basis of both methods which gave similar results, it could be indicated that the granite has one phase of formation during Permian time by post-orogenic movements.

3.2.2. Mesozoic Aged

3.2.2.1. Volkanic Dykes. Presence of dykes, sills and small intrusions cutting the Paleozoic sedimentary rocks in the Istanbul region is known since the 19th Century. These andesitic hypabyssal rocks, which are generally considered to be of Cretaceous age, are mentioned in many regional geological studies (Paeckelmann, 1925; Okay, 1947, 1948; Erguvanlı, 1949; Ketin, 1959) and their distribution is shown schematically in some geological maps of the Istanbul region (Paeckelmann, 1938).

3.2.3. Cenozoic Aged

3.2.3.1. Sultanbeyli Formation. Sultanbeyli Formation is known soil types that consist of silt, sand, gravel from Oligosen and Miyosen age in Cenozoic time.

3.2.4. Quaternary Aged

3.2.4.1. Kuşdili Formation. In generally, Kuşdili Formation being Holosen aged at Late Quaternary consists of clay and mudflat deposits units, so that it makes Kuşdili Formation weak and soft ground against reconstruction. The Late Quaternary Kuşdili Formation, consisting of clay, sand and mud, covers the southern shore of the Küçükçekmece Lake and the Golden**.**

3.2.4.2. Quaternary Alluvium. Quaternary Alluvium and soil / natural fill consist primarily of loose to very loose, medium to fine silt, shelly sand, and dark gray clay and mud. Especially, quaternary and recent alluvial located within the valleys, seashores and lakeshores.

3.2.4.3. Made Ground / Fill / Artificial Fills. A variable thickness of made ground/fill derived from debris, waste material, brick and plastic, thickness of 2. m which overlies Quanternary Alluvium, Kartal, Kuşdili, Pelitli, Sancaktepe Granite and Sultanbeyli Formations.

3.3. Topography

The topographical elevations are about 100 m in the northwest and about 200 m in the northeast of the site decreasing towards to southern direction reaching at between 10 m and -10 m. According to data from OYO, topographical map of study area is shown as a contour map as below (Figure 3.3).

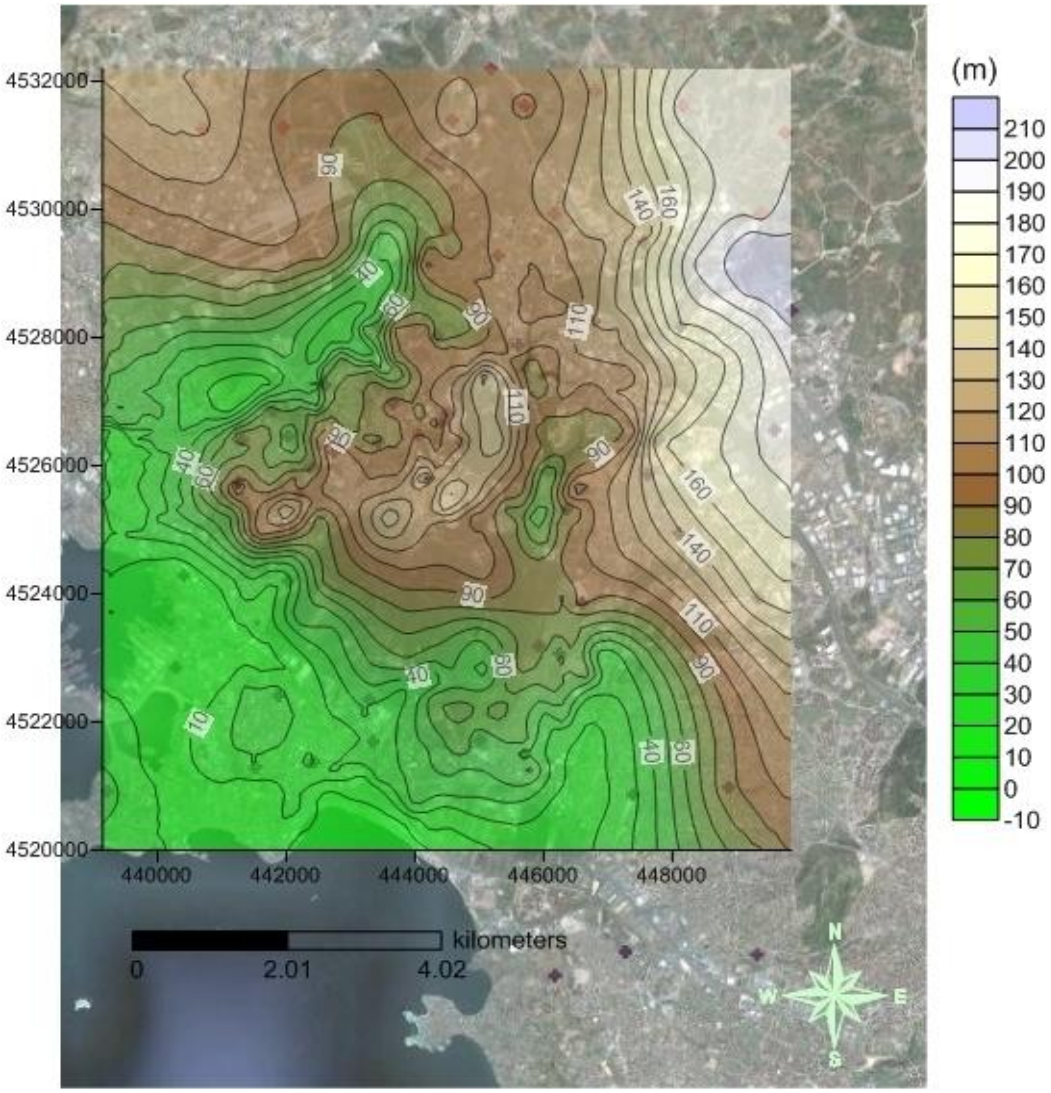

Figure 3.3. Topographical map of investigation area (data of topographical information from OYO Company and our data of site study obtained from GPS instrument). The coordinate unit of this map is given in Universal Transversal Mercator system

3.4. The Distribution of Soil Thickness overlying Bedrock and the Distribution of Bedrock Depth

The thickness of soil layers overlying bedrock affects the amplitude and frequency content of the ground motions; thick deposits of softer soil overlying more rigid formations can trap the seismic waves to an even greater extent than would a thin surficial cover again causing significant amplification. The thickness of sedimentary unit overlying bedrock is increased in approximately 135 m around Sabiha Gökçen Airport and an area like as a valley crossing from north to south. While bedrock elevation reaches approximately 20 m at airport side, it reaches approximately from 20 m at north to - 60 m at south throughout this valley. The map of distribution of soil thickness overlying bedrock is shown as Figure 3.4. The map of distribution of depth of bedrock in study area is presented in Figure 3.5. Coordinate units of these maps are given in Universal Transversal Mercator system.

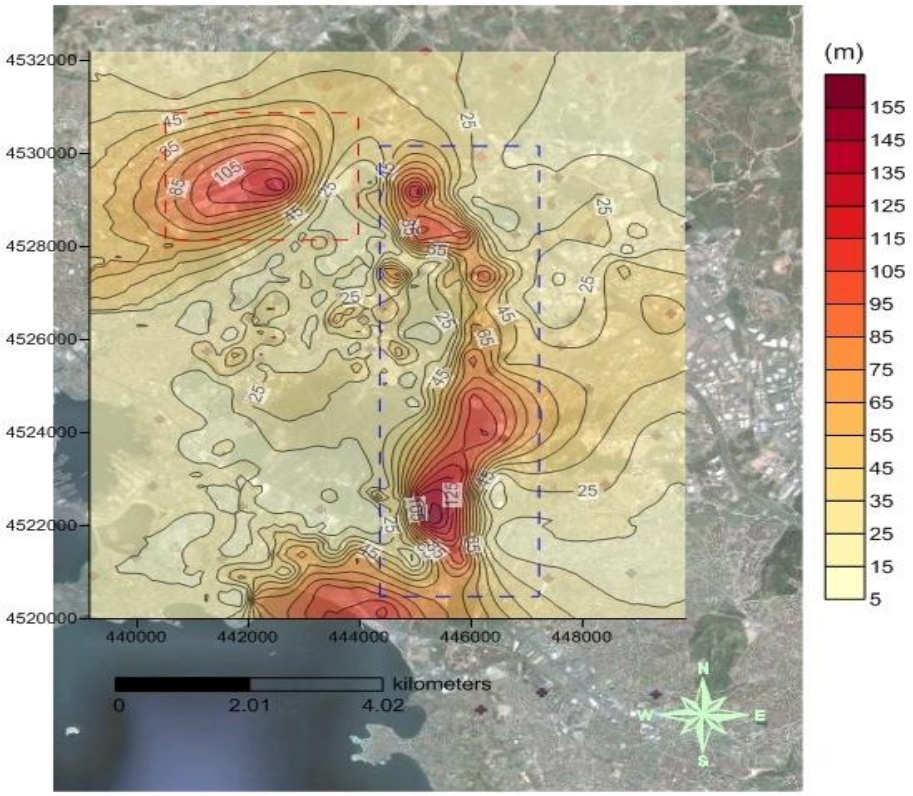

Figure 3.4. Thicknesses of soil layers overlying bedrock in study area. Red triangle shows the site of Sabiha Gökçen Airport and blue triangle shows the area like as a valley crossing from north to south (data from OYO Company)

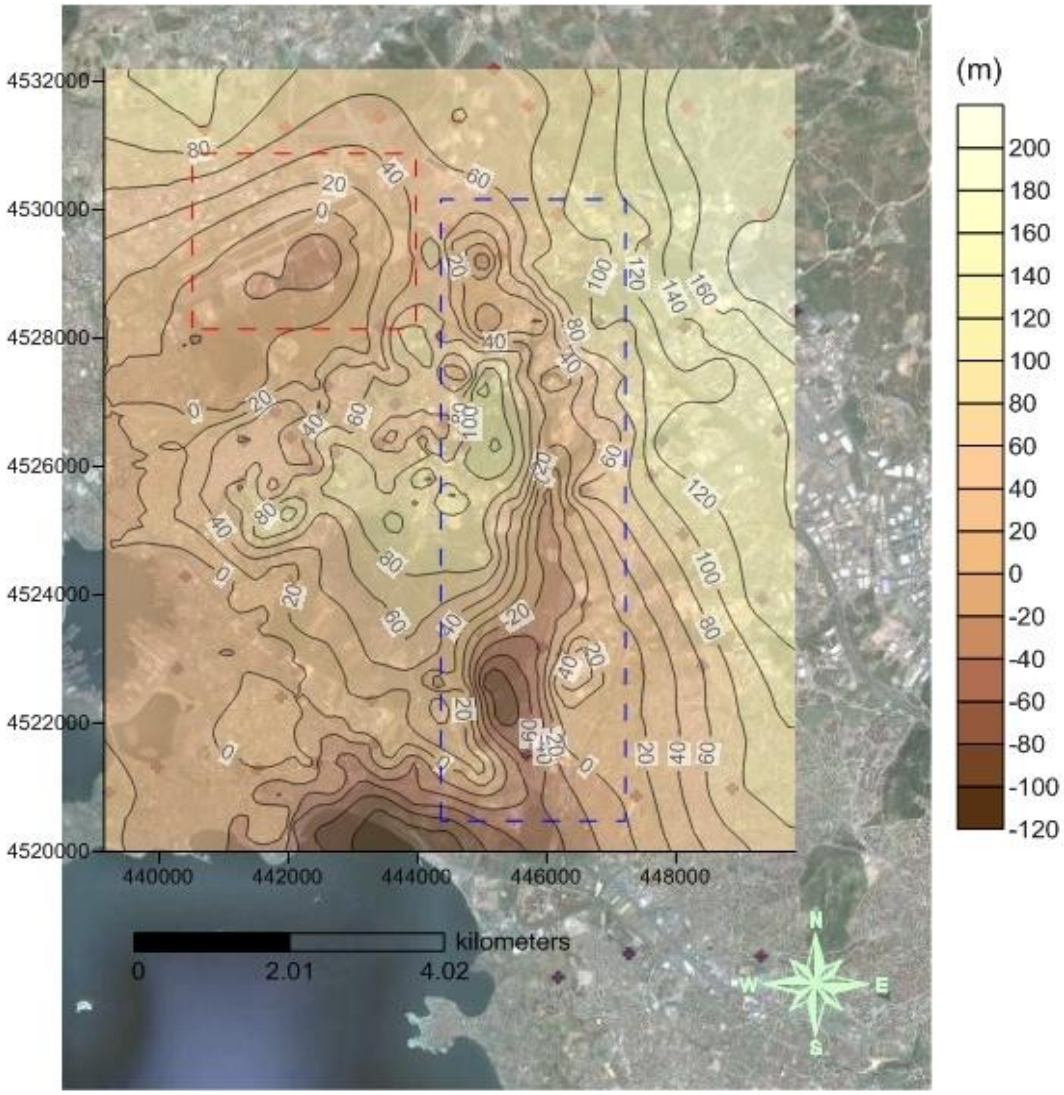

Figure 3.5. The distribution of depths of bedrock according to elevation. Red triangle shows the site of Sabiha Gökçen Airport and blue triangle shows the area like as a valley crossing from north to south (data from OYO Company)

4. MICROTREMOR SURVEY METHODS

There are several different techniques for the analysis of microtremor records. H/V is one of these methods that estimate ground amplification and dominant frequency in a site are analyzed following three different techniques:

1. Direct Spectral Amplitudes
2. Spectral Ratios Relative to a Reference Site
3. The spectral ratios of horizontal components relative to the vertical components

4.1. Horizontal/Vertical Spectral Ratios

4.1.1. Direct Spectral Amplitudes

Direct Spectral Amplitudes can be seen as a very popular method to comment microtremor measurements due to its simplicity. Direct interpretation of spectral amplitudes was used by the groups of Kanai and Kobayashi (Kanai *et al.*, 1954; Kobayashi *et al*., 1986). According to these researchers, the underlying hypotheses are made on these assumptions: First is that microtremors are composed of vertically propagating S waves. Second is that the technique relies on the assumption that the spectrum of the excitation is white noise. The source spectrum of a microtremor is characterized by white noise.

Spectral amplitudes are computed by a Standard Fast Fourier Transform in Direct Spectral Amplitudes Method (Lermo and Chavez-Garcia, 1994). According to them, a spectrum obtained with FFT is described as a function connected with a frequency. In this function, horizontal axis is shown as “frequency’’ or “period”, vertical axis is shown as “spectral amplitude” which was characterized by any wave number at any frequency. The highest amplitude in this spectrum obtained with FFT is convenient with the frequency of the prevailing wave which is known as a dominant wave number or a dominant period, and this period is known as soil dominant period. Some researchers used power spectral density in the calculations (Lermo *et al.*, 1989; Katz,1976; Katz and Bellon, 1978).

According to (Lermo and Chavez-Garcia, 1994), there was no fundamental difference between direct amplitude and power spectral density spectra. The study of Gutierrez and Singh (1992) is best example for direct spectral amplitudes method. These researchers observed that the spectrum of microtremors on a hard rock site was flat for the frequency range of interest. Thus, they used directly the Fourier spectra of microtremors on soft soil sites and corrected for the amplitude level measured at the reference station to estimate the local transfer function. According to them, any peak values could not be seen in spectrum values that are obtained in the reference station (at bedrock). It is assumed that this spectrum value at the bedrock is constant, and a peak value is calculated by dividing spectrum value at soft soils to spectrum value at hard soils. This peak value is used for finding soil amplification and natural frequency.

Nowadays, direct spectral amplitudes method is not preferred directly because this method is composed of the first level of other microtremor analysis methods such as Nakamura's method and reference station method.

4.1.2. Spectral Ratios Relative to a Reference Site

The spectral ratio technique is estimated by using weak and strong motion records practically, and thus it plays an essential role in identification of a common window between the reference and the soft soil seismograms. Besides, the standard spectral ratio method is known as the most reliable method for site response estimation.

Usually, the intense S wave part of the seismogram is extracted with a tapering window and the ratio of smoothed amplitude Fourier spectra is taken to be the transfer function between the soft soil site and the reference station (Lermo and Chavez-Garcia, 1994).

A basic problem occurs when the spectral ratio technique is applied to microtremor records. The basic problem is very difficult to identify a common wave train for the two stations involved. There are two possible solutions to this problem can be given as follows, one is to select data windows using absolute time, without regard to the appearance of the seismogram and the other is to assume that an average of many windows for a given site is representative of its motion at any time (Lermo and Chavez-Garcia, 1994). These researchers assumed the latter. According to them, when spectral ratios are computed, the spectrum of the excitation may not be flat is accepted. On the other hand, a necessary assumption is that the motion recorded at the reference station is representative of the excitation arriving at the interface substratum / sediments, under the soft soil site.

On the other hand, this method is not always easy to be applied in urban areas, because of high instrumentation costs, a high level of noise and the need for long duration experiments (several months), especially in low or moderate seismicity regions.

4.1.3. The Spectral Ratios of Horizontal Components Relative to the Vertical Components (Nakamura's Method)

This method is based on the assumption that the ratio of horizontal and vertical spectra of surface tremor as an approximate transfer function. The H/V technique is a new method in order to determine of ground effect and Yutaka Nakamura developed this method in 1989. This method estimates the site amplification factors without a reference site on the various geological site conditions, it gives the ease of data collection and it can be applied in areas of low or even no seismicity (Nakamura, 1989).

Microtremor observation plays an important role in the validity of Nakamura's method. This method is also shown that if the seismic tremor observation waveform of three components, two horizontal components and vertical component, is available, dynamic characteristics of surface layers can be roughly understood at the seismic observation point. The microtremor observation should be made at midnight when the social activities are stopped nearly completely to avoid effect of artificial noise.

It was assumed that the vertical component of the ambient noise at the ground surface keeps the characteristics of basement ground, is relatively influenced by Rayleigh wave on the sediments and can therefore be used to remove both of the source and the Rayleigh wave effects from the horizontal components (Nakamura, 2008).

According to Nakamura, at Tabata region in 1987, the artificial tremor source has mostly the prevailing vertical motion and tends to induce the Rayleigh waves. This may be the case of Tabata where the effect of train induced tremor was remarkable in the vertical component. In this content, the Rayleigh wave is assumed as noise of microtremor and a method to eliminate the effect of Rayleigh wave is studied.

On the other hand, some of researchers (Lachet and Bard, 1994; Konno and Ohmachi, 1998; Bard 1998) suggested that the peak on H/V ratio can be explained with the fundamental peak of Rayleigh waves. They agree on following two arguments:

1- H/V is basically related to the ellipticity of Rayleigh waves because of the predominance of Rayleigh waves in vertical component.

2- This ellipticity is frequency dependent and exhibits a sharp peak around the fundamental frequency for sites displaying a high enough impedance contrast between the surface and deep materials. This approach, simply comes from the similarity of the figures of H/V ratio of microtremor and H/V of fundamental mode of Rayleigh waves. According to other researchers such as Nakamura, if this approach is true, microtremor should be considered to consist of only Rayleigh wave.

Nogoshi and Igarashi (1971) found that the peak frequency of H/V of Rayleigh wave, the energy of Rayleigh wave is very small, nearly close to the zero. Because of this, peak of H/V can not be explained by Rayleigh wave energy. H/V of microtremor at peak frequency range can be explained with vertical incident SH wave (Nakamura, 2000).

According to Figure 4.1, energy of Rayleigh wave does not appear on the peak of H/V of Rayleigh wave. There is no energy around the peak frequency of H/V and amplitude is almost zero for horizontal and zero for vertical components of Rayleigh waves. On the other hand, Rayleigh wave energy gets its maximum on later frequencies at minimum group velocity of Rayleigh wave and this is nearly equal to trough frequency which is almost two times of H/V peak frequency.

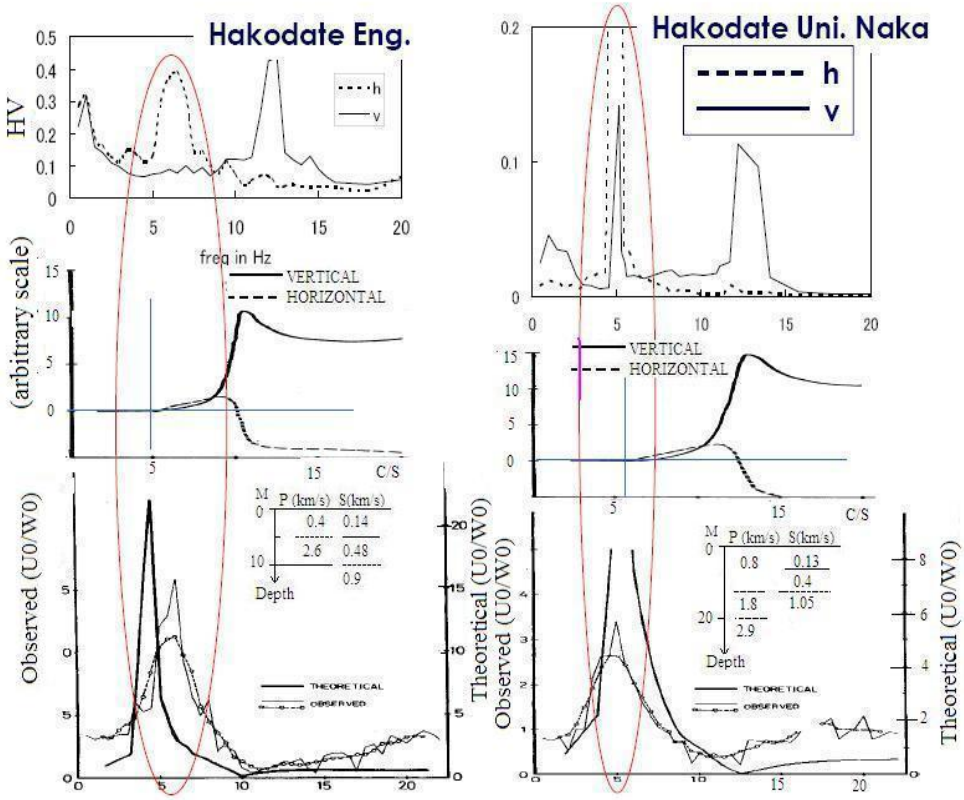

Figure 4.1. Relation of H, V and H/V for microtremor and for Rayleigh wave (Nogoshi and Igarashi, 1971)

Figure 4.2 shows that the change of impedance ratio for frequencies of trough and peak of H/V Minimum group velocity of Rayleigh waves. For trough and minimum group velocity (for almost all impedance ratio values) frequency changes between 1.5 – 2.0. On the other hand, only the peak frequency varies in a wider range for different impedance ratio. The energy of Rayleigh wave is almost zero at peak frequency of H/V, and at the trough frequency of H/V the energy becomes maximum.

On the soft ground, horizontal motion is larger than vertical motion. On the other hand, on the hard ground, both horizontal and vertical motions are similar to each other both on the maximum value and on waveform.

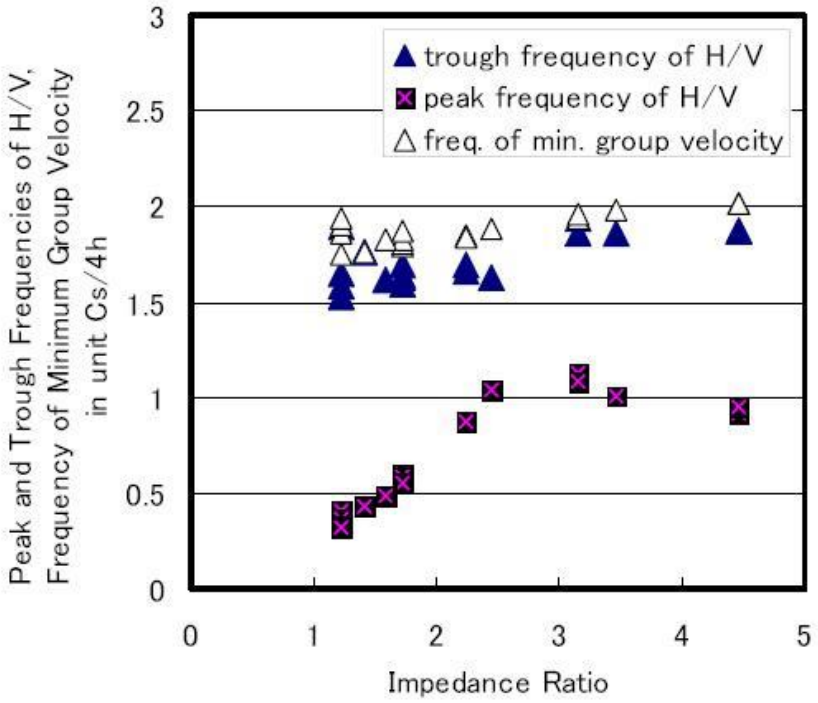

Figure 4.2. Relationship between characteristics of Rayleigh wave and impedance ratio

All these examples prove that, as it was explained by Nakamura (1989). H/V peak is mostly related with SH wave and can not be explained with the Rayleigh waves

4.1.3.1. Principals of H/V Ratio Method. Rayleigh wave should be eliminated from waveforms in order to calculate transfer function correctly. Source effects might be removed from microtremor data by taking the spectral ratio of the horizontal record to the vertical record at a single site (Nakamura, 1989). Nakamura also assumed that only horizontal microtremors are influenced by soil and that source spectral characteristics are maintained in vertical microtremors as well as in horizontal microtremors.

Site effects due to surface geology are generally expressed as the spectral ratio, S_T, between the horizontal component of earthquake recordings at the surface of the soft layer, S_{HS}, and the ones at the ideally horizontal outcropping bedrock, S_{HB} ,

$$S_T = S_{HS} / S_{HB} \tag{4.1}$$

But S_{HS} is readily affected by the surface wave. Since the artificial noise is mostly propagated as Rayleigh wave, S_{HS} of microtremor may possibly be affected by Rayleigh wave.

First assumption is microtremors are composed of several waves, but essentially Rayleigh waves propagating in the soft surface layer overlying a stiff substratum. The effect of Rayleigh wave should be included in the vertical tremor spectrum S_{VS} on the surface, but not included in the vertical tremor spectrum S_{VB} in the base ground.

Second assumption is the effect of the Rayleigh wave (E_{RW}) on the noise motion is included in the vertical spectrum at the surface (EVs), but not at the base of the layer (EV_B):

$$E_{RW} = EVs / EV_B \tag{4.2}$$

The vertical component of microtremor motion is not amplified by the soft soil layer. If there is no Rayleigh wave, $E_{RW} = 1$, E_{RW} will take a value larger than "1" with increasing effect of Rayleigh wave.

Assuming that the effect of Rayleigh waves on microtremor motion is equivalent for the vertical and horizontal components, for a wide frequency range (0.2-20 Hz), the spectral ratio of the horizontal and vertical components of motion at the bottom of the layer is close the unity:

$$S_{HB} / S_{VB} = \boldsymbol{1} \tag{4.3}$$

As shown in Figure 4.3, this value becomes nearly 1.0 for a relatively wide frequency range. Namely, on the firm substrate, propagation is even in all directions.

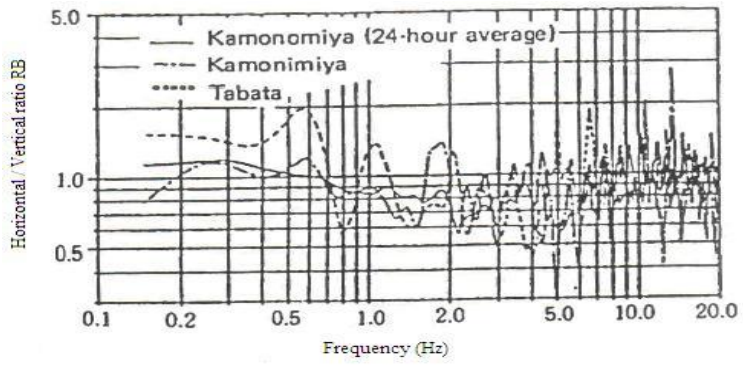

Figure 4.3. Spectrum ratio of horizontal and vertical components in the substrate. Microtremor study was carried out at Kamonomiya and Tabata (Nakamura, 1989)

S_T / E_{RW} may be considered to offer a more reliable transfer function S_{TT} after elimination of the effect of Rayleigh wave.

Namely: $$S_{TT} = S_T / E_{RW} = R_S / R_B \quad (4.4)$$

Where $$R_S = S_{HS} / S_{VS} \quad (4.5)$$

$$R_B = S_{HB} / S_{VB} \quad (4.6)$$

R_S and R_B were obtained by dividing the horizontal tremor spectrum by vertical spectrum, corresponding, respectively, to surface and substrate earthquake tremors. Namely $R_B \approx 1$. and $S_{TT} \approx R_S$. This means that the transfer function of surface layers may be obtained from the tremor on the surface only. In other words, the vertical tremor on the surface retains the characteristics of horizontal tremor of the substrate, thereby substituting the latter. The Rayleigh wave acts to nullify such substitution, but R_S becomes more or less "1" in the frequency range where the Rayleigh wave prevails, and thus it is not remarkable in the estimated transfer function. It may thus be presumed that R_S includes the effect to eliminate the effect of Rayleigh wave (Nakamura, 1989).

Namely, the amplification of the horizontal maximum value by surface layers can be estimated from the ratio of horizontal and vertical maximum values on the surface. It is also considered that the tremor in the substrate is equal in all directions because various wave motions repeat local refraction after principal tremor of earthquake.

5. SHEAR WAVE CALCULATION METHODS

5.1. Refraction Microtremor Method (ReMi)

The refraction microtremor (ReMi) method has been recently developed to obtain near subsurface average shear-wave velocity. 200 meter long array are used to obtain approximately 100 meter depth of investigation (Louie, 2001).

ReMi has been applied to interpret the bottom depth of an uncontrolled landfill and to delineate near surface bedrock topography and involving structure such as fault in addition to shear-wave velocity information. V_S profiles obtained from ReMi also can be used for earthquake site response and liquefaction analysis. The refraction microtremor technique is based on two fundamental ideas: The first idea is that common seismic refraction recording equipment deployed similar to shallow P-wave refraction surveys to record surface waves at frequencies as low as 1. Hz such as ambient noise / microtremor. Depth of penetration is inversely proportional to natural frequency of geophones used. The second idea is that the slowness-frequency (p-f) wavefield transformation is used to separate Rayleigh wave energy from that of other waves and allow identifying true phase velocity against apparent velocities (Pullammanappallil *et al.*, 2003).

The basis of the velocity spectral analysis is known as the p-tau transformation, or ``slant stack" (Thorson and Claerbout, 1985). This transformation takes a record section of multiple seismograms, with seismogram amplitudes relative to distance and time (x-t), and converts it to amplitudes relative to the ray parameter, p, and an intercept time, τ.

$$A(p, \tau) = \int_x A(x, t = \tau + px)\, dx \tag{5.1}$$

where x: Distance; t: Time. This transformation is described as “line integral”.

$$p = dt / dx \tag{5.2}$$

where p = dt/dx is inverse of apparent velocity, Vap, in the x direction and is known as “slowness”. In practically, “x” is composed of separated values, and “t” is composed of separated values:

$$x = j * dx \tag{5.3}$$

j=1,2,3.....,n generally, dx is between 8. -20 m

$$t = i * dt \tag{5.4}$$

i=1,2,3,...,m generally, dt is between 0.001-0.01 sec

$$A(p = p_0 + l\Delta p, \tau = kdt) = \sum A\,(x = jdx, t = idt = \tau + px) \tag{5.5}$$

Equation 5.5 is “p-τ transformation”. Later, this line integral is applied to Fourier transformation (McMechan and Yedlin, 1981).

$$F(p,f = m\Delta f) = \sum A(p, \tau = kdt) e^{-i2\pi m\Delta f\, k\, \Delta t} \tag{5.6}$$

Third step is Velocity Spectral Analysis (Louie, 2001): Power spectrum

$$S(p,f) = F^*(p,f) * F(p,f) \tag{5.7}$$

$$S(|p|,f) = F(p,f) + F(-p,f) = [S(p,f)]_{p\geq 0} + [S(-p,f)]_{p<0} \tag{5.8}$$

Consequently, p-f transformation is completed from x-t space. This transformation from x-t domain to p-f domain is completed. Ray parameter, p, represents horizontal component of slowness along the array. In analyzing more than one seismic refraction record, special p-f image $S_{An}(|p|,f)$, are added by point and point to the total power image.

$$S_{total}(|p|,f) = \sum S(p,f) \tag{5.9}$$

All phases in the record are present in the resulting (p-f) image that shows the power at each combination of phase slowness and frequency. Dispersive phases show the distinct curve of normal modes in low-velocity surface layers: sloping down from high phase velocities (low slowness) at low frequencies, to lower phase velocities (high slowness) at higher frequencies. The distinctive slope of dispersive waves is a real advantage of the p-f analysis. Other arrivals that appear in microtremor records, such as body waves and airwaves, cannot have such a slope. The p-f spectral power image will show where such waves have significant energy. Even if most of the energy in a seismic record is a phase other than Rayleigh waves, the p-f analysis will separate that energy in the slowness-frequency plot away from the dispersion curves this technique interprets. By recording many channels, retaining complete vertical seismograms, and employing the p-f transform, this method can successfully analyze Rayleigh dispersion (Pullammanappallil *et al.,* 2003).

A slowness-frequency (p-f) wavefield transform is used to separate Rayleigh wave energy from that of other waves. Because the noise field can originate from any direction, the wavefield transform is conducted for multiple vectors through the geophone array, all of which are summed. The dispersion curve is defined as the lower envelope of the Rayleigh wave energy in p-f space. Because the lower envelope is picked rather than the energy peak (energy traveling along the profile is slower than that approaching from an angle), this technique may be somewhat more subjective than the others, particularly at low frequencies.

The ReMi method offers important advantages. In contrast to borehole measurements, ReMi tests a much larger volume of the subsurface. The results shows the average shear wave velocity over distances as far as 200 meters (600 feet). Because ReMi is noninvasive and non-destructive, and uses only ambient noise as a seismic source, no permits are required for its use. ReMi seismic lines can be deployed within road sides, at active construction sites, or along highways, without having to disturb work or traffic flow (Pullammanappallil *et al.,* 2003).

5.2. Suspension PS Logging Method

Suspension P-S velocity logging is a method for measurement of seismic wave velocity profiles, shear (V_S), and compression (V_P) wave velocity, it was developed in the mid-1970s to answer the need for a technique that could measure seismic shear-wave velocities in deep, uncased boreholes, it is the first time some researchers used this method at the OYO Corporation of Japan. The method gained acceptance in Japan in the mid-1980s and was used with other velocity measurement methods to characterize earthquake site response technique since 1991.

The Suspension P-S Logging System contains a source and two receivers spaced 1. meter apart, suspended by a cable. The probe length is approximately 7. meters. The armored 4. or 7. conductor cable serves both to support the probe and to convey data to and from a recording/control device on the surface. The probe is lowered into the borehole to a specified depth (a rotary encoder on the winch measures probe depth), where the source generates a pressure wave in the borehole fluid.

Compression (P) and shear (S) waves are created by the seismic source that involves the use of a solenoid hammer. The solenoid hammer produces a pressure wave in the borehole fluid. This pressure wave converts into seismic body waves at the borehole wall. The waves travel in a radial direction from the borehole wall. Receivers contain two-component geophones, one vertical for recording of P-waves, and one horizontal for recording of S-waves (Luna and Jadi, 2000).

The elapsed time between arrivals of the waves at the receivers is carried out to determine the average velocity of one meter high column of soil around the borehole. Source to receiver analysis is also performed for quality assurance.

Advantages of the suspension PS logging are that it is not necessary to clamp the probe against the borehole wall, and because the wavelength of excited shear waves is much greater than the borehole diameter, shear excitation is almost independent of the borehole fluid. As such, geophones in the probe can record the behavior of the borehole wall without clamping the probe. The other advantage of the suspension PS logging is accurate measurement of the shear wave velocity values and because the frequency of the shear wave generated by the source is generally higher than the other methods, wavelengths are shorter and propagation time measurements are more accurate (Kaneko, Kanemori and Tonouchi, 1990).

6. DATA COLLECTION

6.1. Site Study

6.1.1. Field Measurement

For the purpose of determining the soil transfer function and the fundamental frequencies of the Pendik-Tuzla districts of Istanbul, H/V microtremor measurements were carried out at 64 different points during the period of June 2009-October 2009. 26 points of them had been taken in the same locations of borehole points which had been taken by Oyo Company. Figure 6.1 shows H/V microtremor measurement points in study site.

To avoid recording high artificial disturbances such as noise of factory and traffic effects, the locations of measurement points were selected away from source of noise. In addition, measurement points were carried out at different geological formations.

The measurement instruments consist of GÜRALP CMG-6T seismometer being a three-component velocity sensor unit of which natural period is between 30 to 0.01 seconds, power supply, GPS and a laptop. Usually, measurements have to be carried out during clear weather. During the recording, a box was put on the top of seismometer in order to eliminate the effect of noise due to traffic, wind, and animal movements (Figure 6.2 and Figure 6.3).

CMG-6T broadband seismometer has 2. Gb memory disk that stores the records directly. Microtremor records were also transferred from seismometer to computer during recording process. While microtremor records were been taking, these records were seen on the computer screen. Some adjustment were done in field area to the CMG-6T seismometer:

- Seismometer was oriented N-S direction, mass position were centered.

- After connecting power supply to seismometer, necessary acquisition parameters are set up: sampling rate, record length, file names and directory using Scream 4.4 Software. File name was changed at every measurement point. After these setups, recording started.

The record time is determined according to noise levels at the measurement points. In this study, this record time were determined as 25 minutes for each measurement points. Sometimes, because of the destructive effects of noise on the records, this time was increased to 35 minutes to obtain adequate microtremor data.

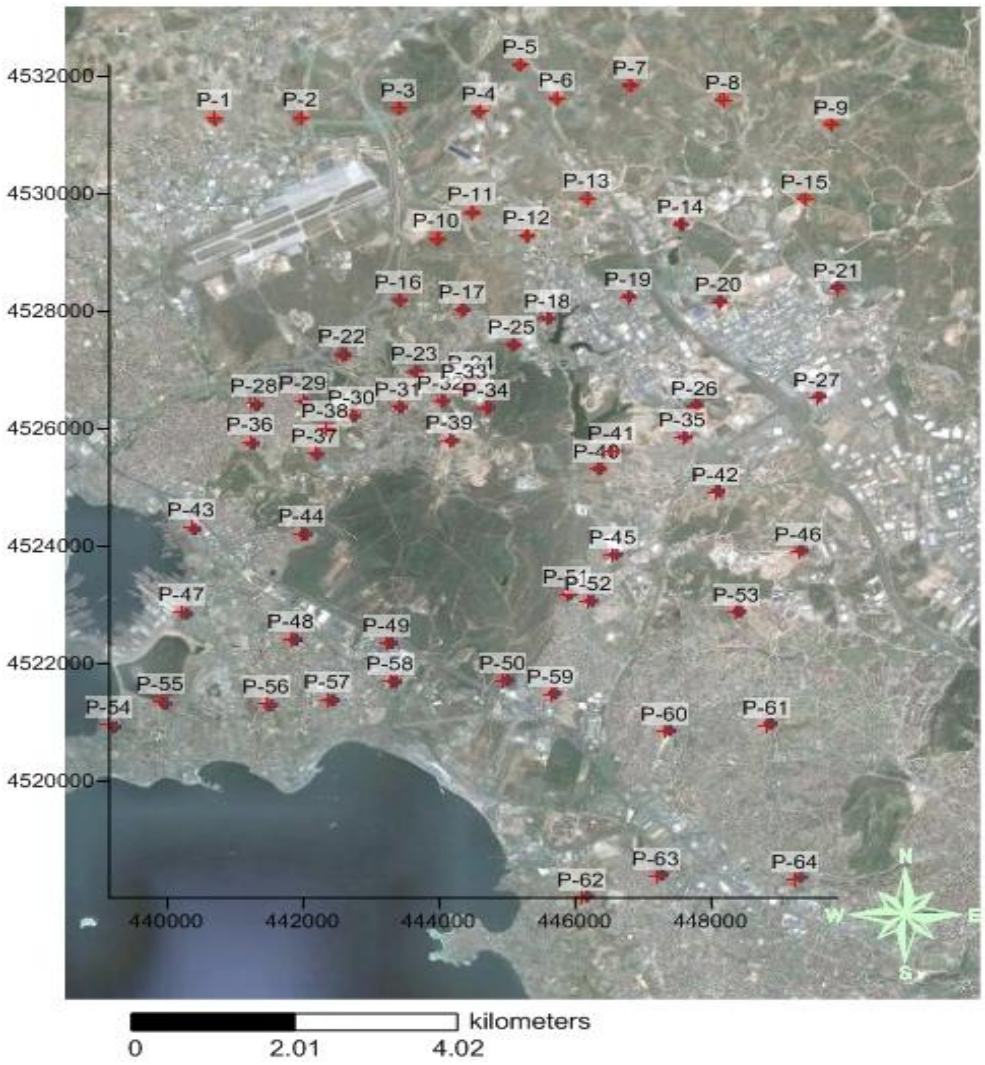

Figure 6.1. Measurement points for H/V study. The coordinate unit of this map is given in Universal Transversal Mercator system

Figure 6.2. Left figure shows seismic equipment in one measurement point. Right one shows seismometer installation next to a borehole to decrease effects of wind, a bucket was put on the seismometer

Figure 6.3. Left figure shows power supply, Right figure shows GÜRALP CMG-6T seismometer

6.1.2. Data Analysis

Three component microtremor data were recorded with a sampling rate of 10 ms. The data were corrected before taking Fourier transform. These are data editing, trend removal, re-sampling and filtering. After the field experiments, the data preparation procedures can be given as below:

At every measurement point, three components (two horizontal and one vertical) of microtremor on the ground were recorded with a duration of ten minutes and written to a file. Later, for each component of one measurement point, data files are combined at Scream 4.4 Software to form a single data file. These separated files were combined by "combine" command in Scream 4.4 Software.

Next, every each data (the new combined files), was converted from GCF format to SAC format files by using "conversion from gcf to sac". In the sac program, when looking at waveform, the data were corrected by trend and mean removal and filtering functions and artificial, high amplitude noises were picked. Band pass filter had filtering range changing between 0.1 – 10. Hz was used generally for each points. Later, high artificial noise must be cleared from the data set in order to increase accuracy of data analysis. For this process, firstly, data sets were converted from SAC format to ASCII format. Later, the data were cleared from these noise .

The first cutting process were applied to the first 30 lines consists of header information for every ASCII records. Later, other cutting processes were done according to selected sections defined previously by viewing the records at a workstation. Consequently, after the elimination of spike or transient type noise, input data were made ready for data analysis in this study, and thus input data were executed in the Fortran program.

After data preparation, for each measurement points, to calculate the H/V ratios, in other words, to determine the values of soil amplification and dominant frequency, the following procedures of data analysis were applied.

The input data that consist of three components at the time domain was converted to frequency domain by the fast fourier transform technique, (fft). This is a necessity in data analysis. It was important that data length must be selected as a power of two (for fft data analysis). In this study, data length is chosen as 4096. This length was reduced to 2048 by changing the sampling interval from 0.01 s to 0.02 s.

Output of Fourier transform was smoothed by a Parzen window with different bandwidths. In this study, the bandwidth was changed from 9. to 60 to obtain reliable estimates.

An increase in bandwidth, in the other words, an increase in the smoothing, made the highest amplitudes being lost and low frequency amplitudes become visible on the spectrum. It is important that to obtain fundamental frequency, smoothing is an essential way to eliminate the highest frequencies.

After the fft, program divides ascii data into seven sub sections and writes to a file for spectrum calculation. The H/V spectral ratios were calculated by dividing the spectrum plus ratio of the square root mean values of horizontal components to the spectra of the vertical component for each seven sub sections. An arithmetic average of these seven sub sections were calculated.

Finally, the H/V spectrum was calculated by a ratio of horizontal to vertical spectra. Soil amplification value was obtained by the ratio of H/V spectrum since amplification effect was not seen on vertical component record.

In order to obtain soil transfer function for one measurement point, Point-5, steps of data preparation was seen in Figure 6.4. Figure 6.5 shows that the estimated H/V spectrum is smoothed by the Parzen window with 9., 19 and 49 bandwidth. The Parzen window of 49 bandwith was selected because of clear peak maximum amplitude. This bandwidth was determined as adequate for obtaining maximum amplitude values and thus we selected 4th H/V plot from 49 bandwith for determining fundamental frequency and amplification. Lastly, according to Figure 6.5, soil amplification 2.1, and fundamental frequency 1.22 Hz. were determined.

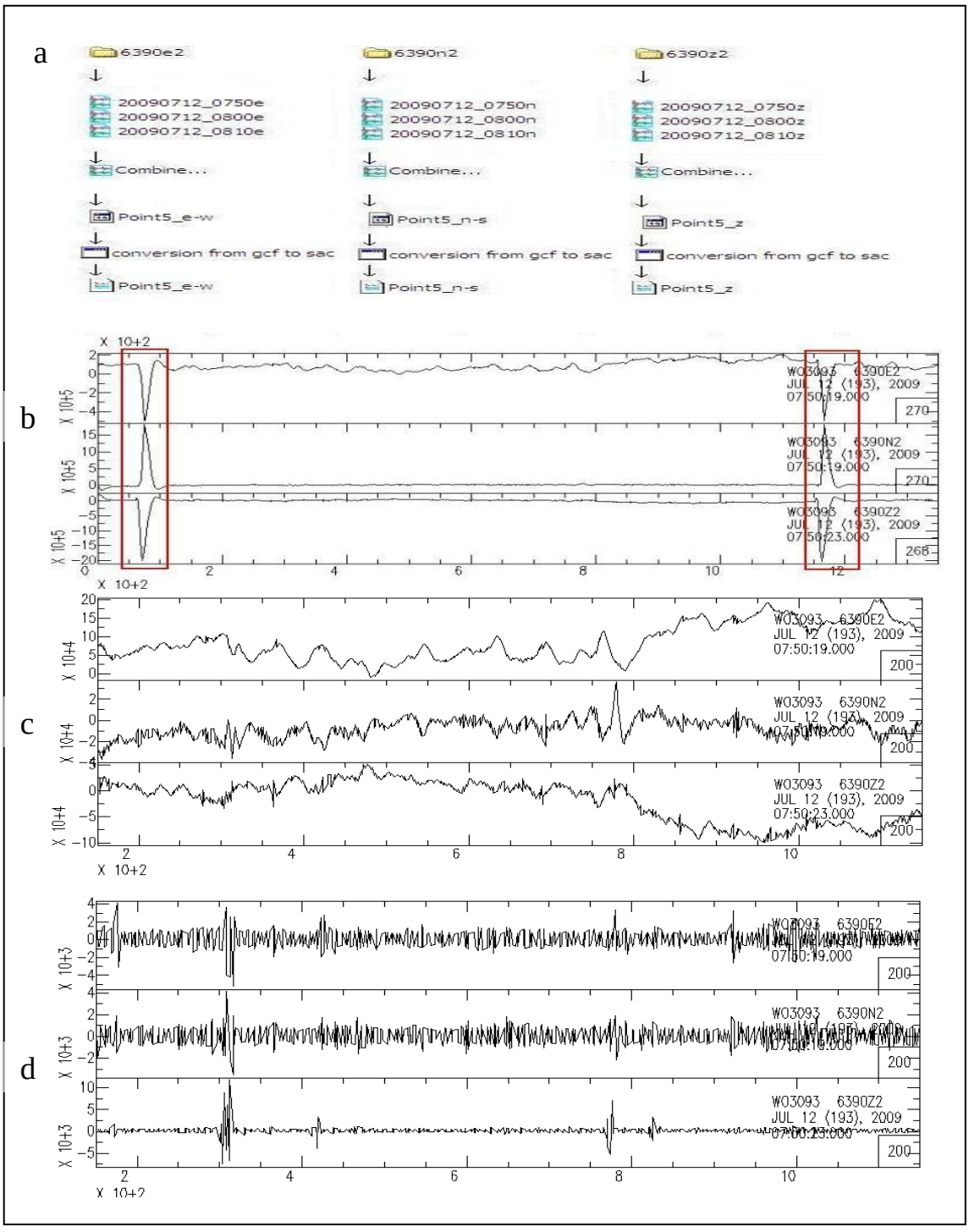

Figure 6.4. Steps of data preparation for point-5. Combination and conversion of data set (a). Viewing the data and selection of high amplitude noises (b). After the elimination of high amplitude noises, the data were corrected by trend and mean removal (c). Band pass filter is applied, its frequency range is between 0.1- 10 Hz (d)

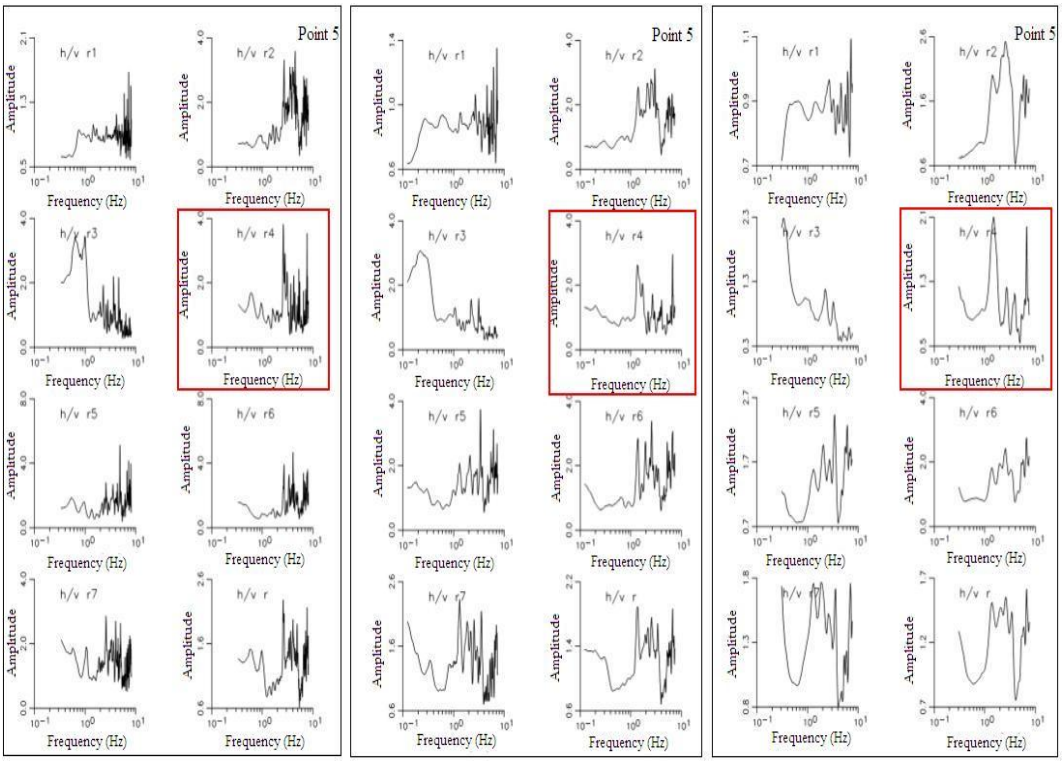

Figure 6.5. H/V spectrum values were smoothed by Parzen window with bandwidth of 9 (left), 19 (middle) and 49 (right) in order to obtain accurately dominant frequency for point-5

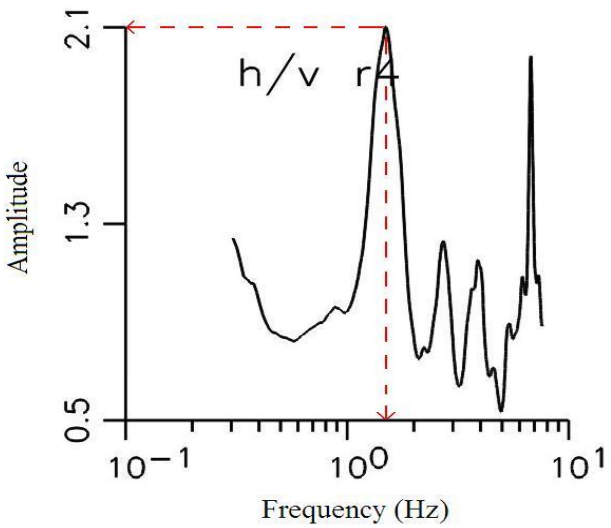

Figure 6.6. H/V amplification spectrum for measurement point-5

The other 63 measurement points, the same steps were used to obtain maximum amplification and dominant frequency using Nakamura method. The Table 6.1 shows the results obtained from this study.

Table 6.1. The result of microtremor study

H/V Study Points	Soil Amplification	Dominant Frequency (Hz)	Dominant Period (sec)	H/V Study Points (continued)	Soil Amplification	Dominant Frequency (Hz)	Dominant Period (sec)
Point-1	2.9	0.35	2.86	Point-34	4.2	0.9	1.11
Point-2	4.8	0.25	4.00	Point-35	1.12	0.47	2.12
Point-3	8.3	0.3	3.33	Point-36	1.7	1.9	0.53
Point-4	4.6	0.3	3.33	Point-37	4.3	0.7	1.43
Point-5	2.1	1.22	0.82	Point-38	2.3	2.1	0.48
Point-6	1.7	1.4	0.71	Point-39	2.88	0.9	1.11
Point-7	1.55	2.05	0.49	Point-40	5.2	1.05	0.95
Point-8	2.1	1.2	0.83	Point-41	3.6	1.1	0.91
Point-9	0.7	4	0.25	Point-42	4	0.5	2.00
Point-10	2.6	0.85	1.18	Point-43	2.4	1.4	0.71
Point-11	5.7	0.5	2.00	Point-44	2.72	1.05	0.95
Point-12	10	0.2	5.00	Point-45	3.9	0.9	1.11
Point-13	3.3	0.65	1.54	Point-46	2.3	1.2	0.83
Point-14	2.1	1.3	0.77	Point-47	2.3	2.6	0.38
Point-15	2	1.5	0.67	Point-48	2.4	1	1.00
Point-16	1.8	1.3	0.77	Point-49	3.8	1.02	0.98
Point-17	1.55	1.4	0.71	Point-50	2.5	1.2	0.83
Point-18	5	0.97	1.03	Point-51	4	1	1.00
Point-19	1.7	1	1.00	Point-52	5.5	1.05	0.95
Point-20	2.92	0.95	1.05	Point-53	2.3	1.2	0.83
Point-21	3.5	0.4	2.50	Point-54	4	0.5	2.00
Point-22	3.8	0.9	1.11	Point-55	3.5	0.7	1.43
Point-23	3.32	0.92	1.09	Point-56	3.5	0.8	1.25
Point-24	3	0.98	1.02	Point-57	3.8	0.9	1.11
Point-25	2.5	1.7	0.59	Point-58	4	0.65	1.54
Point-26	3.7	0.7	1.43	Point-59	4.5	1.2	0.83
Point-27	7.5	0.2	5.00	Point-60	2.2	2.1	0.48
Point-28	2.4	1.3	0.77	Point-61	4	0.5	2.00
Point-29	2.96	0.76	1.32	Point-62	3.4	0.5	2.00
Point-30	3.3	0.6	1.67	Point-63	2	1.6	0.63
Point-31	2.4	1.3	0.77	Point-64	2.6	2	0.50
Point-32	2.2	1.4	0.71				
Point-33	6.88	0.65	1.54				

6.2. Model Study

6.2.1. Data Preparation

In the model study, one dimensional model was prepared for different measurement points which consist of the results of the shear velocity that had been obtained by Oyo Company using ReMi and PS logging methods in selected sites. These measurement points were selected according to bedrock location information. Figure 6.6 shows these points for model study. The location of these points were converted to Geographic coordinate systems from Universal Transverse Mercator (UTM) system by "J-trans13" and "Coordinate Conversion program 4.5" to show the measurement points of ReMi and PS logging methods in Google map.

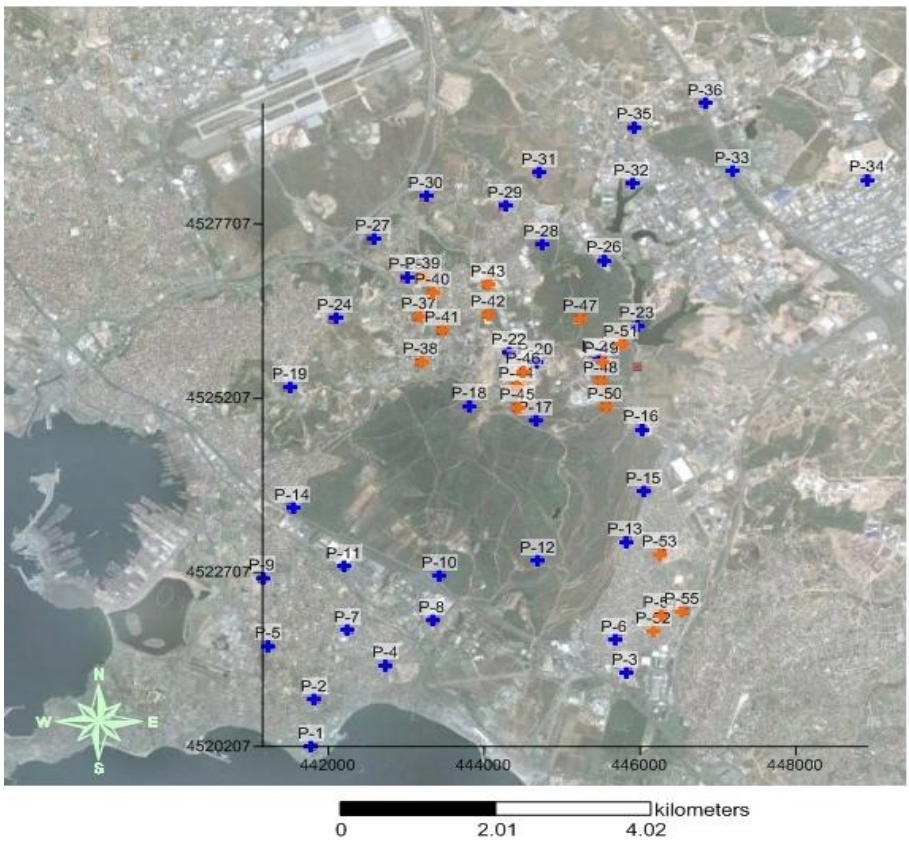

Figure 6.7. Measurement points for model study. Red points show ReMi measurement points, blue points shows PS measurement points. **T**he coordinate unit of this map is given in Universal Transversal Mercator system

Firstly, one dimensional model was planned to evaluate the effect of local soil conditions on ground response using the Shake 91 program. This model consists of N horizontal layers which extend to bedrock depth, and each layer is homogeneous and isotropic and is characterized by the thickness, shear velocity, density and damping parameter. Damping parameters, and densities are calculated using empirical formulas.

Density, d, is obtained by below formula for each model points and its unit is g/cm^3:

$$d = (1.6)+(0.2)*Vp \tag{6.1}$$

where Vp is km/sec .

Damping parameter, ξ, is known as inverse of quality factor that is related to Shear wave velocity. Quality factor, Qs, is calculated using below formula:

$$Qs = 0.1*Vs \tag{6.2}$$

Input data were prepared according to the information based on thicknesses of the layers, their shear wave velocities, their densities and their damping parameters.

The response for this design motion was computed by Shake 91 program. Soil system extends infinitely in the horizontal direction, each layer in the system is completely defined by its values of velocity, density or thickness and the responses in the system are caused by the upward propagation of shear waves from the underlying rock formation were the most important assumptions for the program.

6.2.2. Data Analysis

In our model studies, one dimensional model was prepared for different 56 measurement points. To give an example, measurement points-13 was prepared in Figure 6.8.

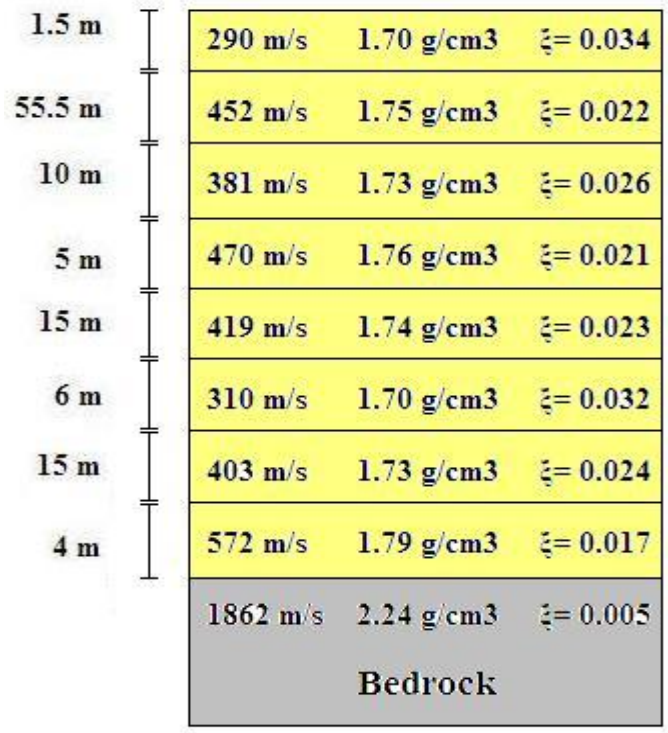

Figure 6.8. One dimensional model for measurement point-13

According to this model, input data were prepared (Figure 6.9). All values are converted British imperial system for Shake 91 program. Shear wave velocities for the sub layers are given as feet/second unit. The thicknesses of sub layers are in feet unit. Densities of layers are in kips cubic foot, kcf, unit also. Later to obtain amplification spectrum, bedrock structures are classified according to geologic units. These are artificial fill at zero - 1.5 m depths, Sultanbeyli Formation at 1.5 - 112 m depths and Sancaktepe Granite at 112 - 124 m depth. Sancaktepe Granite is determined as bedrock formation. Since soil profiles were overlying the bedrock, ninth sub layer equals to one, and frequency step were selected 0.125 units. In our model studied, at some measurement points, the bedrock was outcrop to rock surface, thus last sub layer equals to zero. Input motion is selected real earthquake data that is the Loma Prieta Earthquake, in 1989, and its peak acceleration is 0. 1128945 gal. After these adjustments, input data are executed in Shake 91 program. Figure 6.10 depicts the result values of this point, and thus maximum amplification of 9.85, fundamental frequency of 0.96 Hz and dominant soil period of 1.04 sec are found. In order to justify the calculation of dominant soil period or frequency values in Shake 91 program, soil periods also were calculated from below empirical formula,

$$T = \sum_{i=1}^{n} 4Hi / Vsi \qquad (6.3)$$

Where T is the site dominant period, H is the depth to bedrock, and Vs is the shear wave velocity of the soil (Bard and Bouchon, 1985).

Soil period values estimated from empirical formula is a little higher than the values calculated by Shake 91. For Point-13, while dominant soil period is calculated as 1.07 sec with using empirical formula, Shake 91 program calculated 1.04 sec. We noticed that soil dominant periods calculated from empirical formula are close to Nakamura study.

Above steps were repeated for the other 55 measurement points. The results of the model study are shown in Table 6.2.

```
Option 2 -- Soil Profile
    2
    1    9              input:Diam @ .1g
    1                    4.92                .034      .106       951.
    2                  182.08                .022      .109      1482.
    3                   32.80                .026      .108      1250.
    4                   16.40                .021      .110      1541.
    5                   49.21                .023      .108      1374.
    6                   19.68                .032      .106      1017.
    7                   49.21                .024      .108      1322.
    8                   13.12                .017      .112      1876.
    9                                        .005      .140      6108.
option 10 -- compute & save amplification spectrum:
   10
    9    1     1    0     0.125      - surface/rock outcrop
execution will stop when program encounters 0
    0
```

Figure 6.9. Input data for measurement point - 13

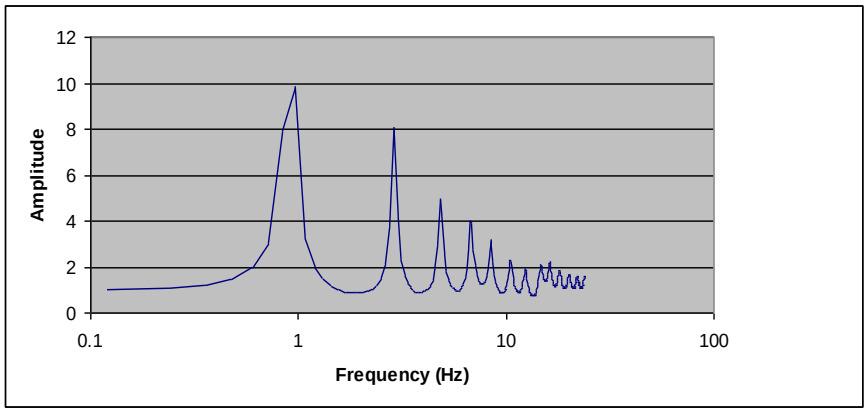

Figure 6.10. Amplification spectrum for measurement point-13 according to Shake 91 program

Table 6. 2. The results of model study

Model Study Points	Soil Amplification	Dominant Frequency (Hz)	Dominant Period (sec)	Model Study Points (continued)	Soil Amplification	Dominant Frequency (Hz)	Dominant Period (sec)
Point-1	2.35	8.59	0.12	Point-29	1.91	9.66	0.10
Point-2	16.15	1.61	0.62	Point-30	2.67	3.47	0.29
Point-3	18.48	1.06	0.94	Point-31	18.21	1.88	0.53
Point-4	15.73	1.53	0.66	Point-32	22.47	1.27	0.79
Point-5	2.58	9.06	0.11	Point-33	2.27	5.18	0.19
Point-6	14.63	0.88	1.13	Point-34	5.35	6.58	0.15
Point-7	6	4.40	0.23	Point-35	2.7	5.64	0.18
Point-8	4.86	9.01	0.11	Point-36	2.73	3.99	0.25
Point-9	3.16	9.90	0.10	Point-37	2.53	9.88	0.10
Point-10	1.11	9.31	0.11	Point-38	5.59	2.84	0.35
Point-11	3	9.72	0.10	Point-39	3.86	3.01	0.33
Point-12	2.61	3.36	0.30	Point-40	6.5	5.64	0.18
Point-13	9.85	0.93	1.07	Point-41	1.58	8.56	0.12
Point-14	5.82	10.00	0.10	Point-42	1.82	8.61	0.12
Point-15	17.49	2.87	0.35	Point-43	2.96	2.23	0.45
Point-16	10.74	0.97	1.03	Point-44	2.46	2.99	0.33
Point-17	2	6.56	0.15	Point-45	3.97	2.62	0.38
Point-18	1.98	4.27	0.23	Point-46	1.86	2.04	0.49
Point-19	2.39	4.89	0.20	Point-47	3.19	3.13	0.32
Point-20	1.73	2.14	0.47	Point-48	3.82	2.09	0.48
Point-21	1.37	8.66	0.12	Point-49	2.33	5.46	0.18
Point-22	2.88	5.31	0.19	Point-50	9.08	1.89	0.53
Point-23	15.89	1.82	0.55	Point-51	15.46	1.60	0.62
Point-24	4.39	9.83	0.10	Point-52	10.65	1.64	0.61
Point-25	3.22	6.25	0.16	Point-53	13.25	2.12	0.47
Point-26	1.45	2.22	0.45	Point-54	13.34	1.82	0.55
Point-27	2.55	6.92	0.14	Point-55	5.99	3.27	0.31
Point-28	14.37	1.30	0.77	Point-56	6.33	6.28	0.16

7. THE RESULT OF STUDIES

Soil amplification, dominant frequency and period values estimated from H/V and model studies are presented as contour maps. Furthermore, the areas of H/V and model studies were divided into a series of horizontal cross sections to understand the changes of the values of soil amplification and dominant period compared to overburden thickness.

The location of measurement points were converted to Universal Transverse Mercator (UTM) system from Geographic coordinate systems using "J-trans13" and "Coordinate Conversion program 4.5" to plot these results in a Surfer 9 program. The coordinate unit of these contour maps are given in Universal Transversal Mercator system.

7.1. The results of H/V Study

Figure 7.1, 7.2 and 7.3 shows the distribution of soil amplification, dominant frequency and period values obtained from H/V study, respectively.

Firstly, the results of H/V microtremor study indicate that four different regions of study area have site amplifications greater than 3.7 value. These regions can be given as below:

1- Orhanlı region that is an area between the northeast of the Sabiha Gökcen Airport and Tuzla Leather - Industry Free Zone.

2- Aydınlı region that is the middle of the study area, located in southeast of Tuzla Marple Industry zone.

3- Sekerpınar region that is the north of the study area.

4- The southeast of Abduş Lake

Especially Orhanlı region has site amplification levels reaching to 10. While Aydınlı and Sekerpınar have values changing between 3.7 and 7., the southeast of Abduş Lake has values between 3.7 and 4. Besides, while dominant soil periods are between 1.4 and 5. sec (0.2-0.8 Hz) at Orhanlı and Sekerpınar regions, Aydınlı Region has dominant soil period being in a range between 0.9 and 1. sec (1.- 1.1 Hz). Dominant period varies between 1. and 1.8 sec (0.6 – 1. Hz) in the southeast of Abduş Lake.

Furthermore, when we look at remaining areas (the west and northeast and southeast of the investigated area), soil amplification level has approximately at 2.7. At these sites, dominant period take values between 0.5 and 0.8 sec (1.2-1.9 Hz).

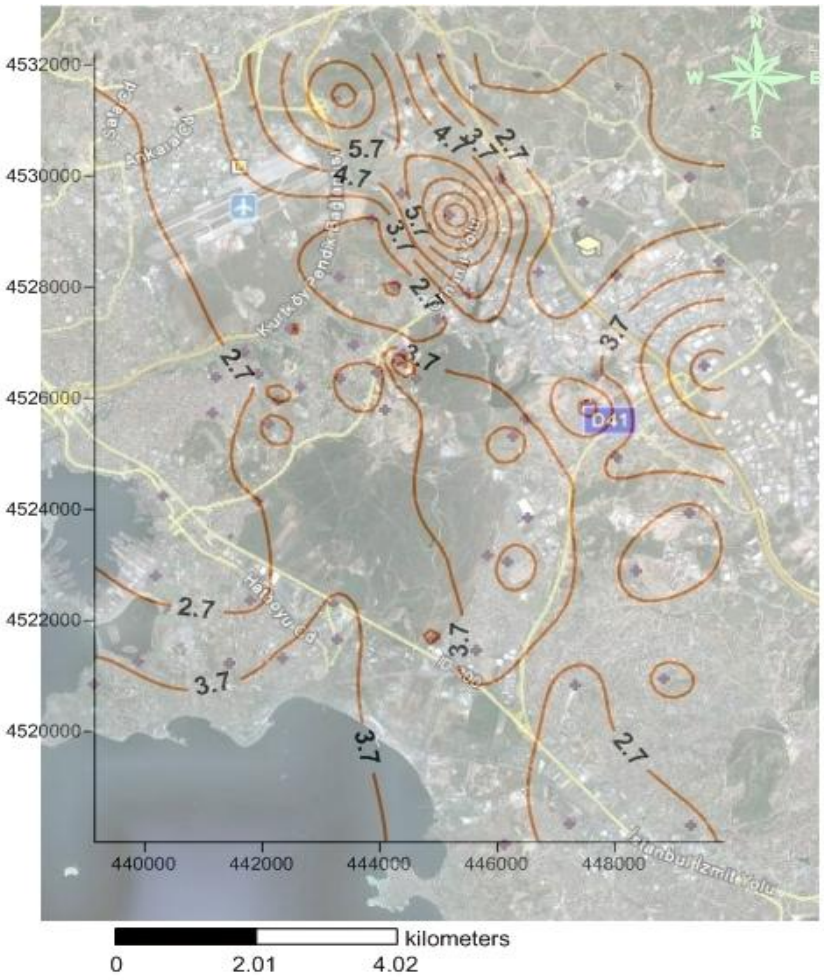

Figure 7.1. Distribution of soil amplification values from H/V study

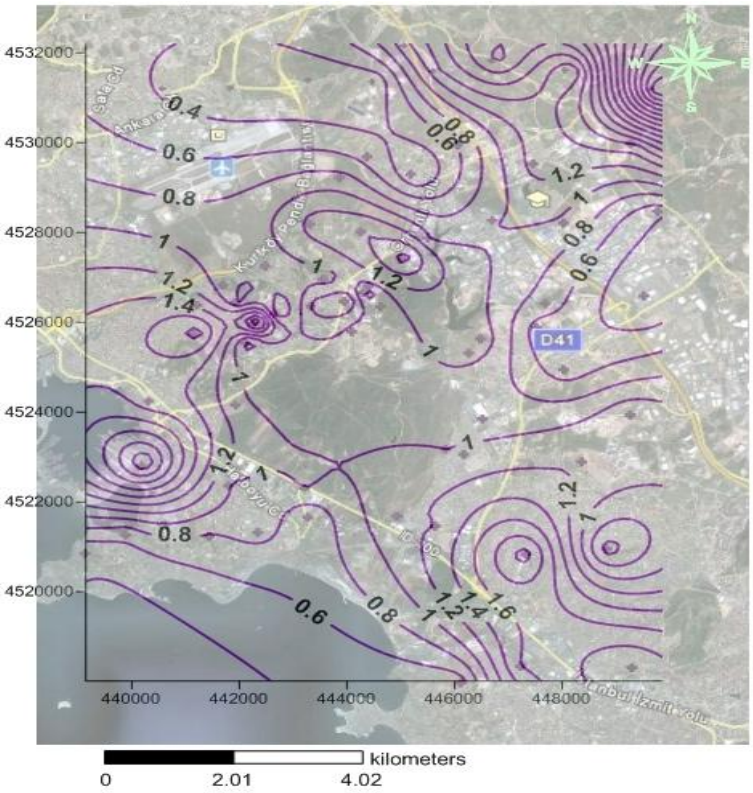

Figure 7.2. Distribution of dominant frequency values from H/V study

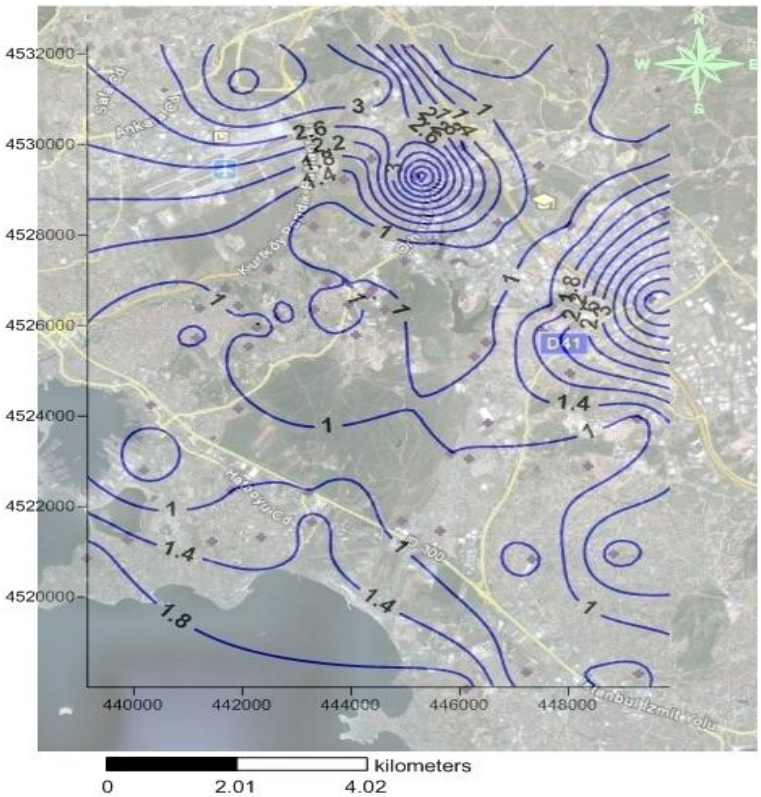

Figure 7.3. Distribution of dominant period values from H/V study

Figure 7.4 shows that the area of H/V study was divided into ten horizontal lines to understand the changes of soil amplification and dominant period comparing with respect to bedrock thickness. Each thickness of sedimentary units overlying bedrock were determined according to Basement Morphology map of Tertiary – Quaternary sediments (Özgül *et al.,* 2005), and contour maps of bedrock depth which belong to OYO for the H/V measurements points. All lines explaining the changes of the values of soil amplification and dominant period compared with respect to bedrock thickness are presented as an graphics (from Figure 7.6 to 7.9). Explanation of these graphics is given in Figure 7.5. Locations of H/V measurement points are not aligned in horizontal direction.

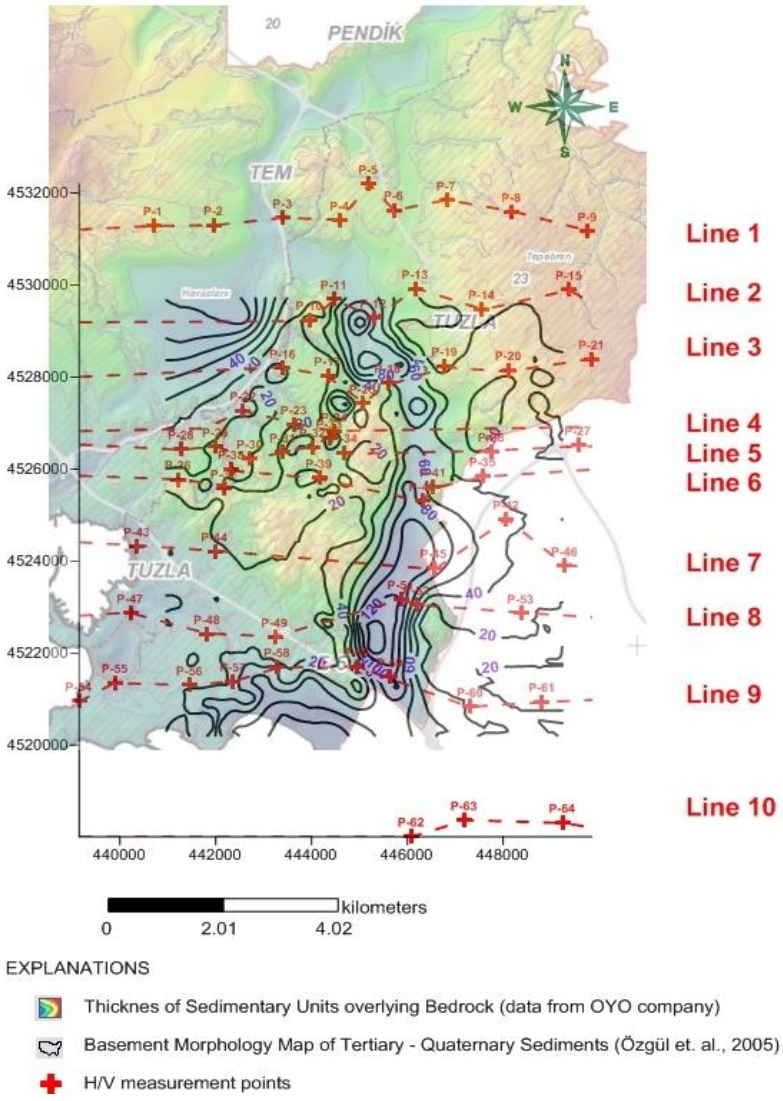

Figure 7.4. Ten horizontal lines over the H/V measurement field

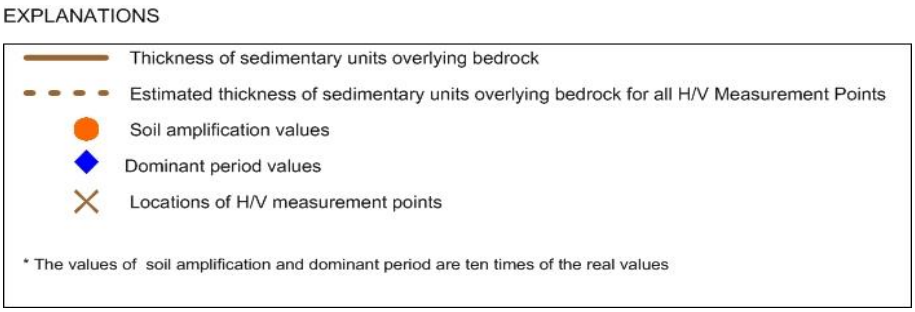

Figure 7.5. Explanations for ten graphics that are given in Figure 7.6 – 7.9

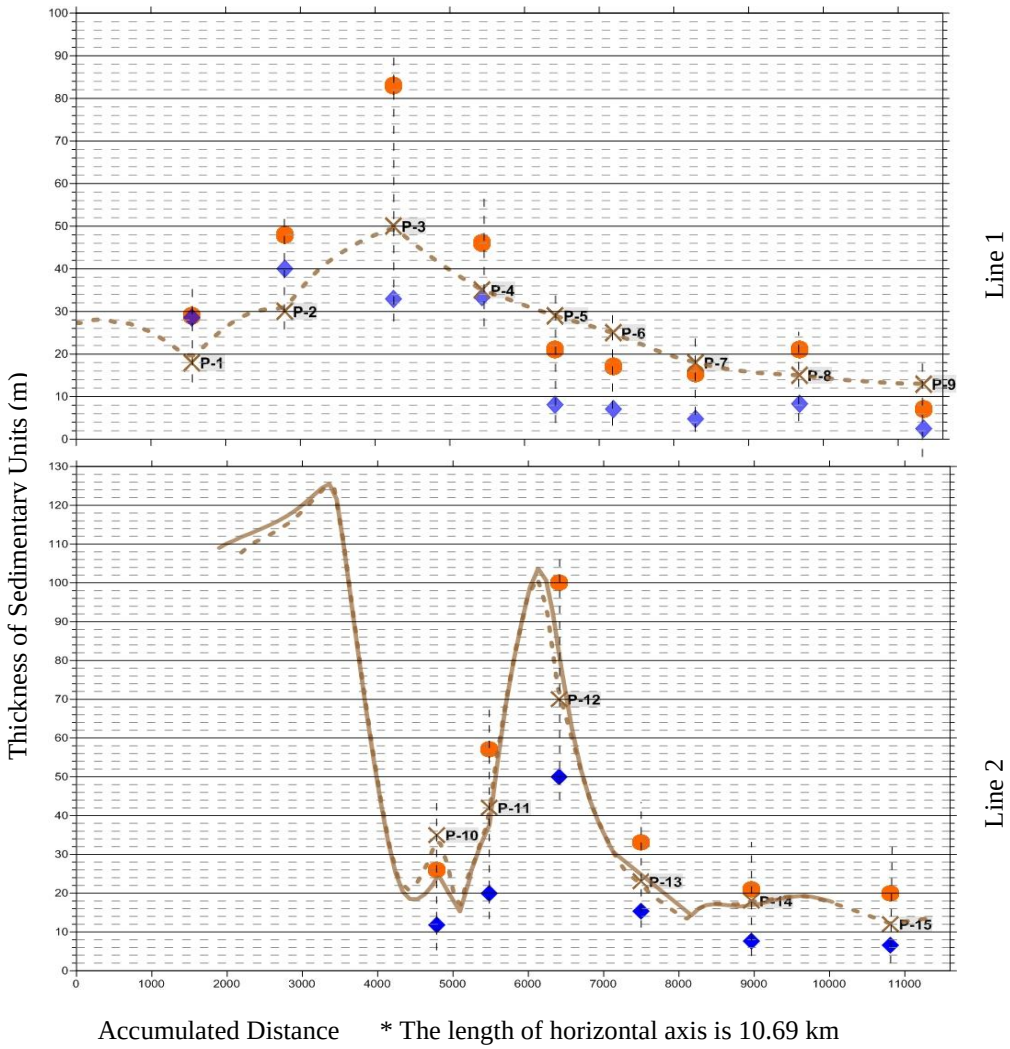

Figure 7.6. Line 1 (top) and 2 (bottom) show the changes of the values of soil amplification and dominant period comparing with respect to bedrock thickness

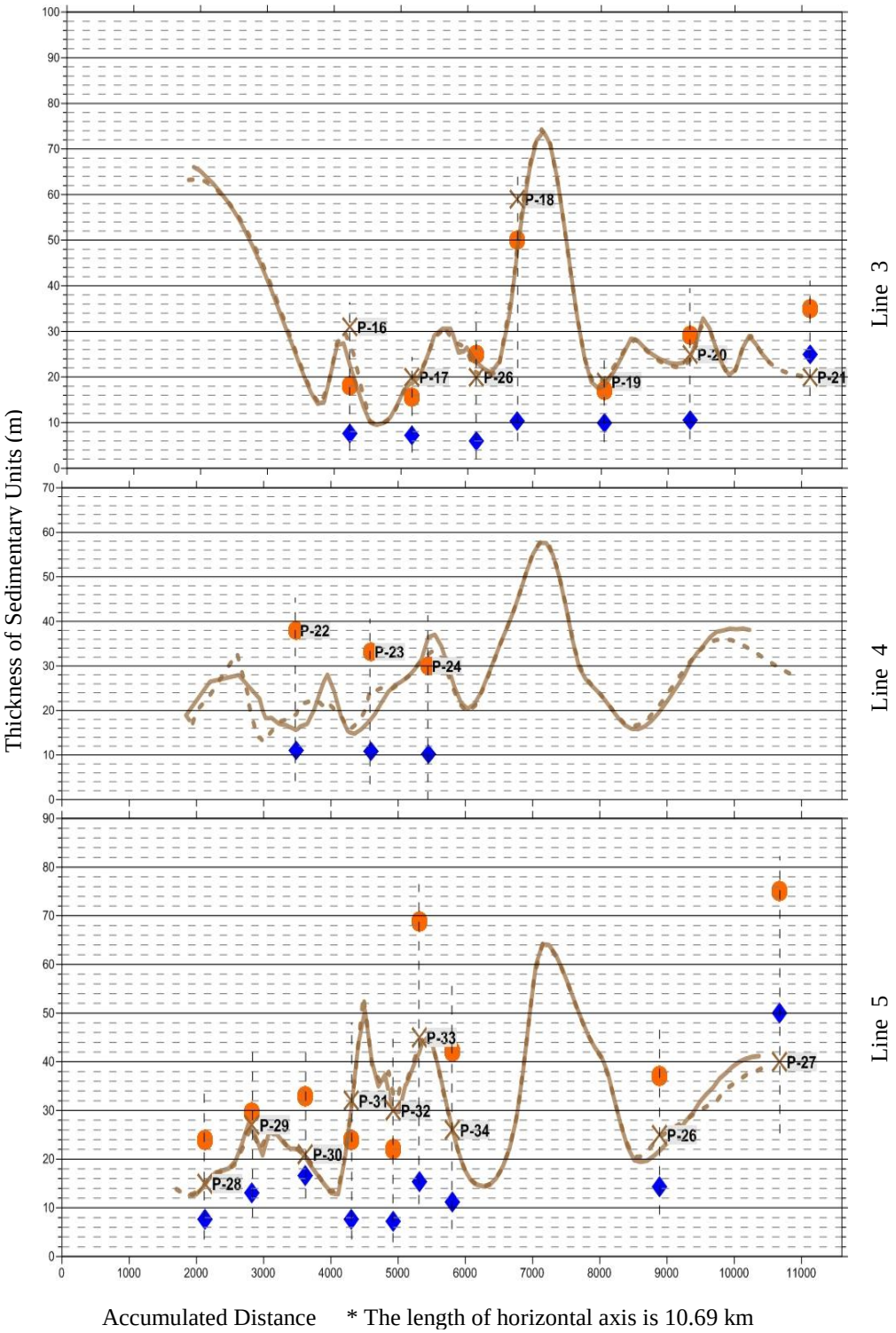

Figure 7.7. Line 3 (top), 4 (middle) and 5 (bottom) show the changes of the values of soil amplification and dominant period comparing with respect to bedrock thickness

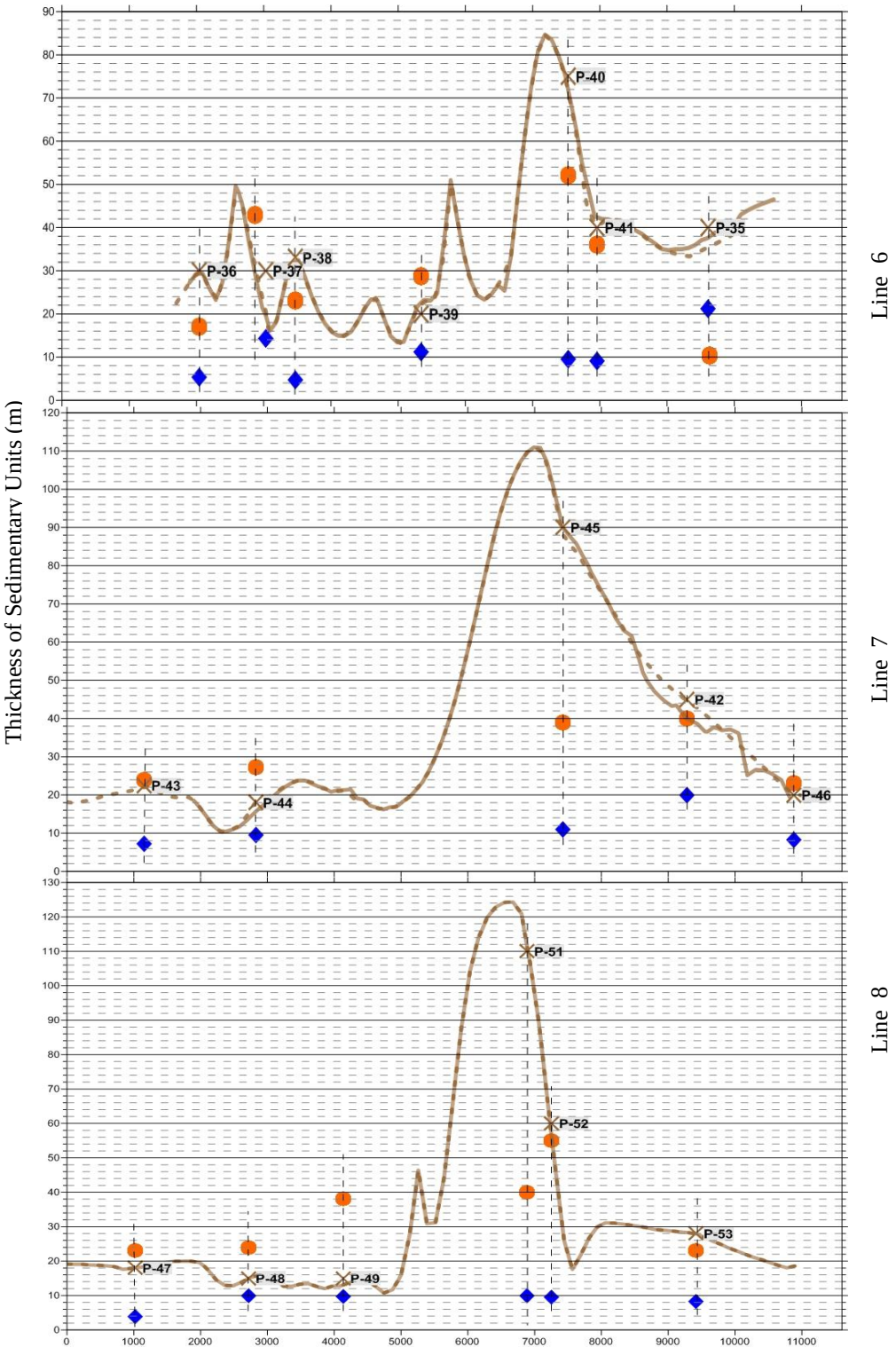

Figure 7.8. Line 6 (top), 7 (middle) and 8 (bottom) show the changes of the values of soil amplification and dominant period comparing with respect to bedrock thickness

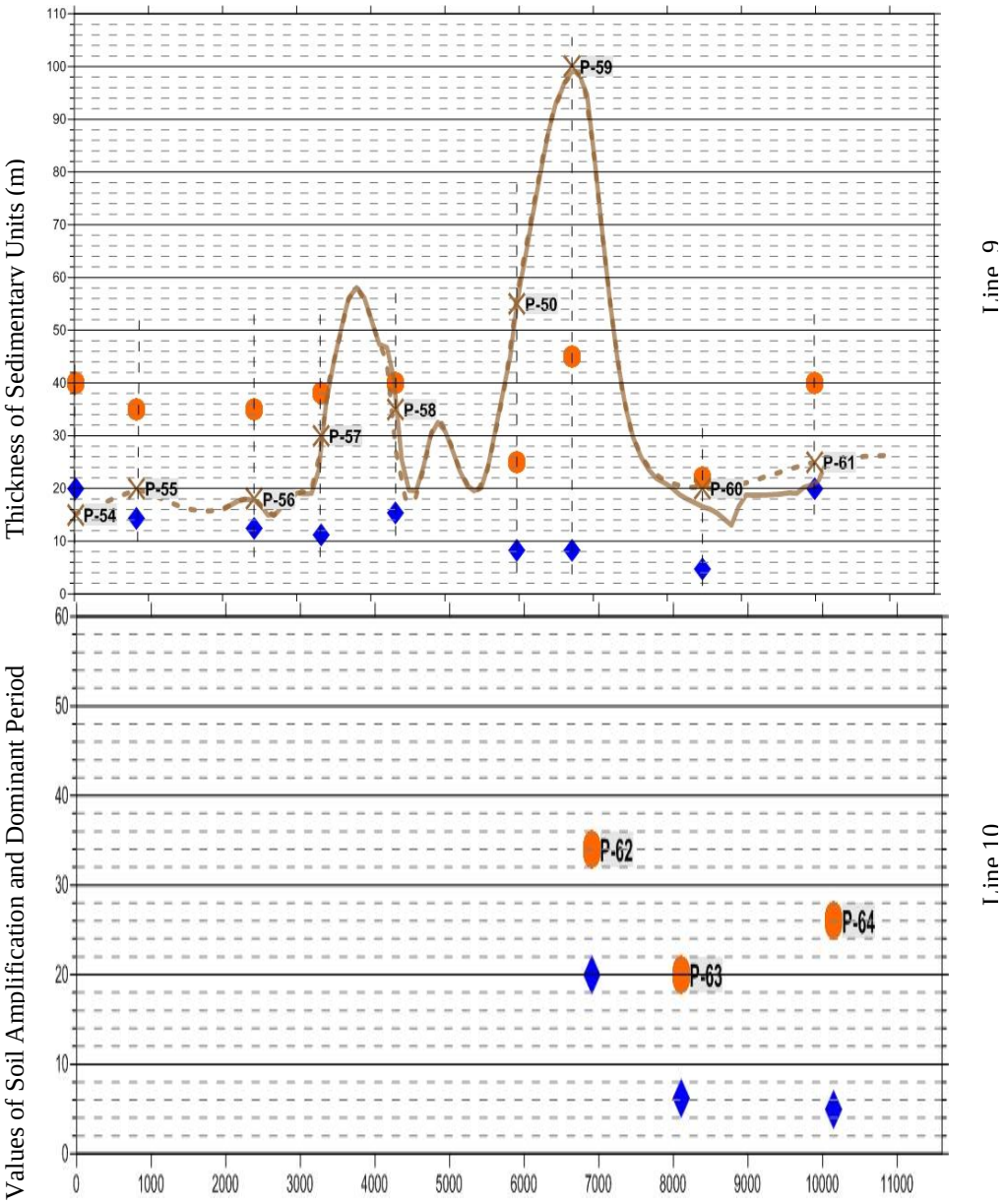

Figure 7.9. Line 9 (top) shows the changes of the values of soil amplification and dominant period comparing with respect to bedrock thickness. Line 10 (bottom) shows only the values of soil amplification and dominant period . Here bedrock thickness is unkown

7.2. The Results of Model Study

Figure 7.10, 7.11 and 7.12 show the distribution of soil amplification, dominant frequency and period values obtained from model study, respectively.

The result of model study indicates that soil amplification values change between 7.-13 values in Aydınlı Region, 7.-16 values in Orhanlı Region and 7.-13 values in south of the study area. Dominant soil periods are greater than 0.4 sec in these areas and dominant frequency are changing between 1.8 - 3.8 Hz in these there regions. We could not estimate site effect values remaining parts of the study area because of inadequate model points.

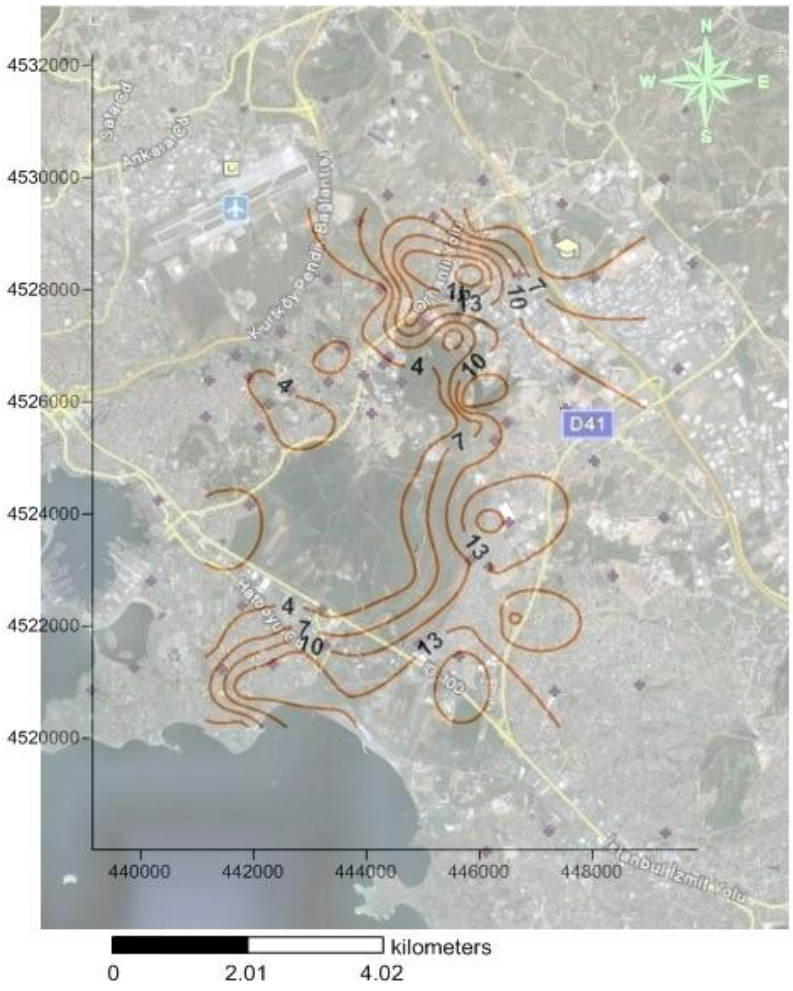

Figure 7.10. Distribution of soil amplification values from model study

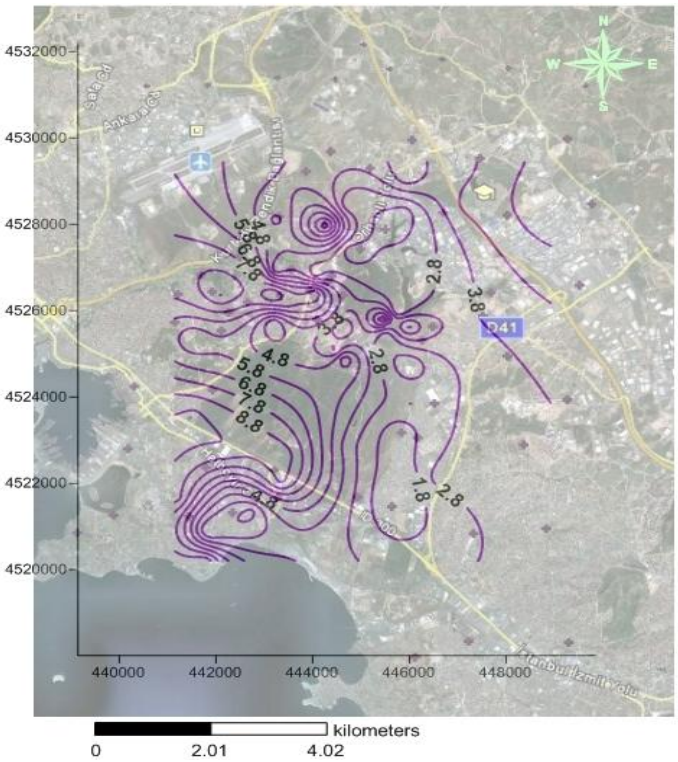

Figure 7.11. Distribution of dominant frequency values from model study

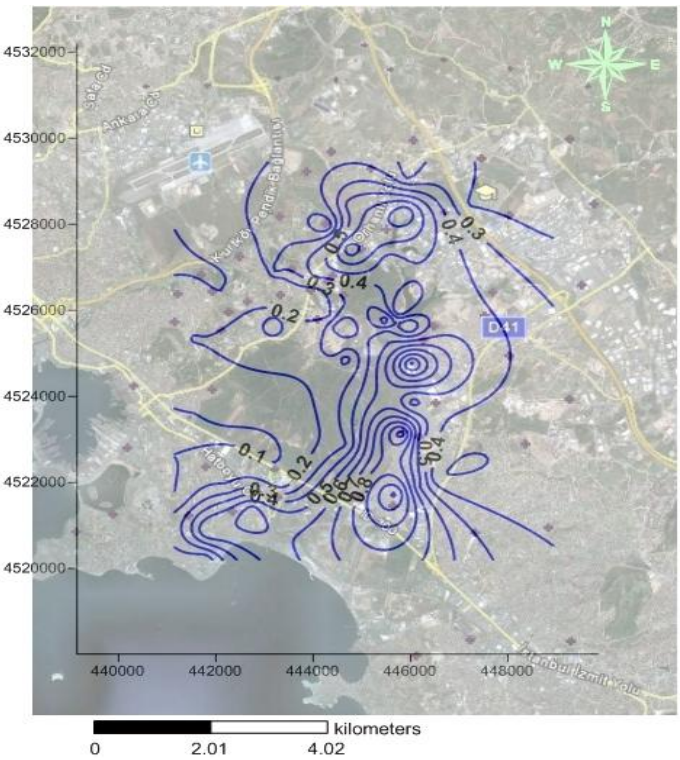

Figure 7.12. Distribution of dominant period values from model study

Figure 7.13 shows that the area of model study was divided into seven horizontal lines and one vertical lines to understand how soil amplification and dominant period are changing with sedimentary thickness. Each thickness of sedimentary units overlying bedrock were determined according contour maps of bedrock depth which belong to OYO Company. All lines explaining the changes of the values of soil amplification and dominant period compared with respect to bedrock thickness are presented as a graphic from Figure 7.15 to 7.17. Explanation of these graphics is given in Figure 7.14. Locations of Model measurement points are not aligned in horizontal direction.

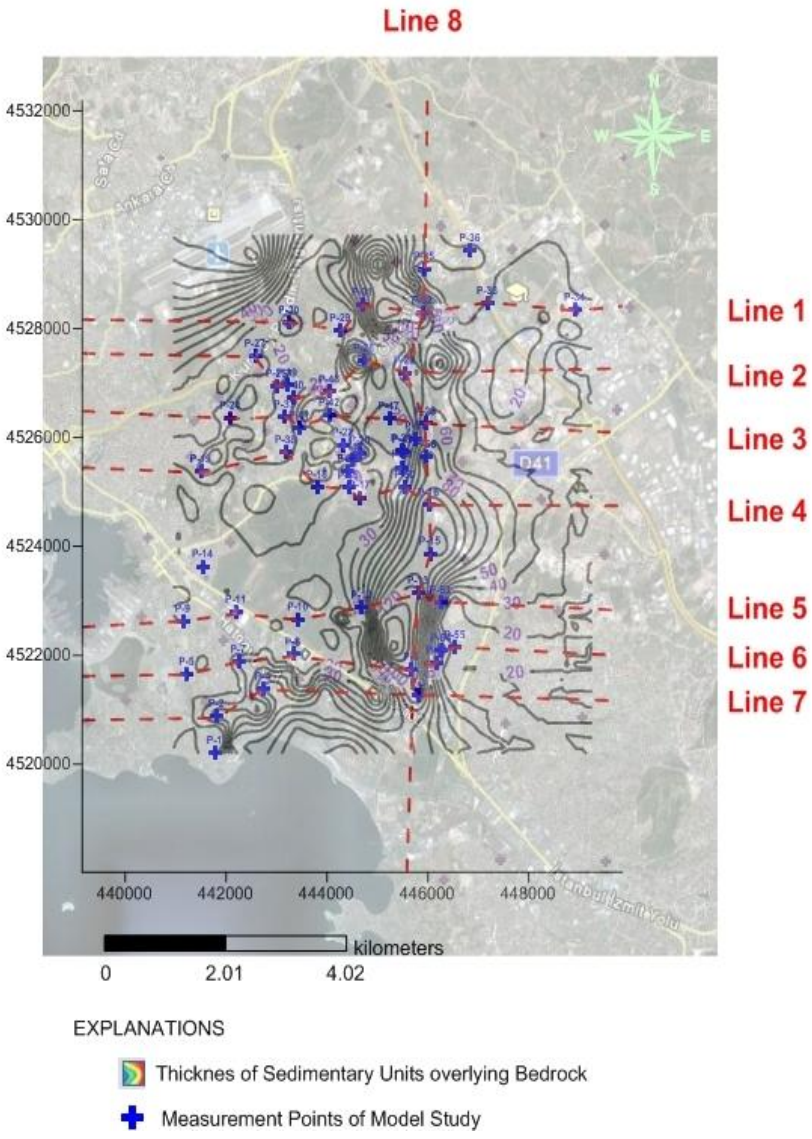

Figure 7.13. Eight lines over the field of model measurement

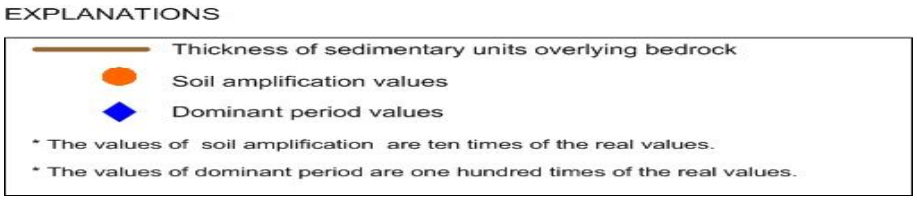

Figure 7.14. Explanations for eight graphics that are given in Figure 7.15 – 7.17

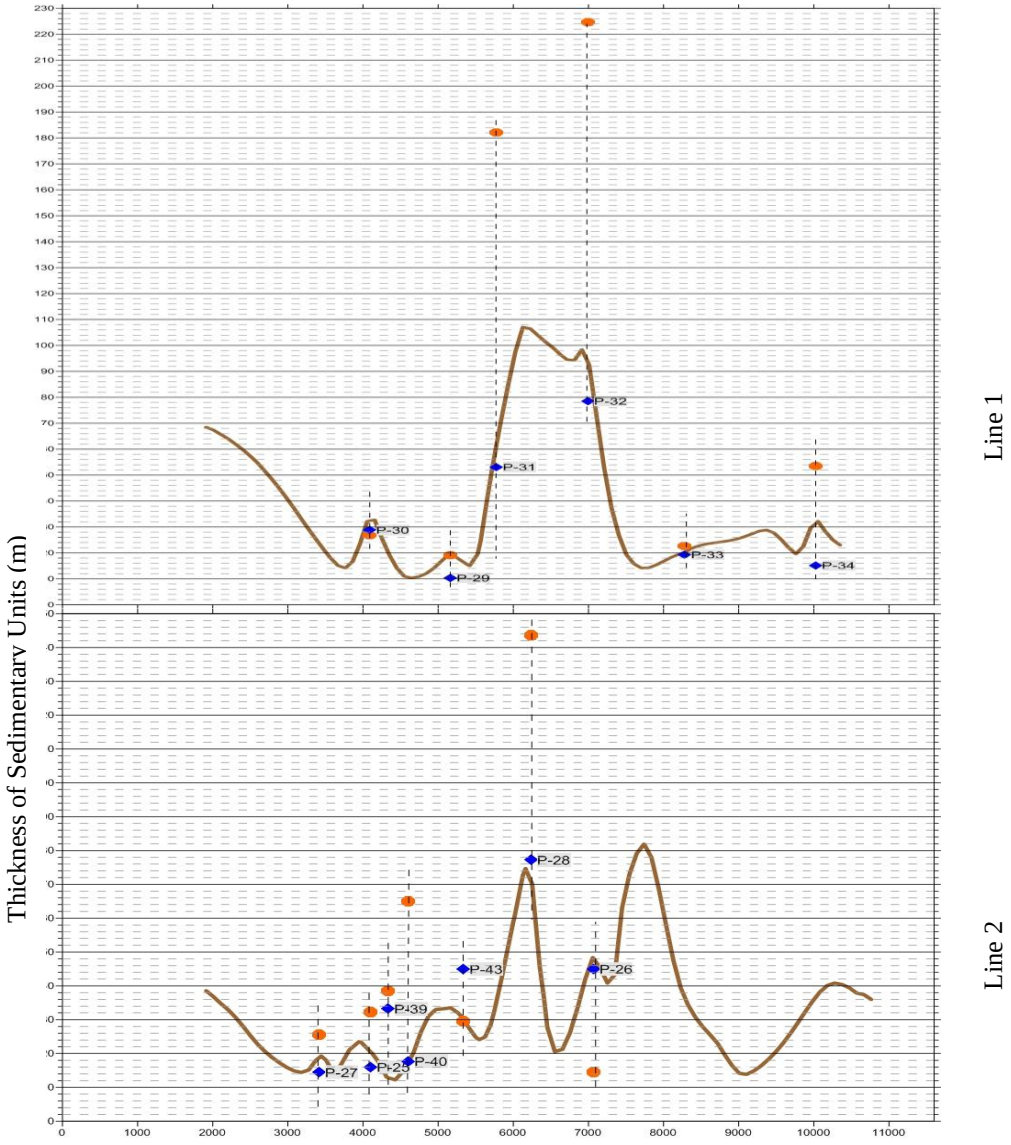

Figure 7.15. Line 1 (top) and 2 (bottom) show the changes of the values of soil amplification and dominant period comparing with respect to bedrock thickness

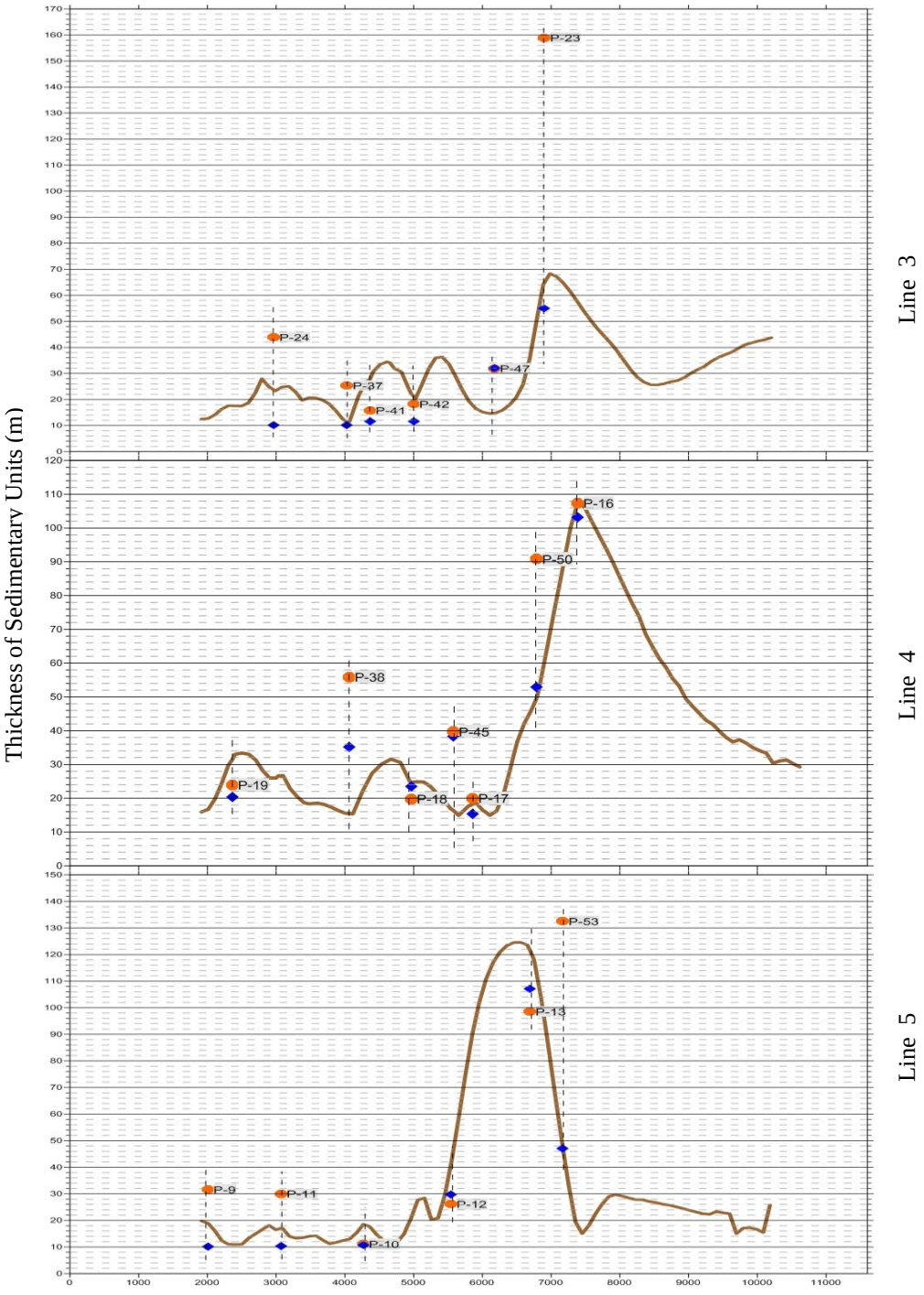

Figure 7.16. Line 3 (top), 4 (middle) and 5 (bottom) show the changes of the values of soil amplification and dominant period comparing with respect to bedrock thickness

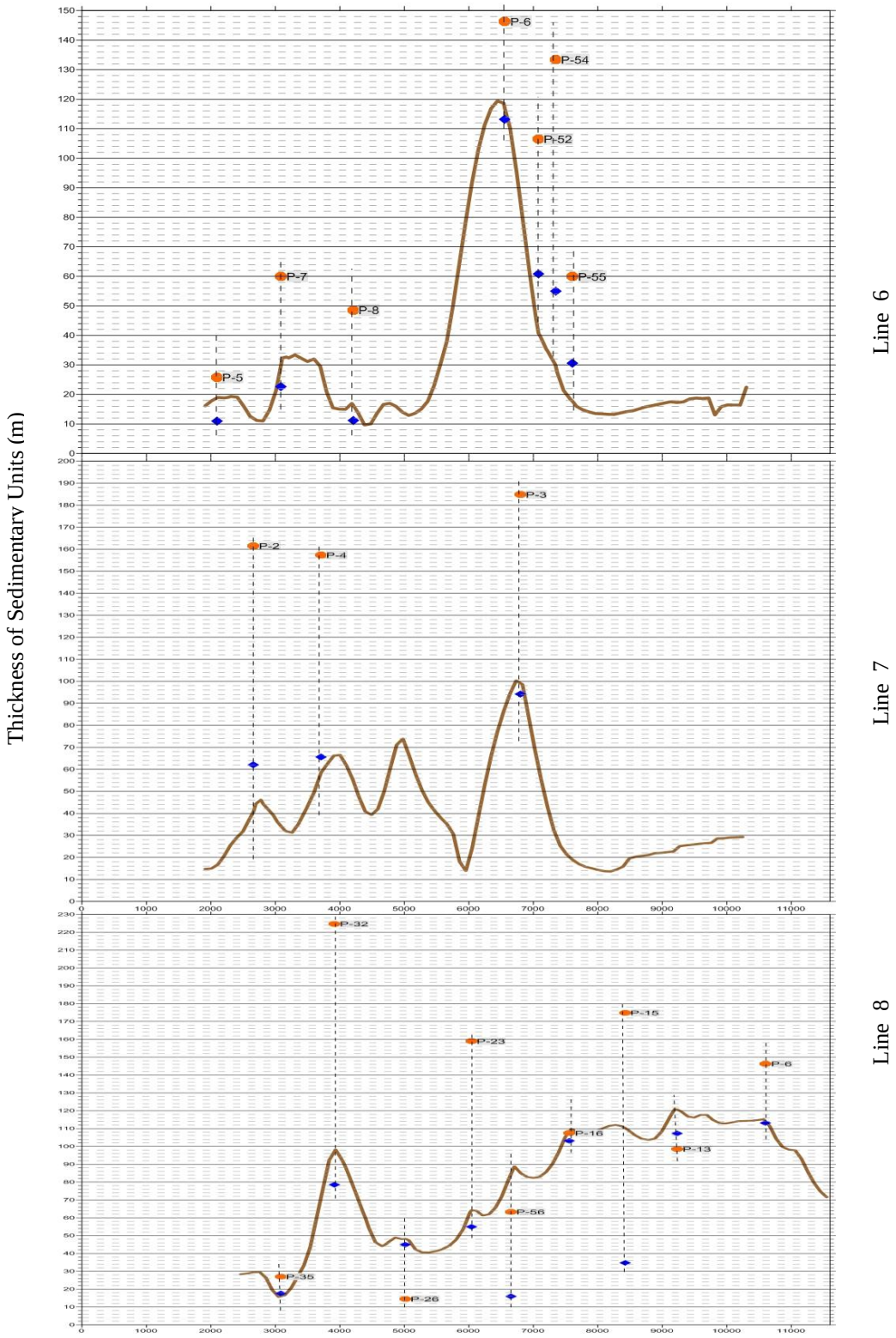

Figure 7.17. Line 6 (top), 7 (middle) and 8 (bottom) show the changes of the values of soil amplification and dominant period comparing with respect to bedrock thickness

8. DISCUSSION AND CONCLUSION

Our results have significant implications for the Tuzla–Pendik study areas. Both H/V microtremor study and model study indicate that highest amplification values are estimated in three regions, Orhanlı, Aydınlı and south of the study area. According to geological structure of these three areas, approximately up to 120 m thickness of Cenozoic formations, Kuşdili and Sultanbeyli formations, overlying the bedrock formations play important role in the increase of soil amplification values. We think that strong amplification are seen in these regions because of thick and soft structure of Kuşdili and Sultanbeyli formations. Figure 8.1 shows the distrubution of soil amplification, dominant frequency and period obtaining from both studies according to Basement Morphology map of Tertiary – Quaternary sediments .

H/V study is known that its soil amplification values were high due to the vertical motion records which were also affected by local geological conditions. In this study, the highest amplification value is 10 in Orhanlı region.

Furthermore, the values of site amplification estimated by using the Shake program for model study were higher than those estimated by the microtremor method. The reason for this discrepancy may be due to density, damping values are obtained by empirical values and interpretation made by not taking environmental effects and not considering topography of the bedrock. Highest soil amplification value is estimated by model study as 22 in the Orhanlı region.

On the other hand, the lowest estimated amplification from H/V study is obtained in northeast, southeast and west site of the study areas. These sites consist of approximately 20 m thickness of sedimentary units above the bedrock formations and some site of these areas bedrock lying down as outcrop, and thus we determined that these sites have better ground properties. The result of model study gives district information about these remaining areas because of absence of H/V measurement points.

Soil dominant period values obtained from H/V study in especially Orhanlı region and north of the study site were found much more bigger than other two regions, Aydınlı and south of the study site. According to model studies, the highest fundamental period approximately changing from 0.4 to 1. sec were estimated in Aydınlı, Orhanlı and South of site.

When we compared our results in the Abduş Lake area with the results of Kurtuluş *et al.,* (2008), soil amplification and dominant period had been calculated as 3.3 unit and 0.79 sec, respectively. A good agreement between soil amplifications are found, but dominant ground period values are estimated as much lower than our studies. According to our H/V study, dominant ground period are changing from 1. to 1.4 sec. The dominant frequency values in the studies of Zülfikar *et al*., (2007), Birgören and Özel, (2006) and Birgören *et al*., (2008) are similar to the values in our study. Table 8.1 shows the comparison of values between our studies and mentioned studies.

Based on the above discussions it is clear that both the thickness of Cenozoic sedimentary layers overlying Paleozoic bedrocks and these layers' dynamic soil properties, "shear wave velocity, damping ratios and density" play significant role in the maximum soil amplification and the fundamental soil period and frequency. The fact that soil layers above the bedrock will amplify the frequency interval of an earthquake wave has much more influence on the site effect. This circumstance is important to construct earthquake – resistant buildings. A rise in seismic vulnerability, resonance effect, will be done when the fundamental period of structures are very close to the soil fundamental period. This fact seems to be dangerous in disaster mitigation point of view.

Table 8.1. Comparison between our studies and other three studies

Researchers	Location of Their Studies	Soil Amplification	Dominant Frequency (Hz)	Dominant Period (sec)	Our Studies
Kurtuluş *et al.* , (2008)	around the Abduş Lake	**3.3**	**1.26**	**0.79**	
		2.7 - 3.7	0.71 - 1.0	1.0 - 1.4	H/V Study
Zülfikar *et al.*, (2007) Birgören and Özel, (2006) Birgören et *al.* , (2008)	R 44 - ITFTU		**3.0 - 5.0**		
			4.9		Model Study
	R 59 - TUMEZ		**2.0 - 3.0**		
			2.8		Model Study
	R 12 - TUZAL		**1.5**		
			1.1		H/V Study

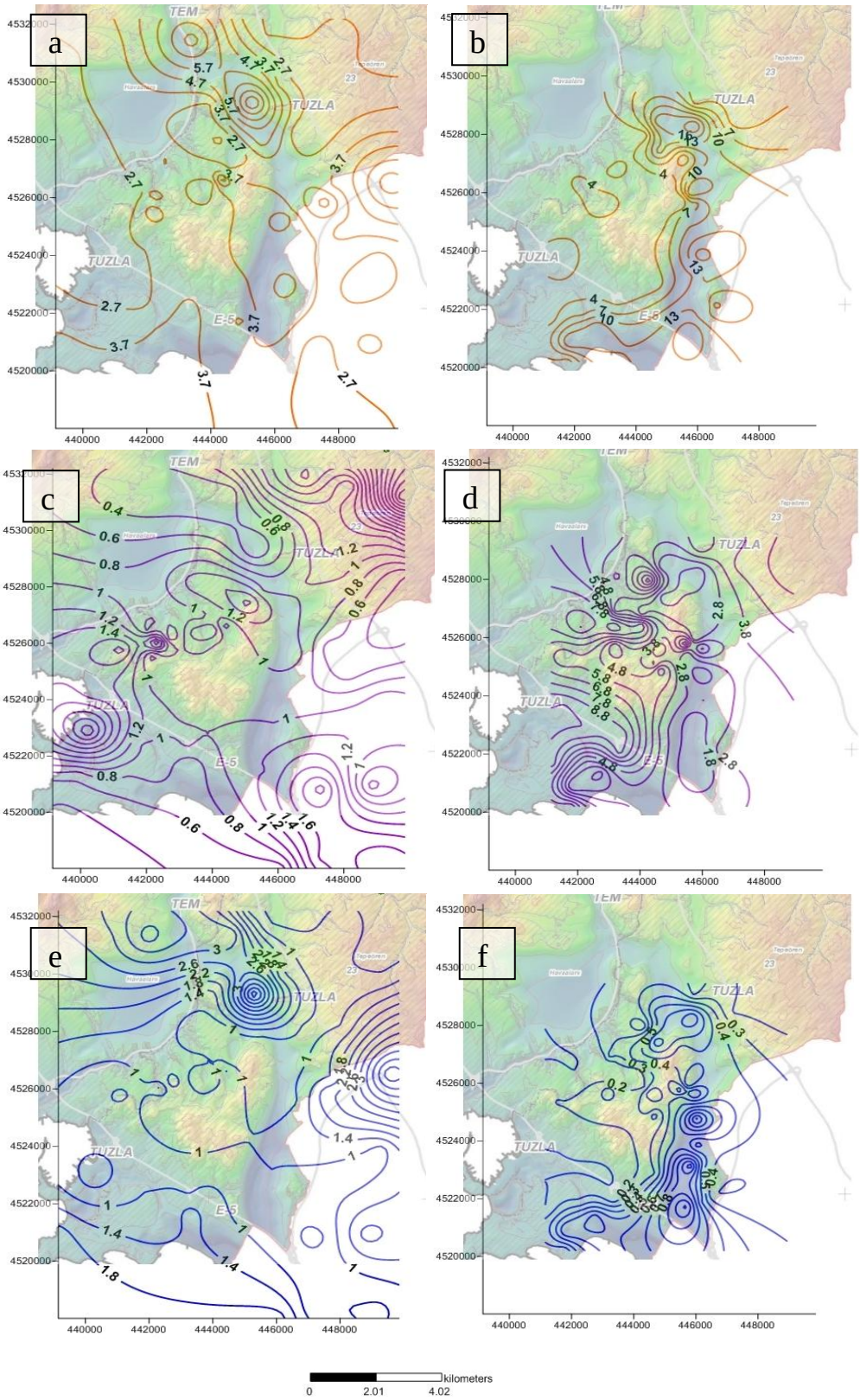

Figure 8.1. The distribution of soil amplification (a, b), dominant frequency (c,d) and period (e,f) obtaining from H/V and model studies, respectively according to basement morphology map is given by Özgül *et al.*, 2005

APPENDIX A: H/V SPECTRUM

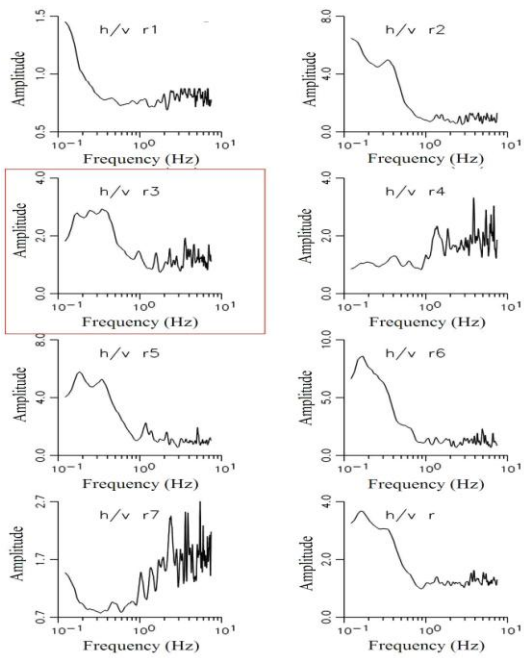

Point - 1. Parzen window with bandwidth of 19

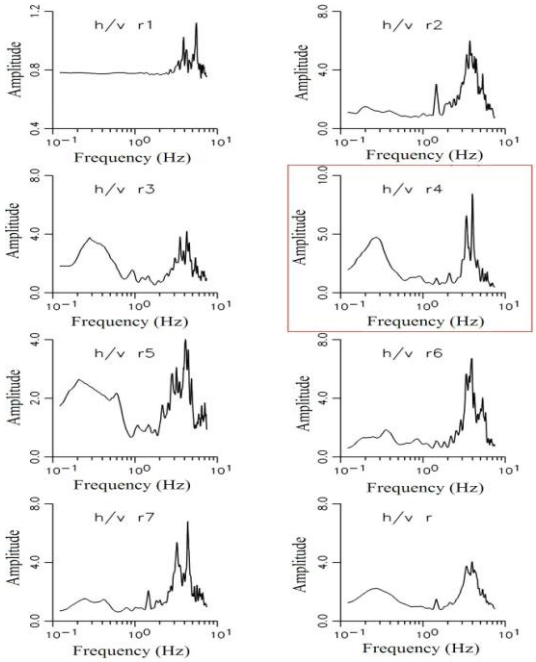

Point - 2. Parzen window with bandwidth of 19

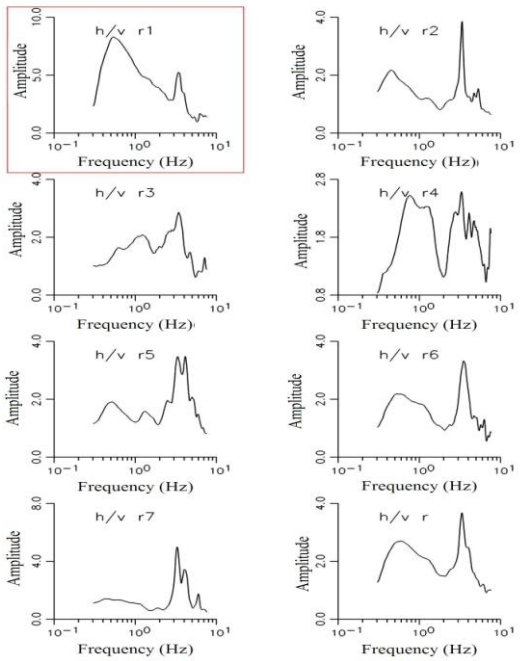

Point – 3. Parzen window with bandwidth of 49

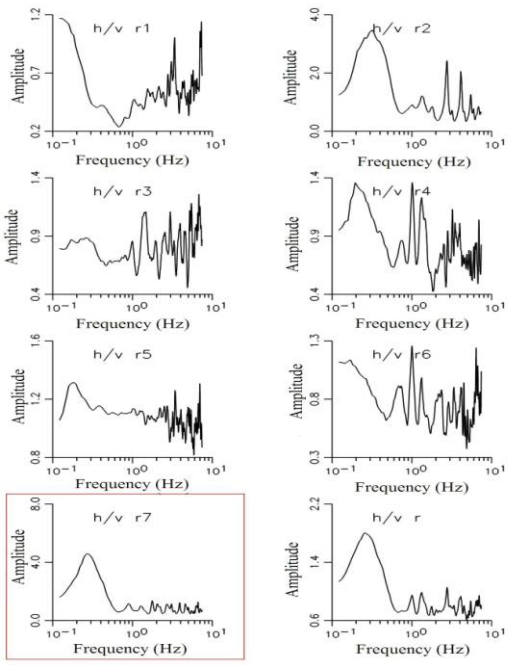

Point – 4. Parzen window with bandwidth of 19

Figure A.1. H/V spectra of points 1- 4

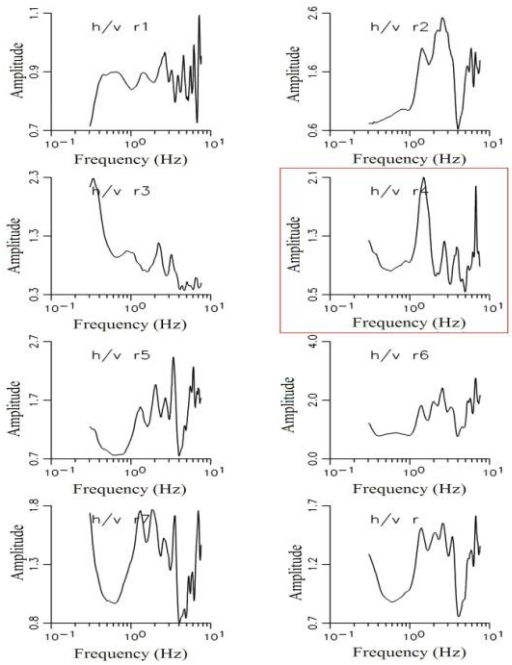

Point – 5. Parzen window with bandwidth of 49

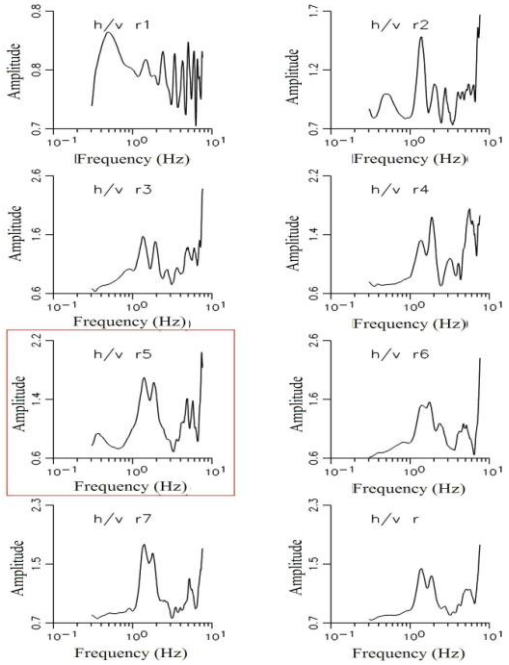

Point – 6. Parzen window with bandwidth of 49

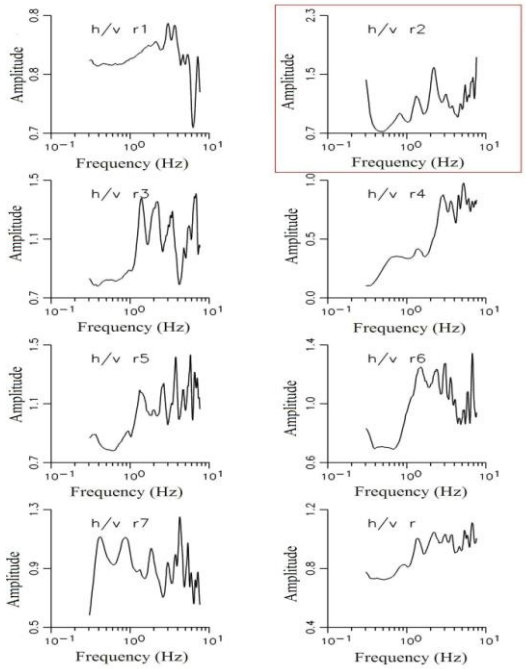

Point – 7. Parzen window with bandwidth of 49

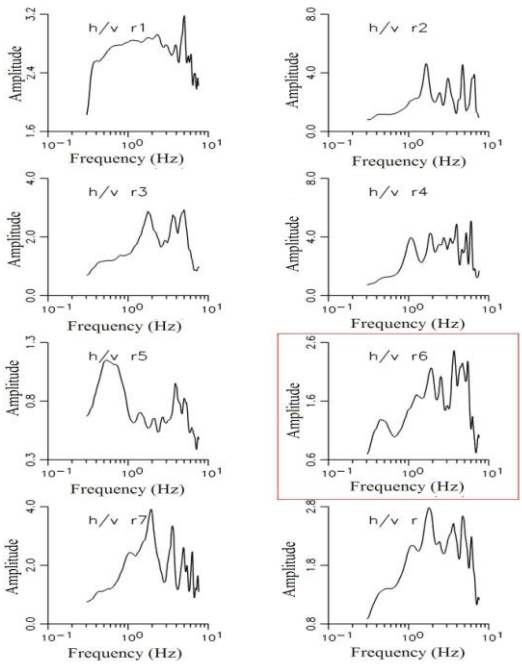

Point – 8. Parzen window with bandwidth of 49

Figure A.2. H/V spectra of points 5 - 8

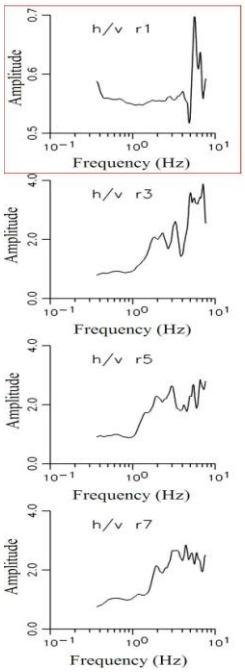

Point – 9. Parzen window with bandwidth of 60

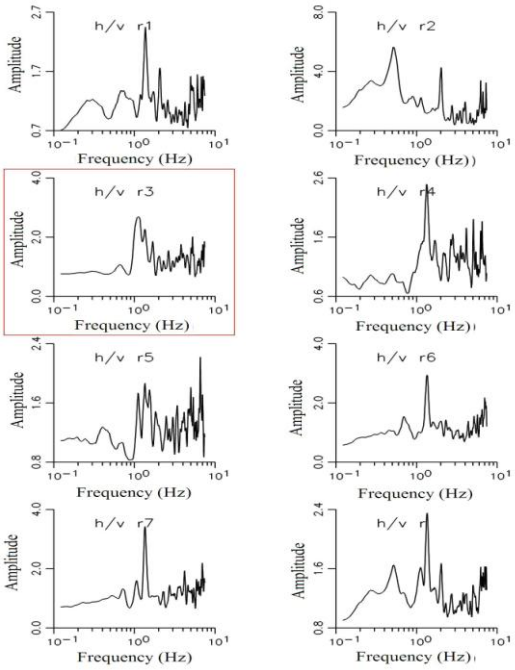

Point – 10. Parzen window with bandwidth of 19

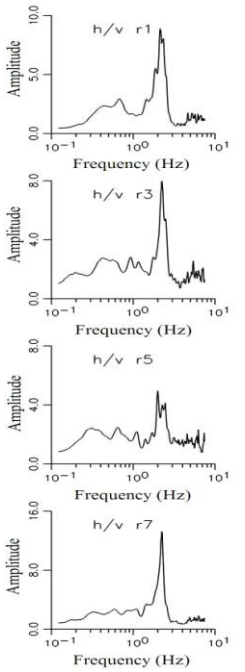

Point – 11. Parzen window with bandwidth of 19

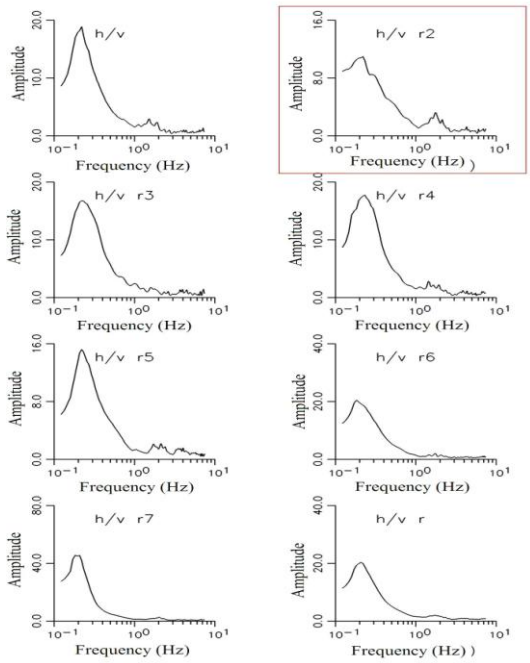

Point – 12. Parzen window with bandwidth of 19

Figure A.3. H/V spectra of points 9-12

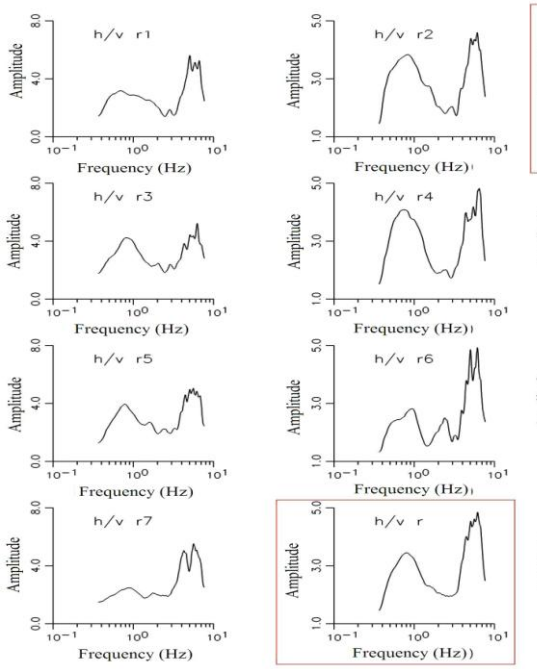

Point – 13. Parzen window with bandwidth of 60

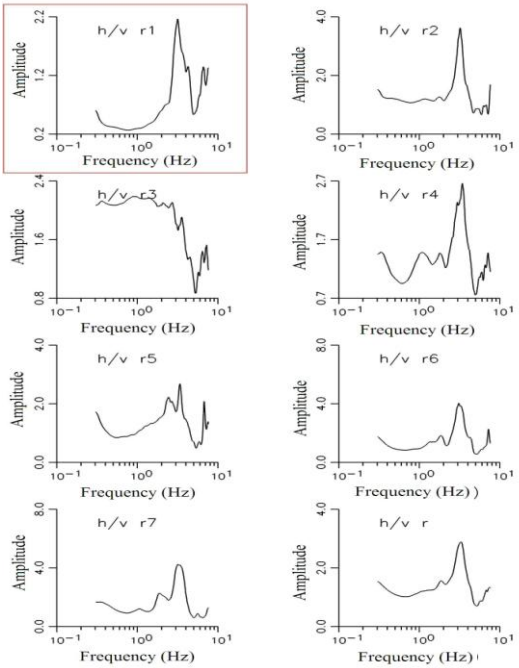

Point – 14. Parzen window with bandwidth of 49

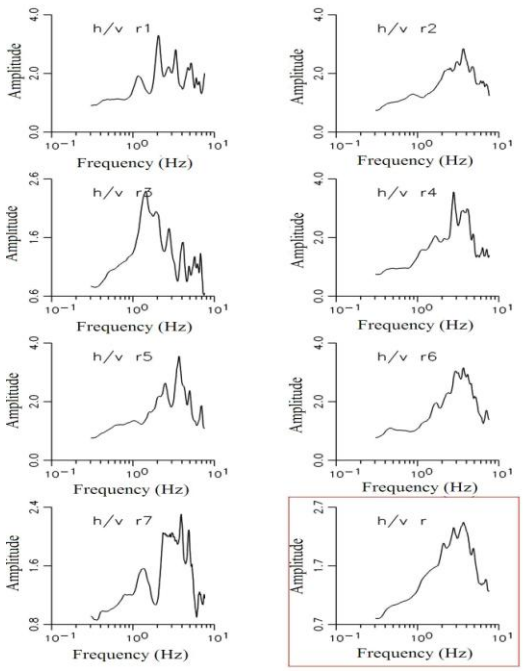

Point – 15. Parzen window with bandwidth of 49

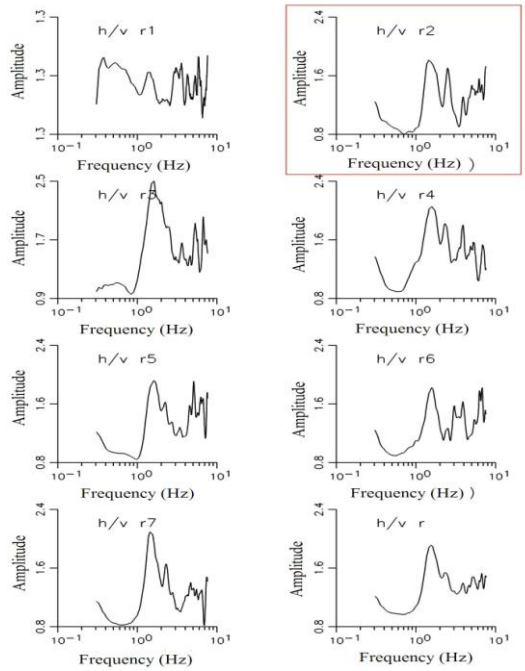

Point – 16. Parzen window with bandwidth of 49

Figure A.4. H/V spectra of points 13 - 16

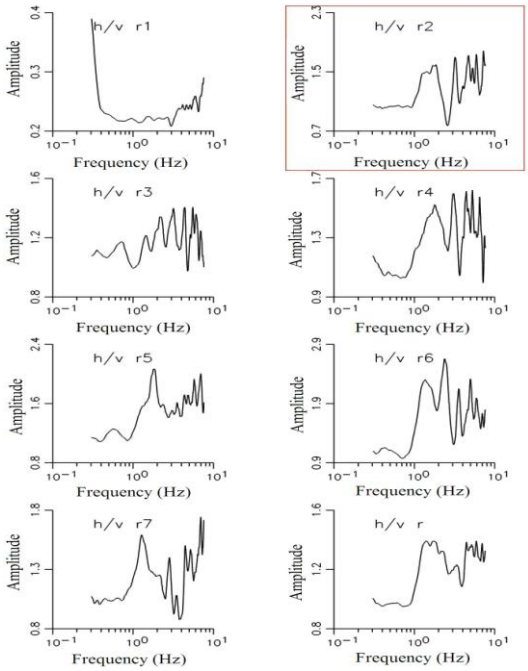

Point – 17. Parzen window with bandwidth of 49

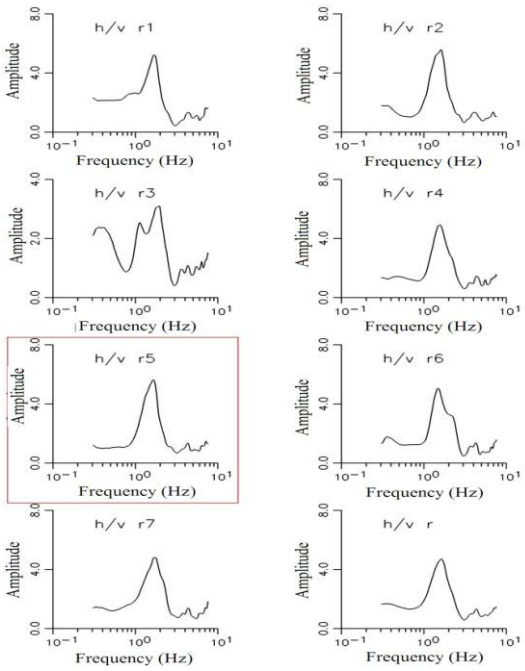

Point – 18. Parzen window with bandwidth of 49

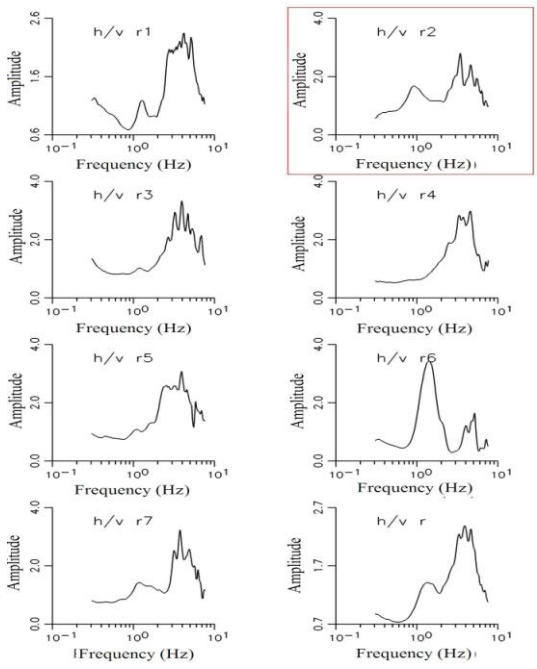

Point – 19. Parzen window with bandwidth of 49

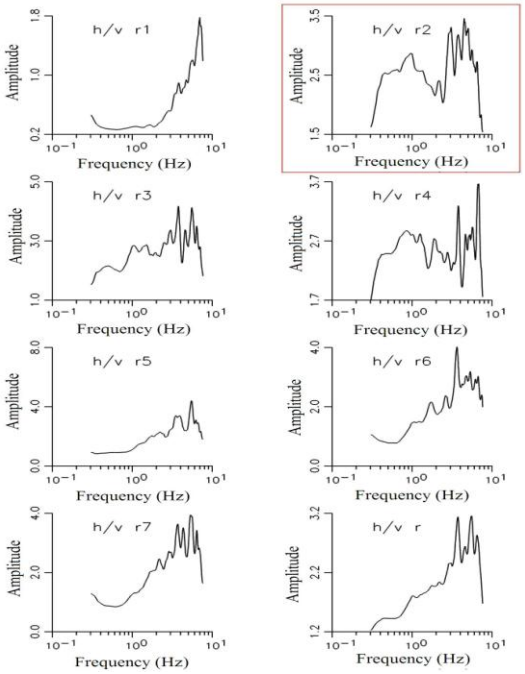

Point – 20. Parzen window with bandwidth of 49

Figure A.5. H/V spectra of points 17 - 20

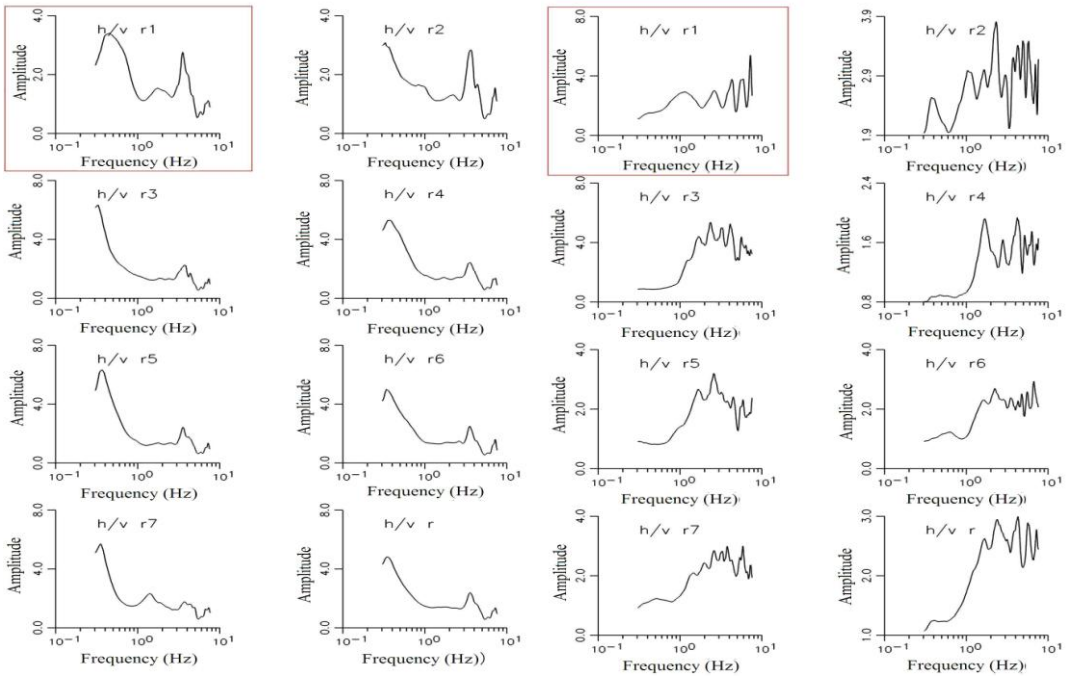

Point – 21. Parzen window with bandwidth of 49

Point – 22. Parzen window with bandwidth of 49

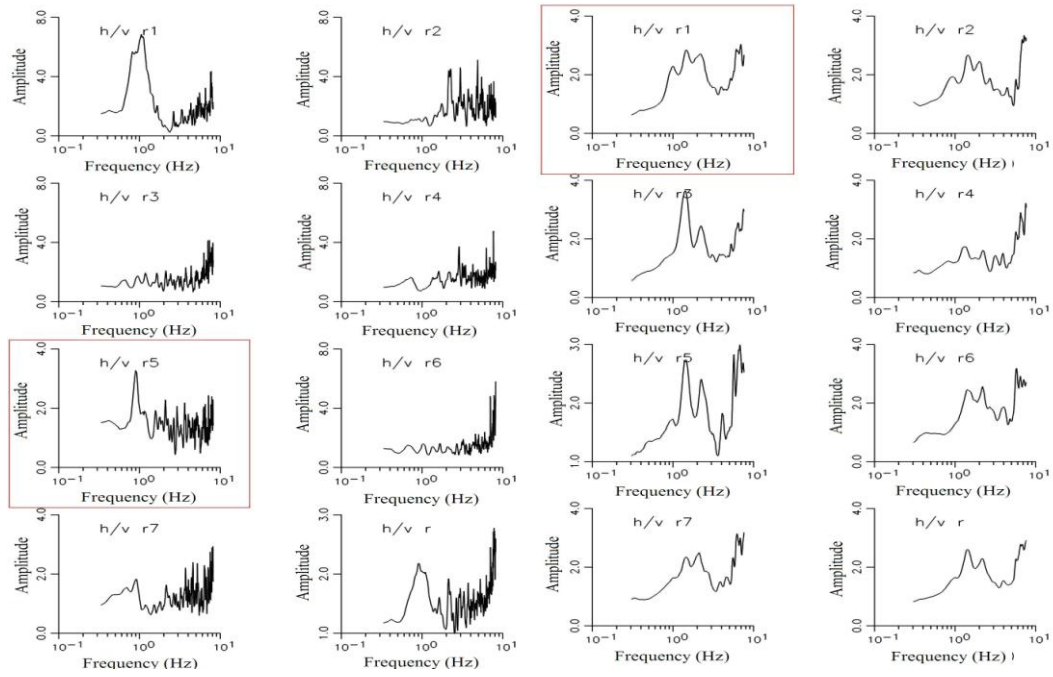

Point – 23. Parzen window with bandwidth of 9

Point – 24. Parzen window with bandwidth of 49

Figure A.6. H/V spectra of points 21 - 24

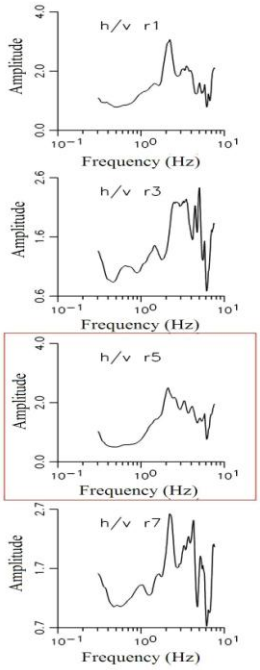

Point – 25. Parzen window with bandwidth of 49

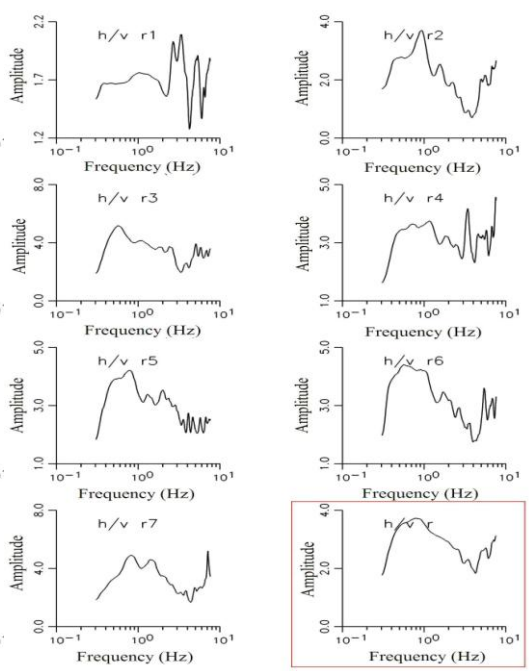

Point – 26. Parzen window with bandwidth of 49

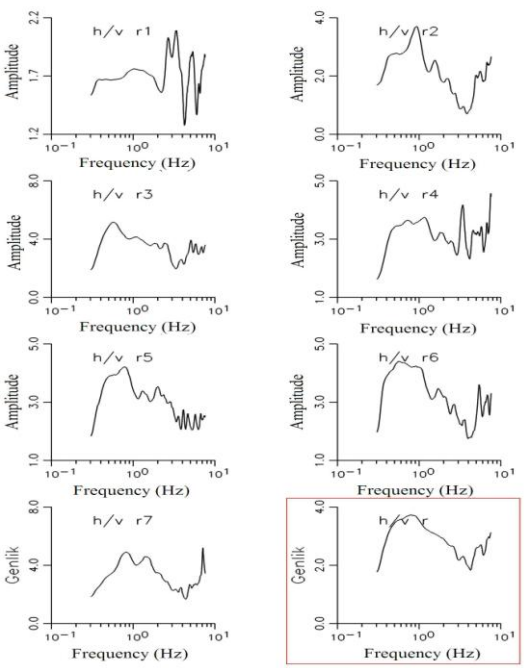

Point – 27. Parzen window with bandwidth of 49

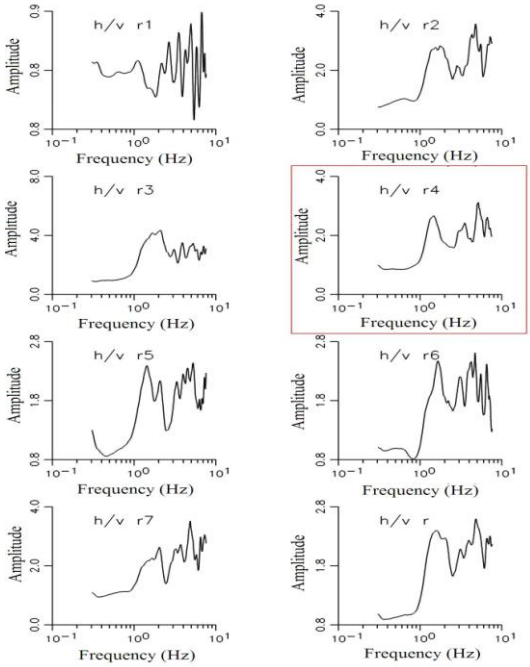

Point – 28. Parzen window with bandwidth of 49

Figure A.7. H/V spectra of points 25 - 28

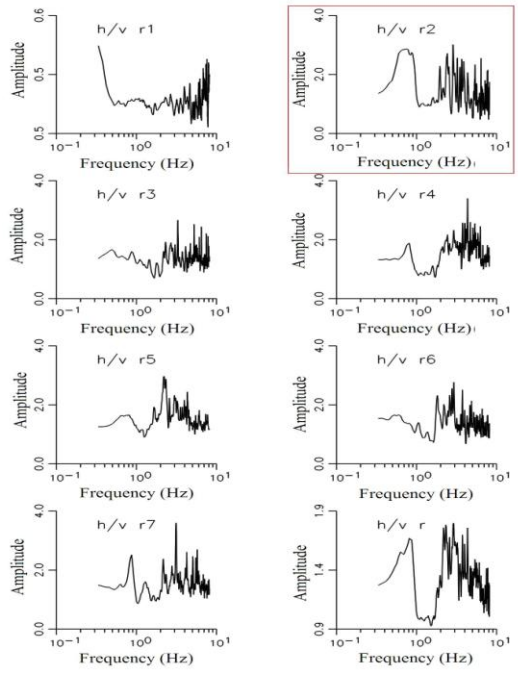

Point – 29. Parzen window with bandwidth of 9

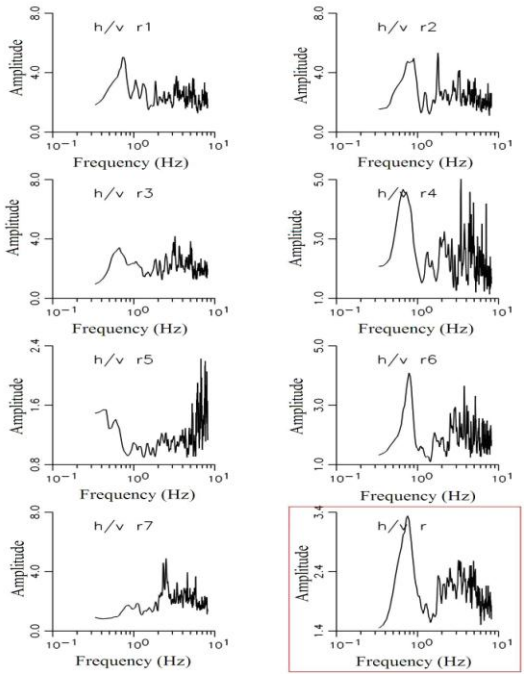

Point – 30. Parzen window with bandwidth of 9

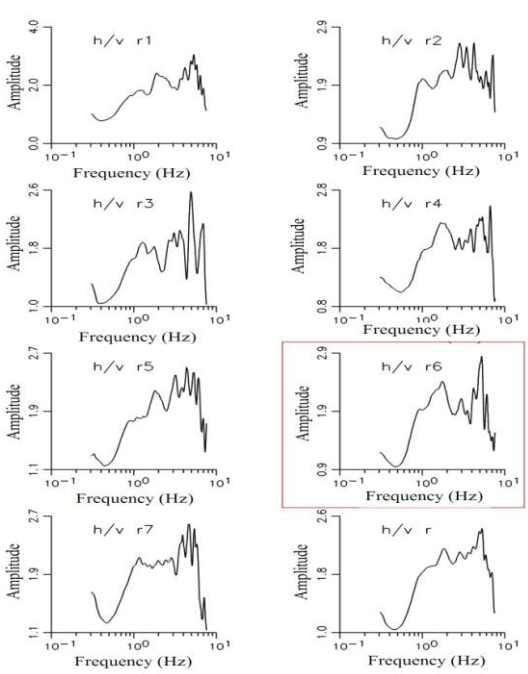

Point – 31. Parzen window with bandwidth of 49

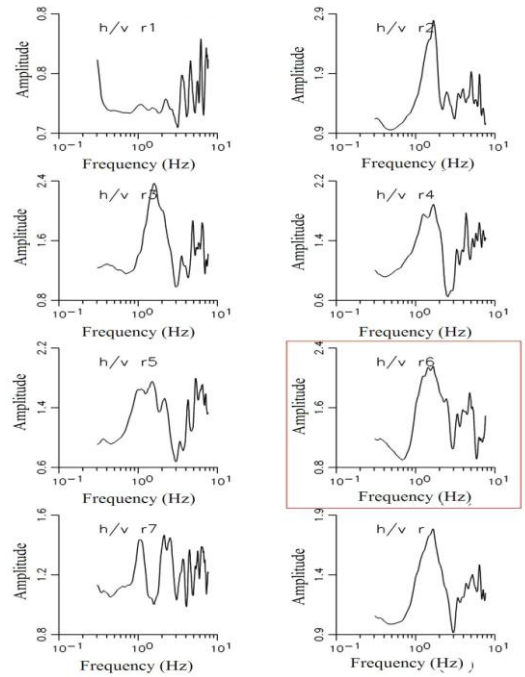

Point – 32. Parzen window with bandwidth of 49

Figure A.8. H/V spectra of points 29 - 32

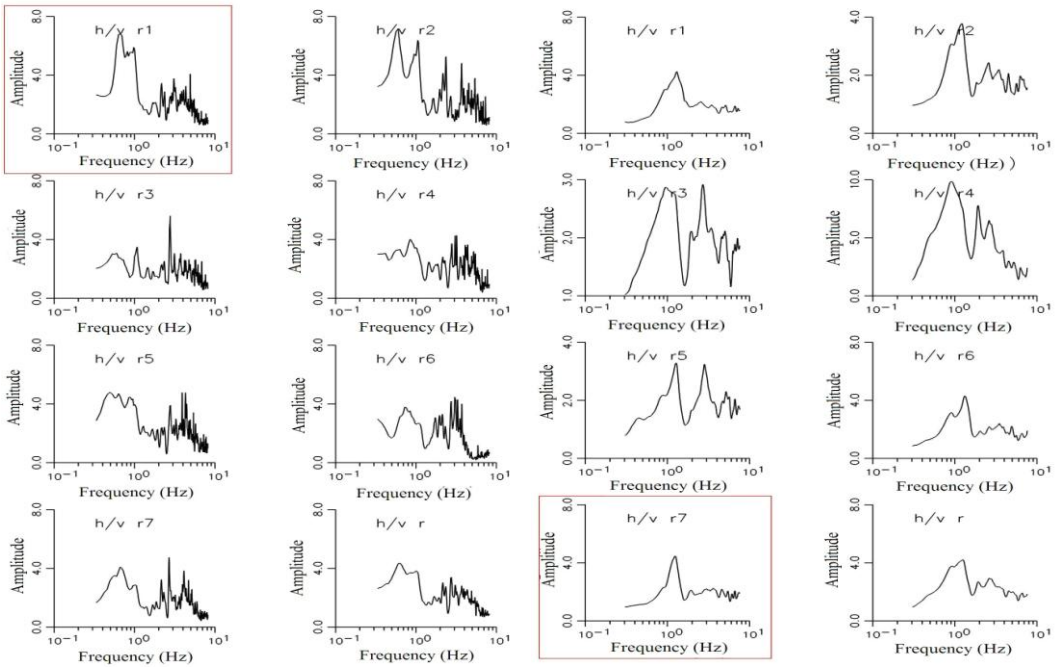

Point – 33. Parzen window with bandwidth of 9

Point – 34. Parzen window with bandwidth of 49

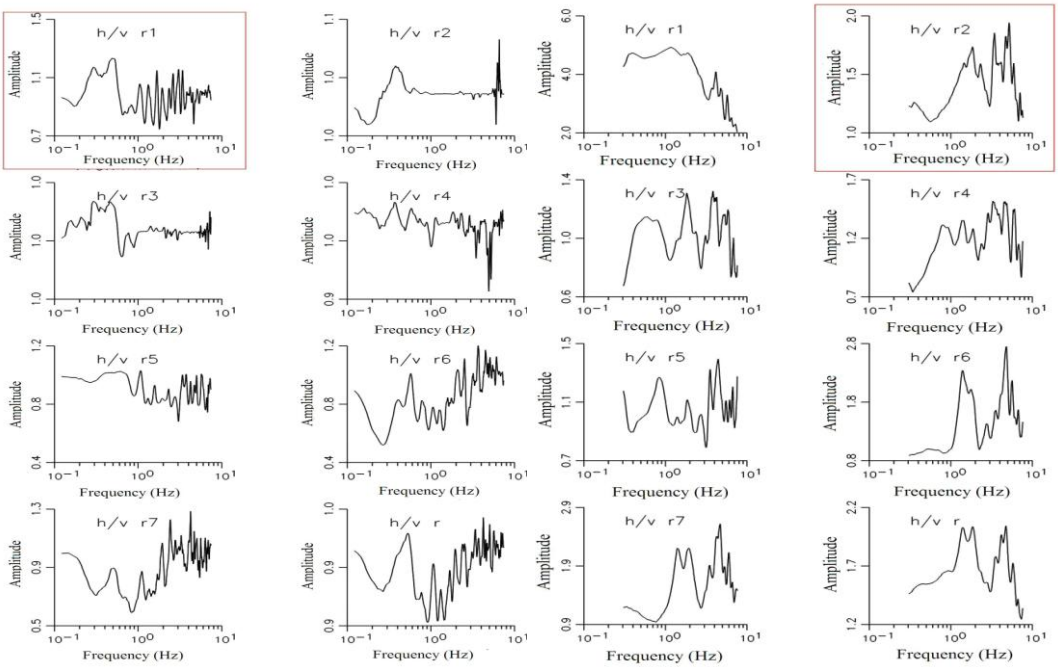

Point – 35. Parzen window with bandwidth of 19

Point – 36. Parzen window with bandwidth of 49

Figure A.9. H/V spectra of points 33 - 36

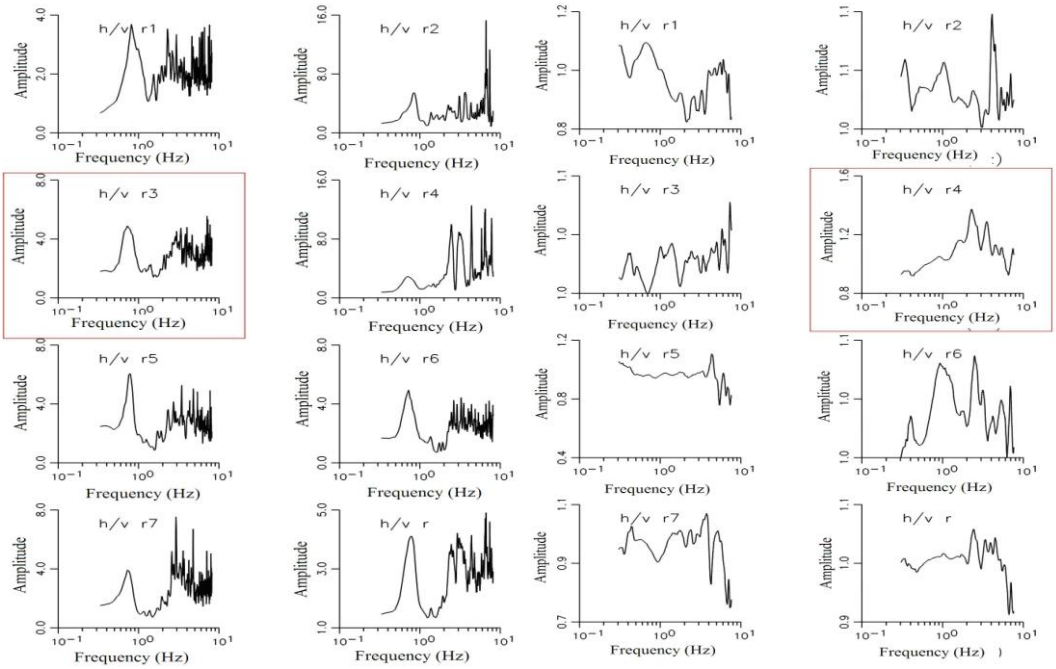

Point – 37. Parzen window with bandwidth of 9

Point – 38. Parzen window with bandwidth of 49

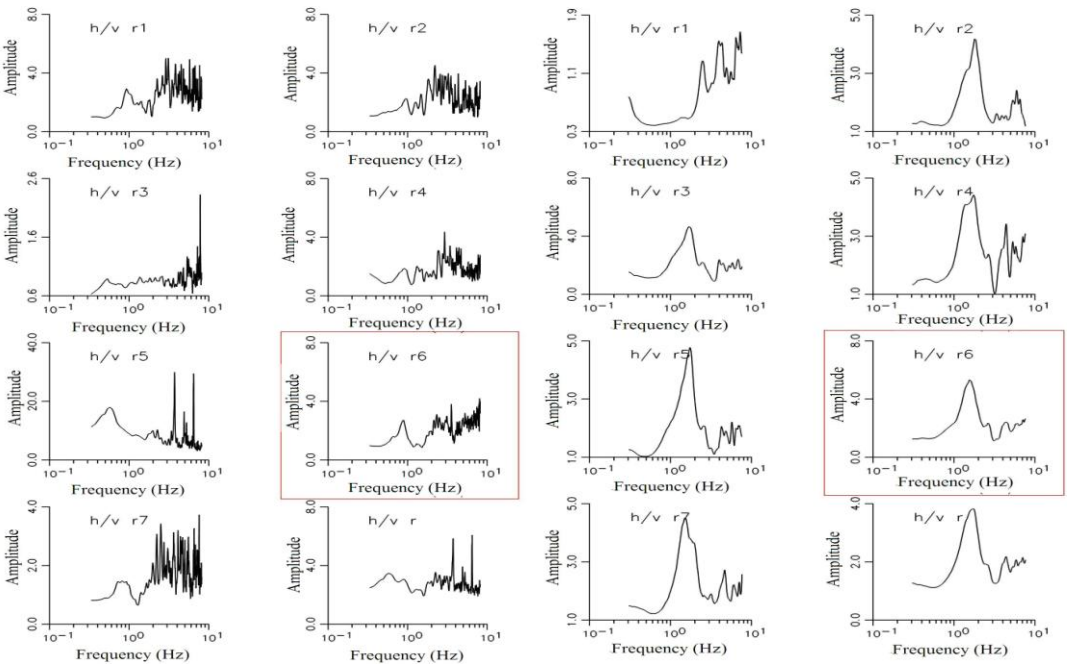

Point – 39. Parzen window with bandwidth of 9

Point – 40. Parzen window with bandwidth of 49

Figure A.10. H/V spectra of points 37 - 40

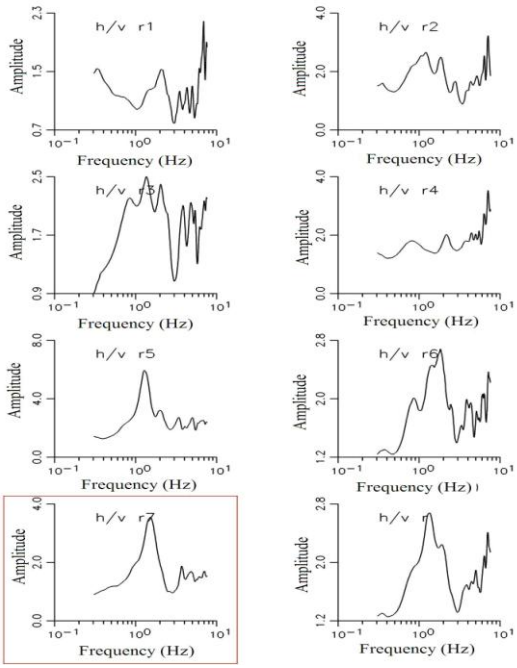

Point – 41. Parzen window with bandwidth of 49

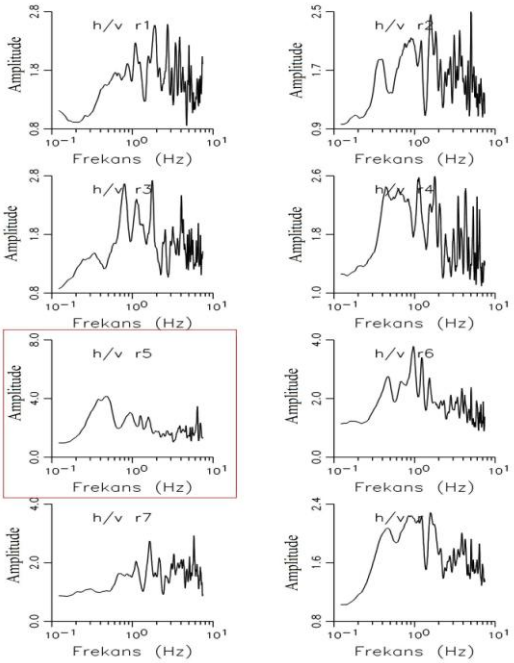

Point – 42. Parzen window with bandwidth of 19

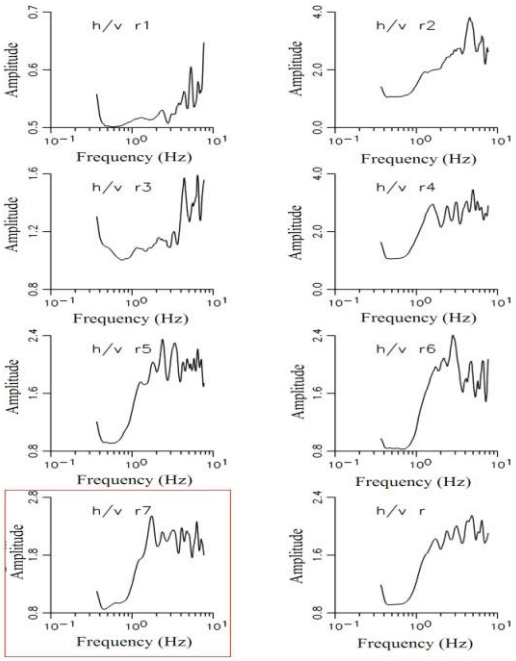

Point – 43. Parzen window with bandwidth of 60

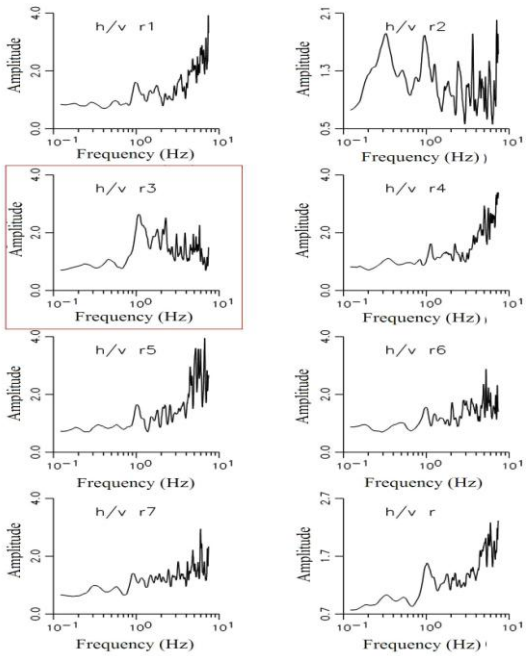

Point – 44. Parzen window with bandwidth of 19

Figure A.11. H/V spectra of points 41 - 44

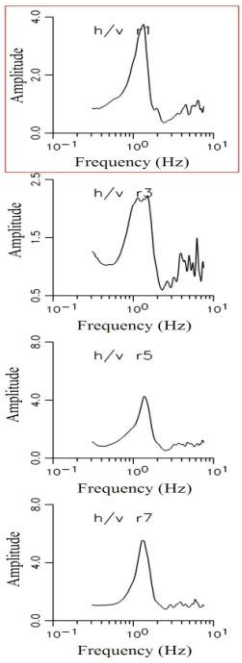

Point – 45. Parzen window with bandwidth of 49

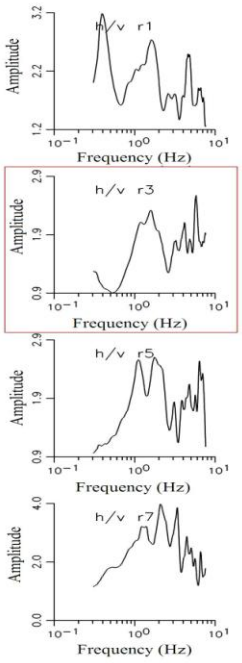

Point – 46. Parzen window with bandwidth of 49

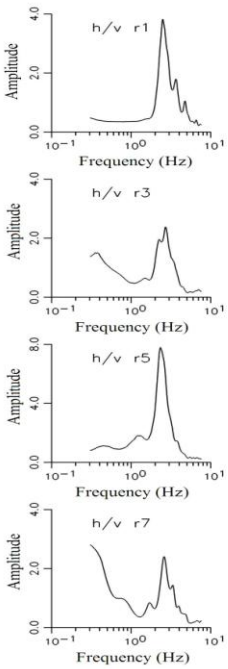

Point – 47. Parzen window with bandwidth of 49

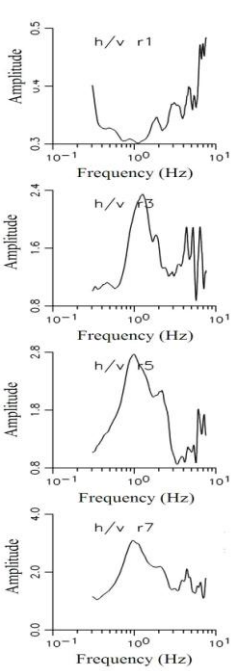

Point – 48. Parzen window with bandwidth of 49

Figure A.12. H/V spectra of points 45 - 48

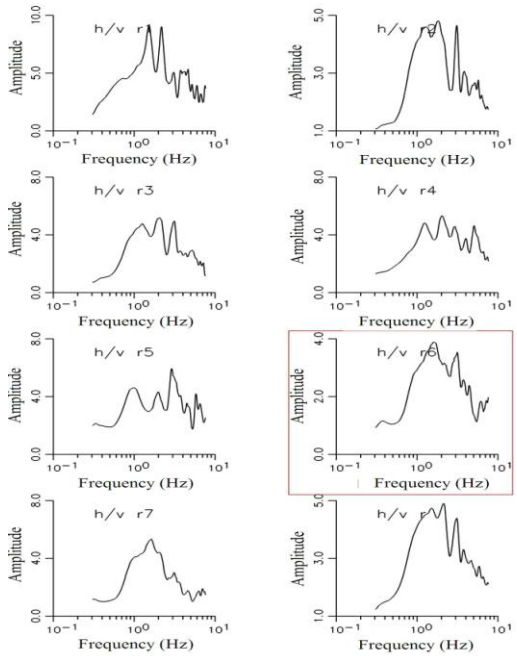

Point – 49. Parzen window with bandwidth of 49

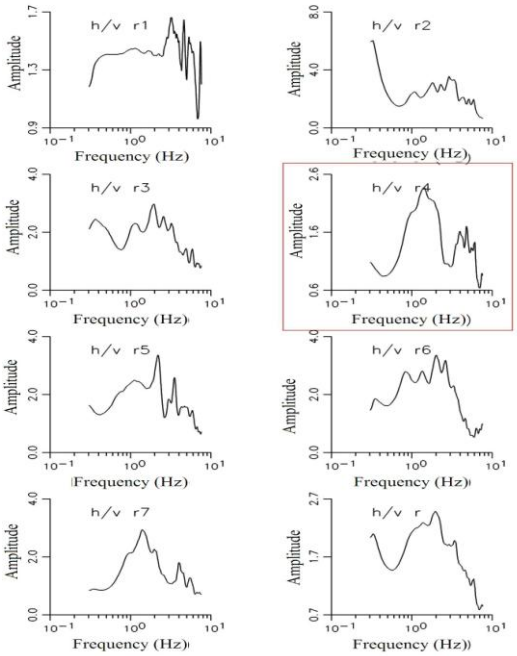

Point – 50. Parzen window with bandwidth of 49

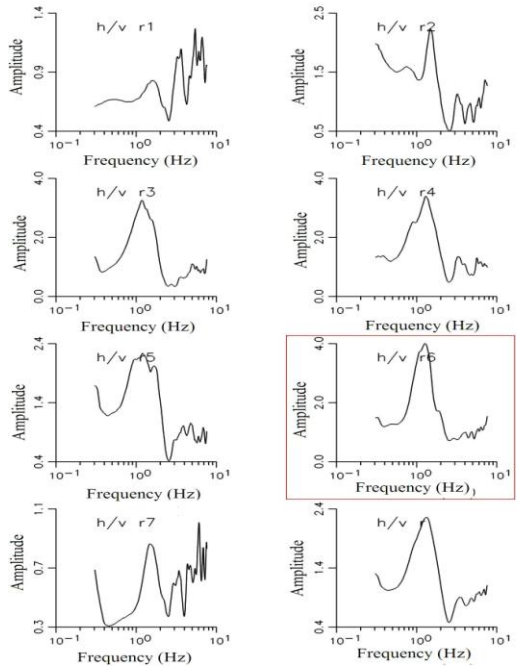

Point – 51. Parzen window with bandwidth of 49

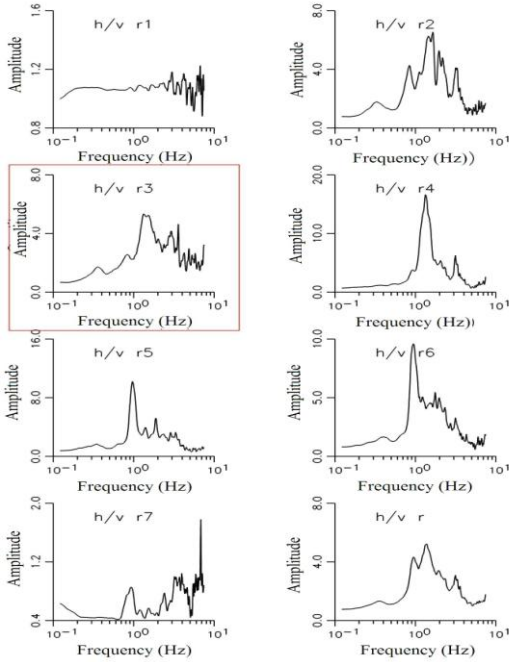

Point – 52. Parzen window with bandwidth of 19

Figure A.13. H/V spectra of points 49 - 52

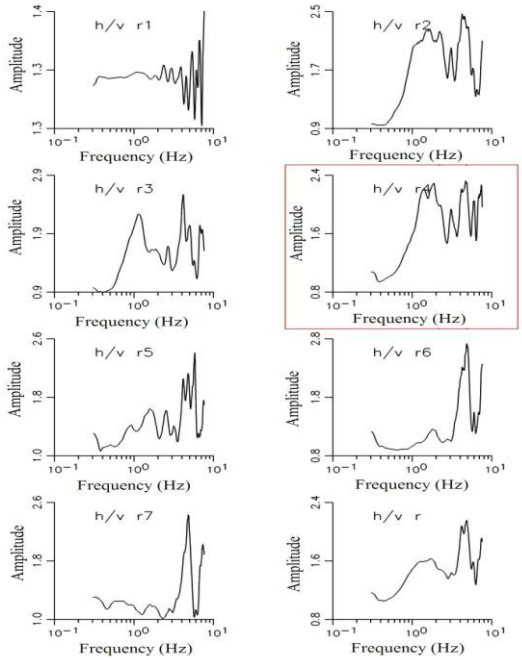

Point – 53. Parzen window with bandwidth of 49

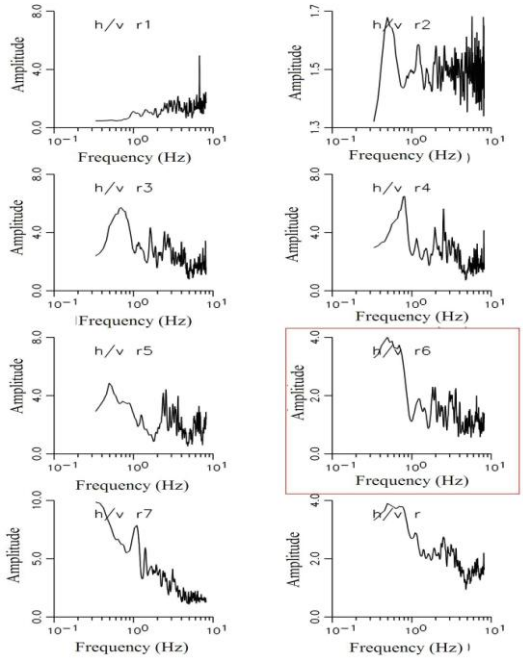

Point – 54. Parzen window with bandwidth of 9

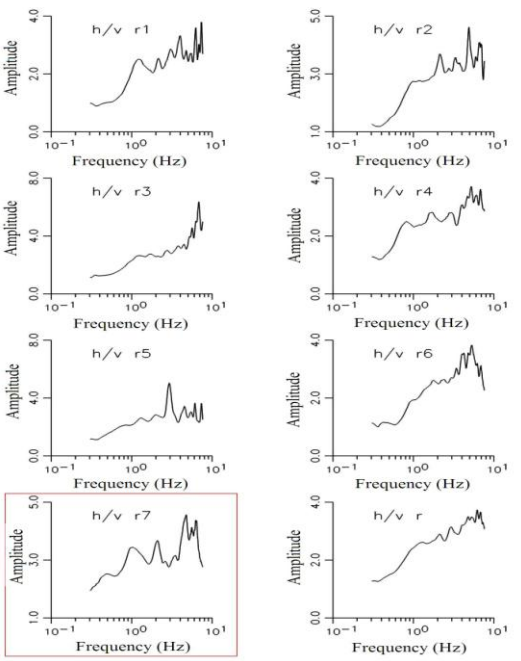

Point – 55. Parzen window with bandwidth of 49

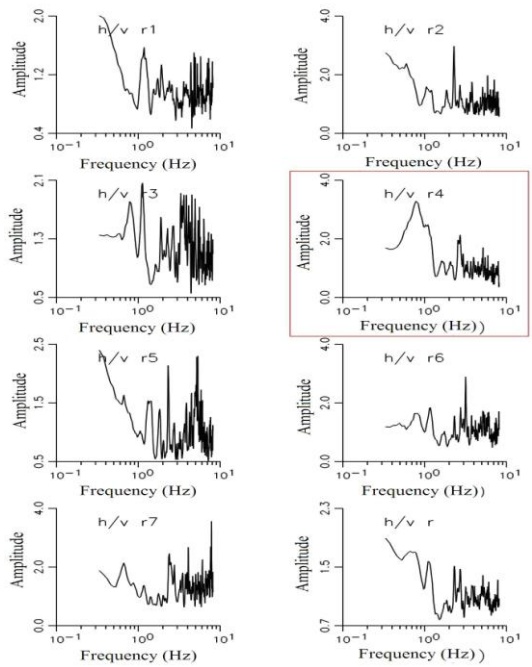

Point – 56. Parzen window with bandwidth of 9

Figure A.14. H/V spectra of points 53 - 56

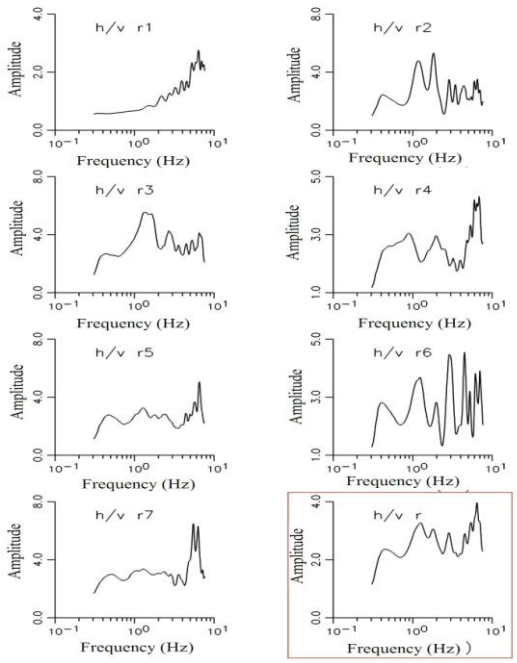

Point – 57. Parzen window with bandwidth of 49

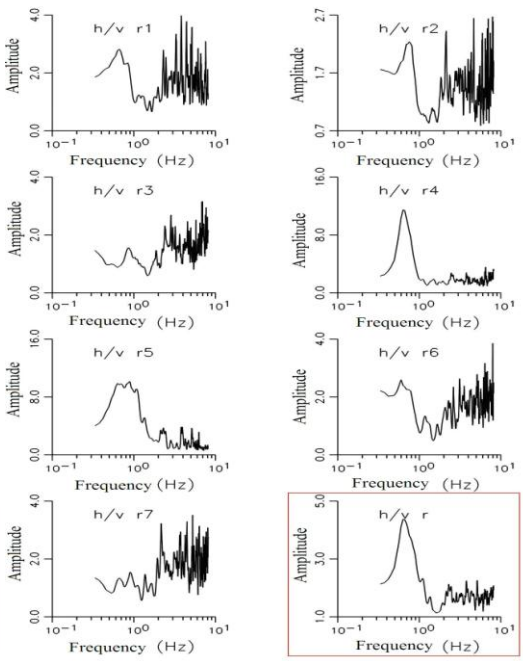

Point – 58. Parzen window with bandwidth of 9

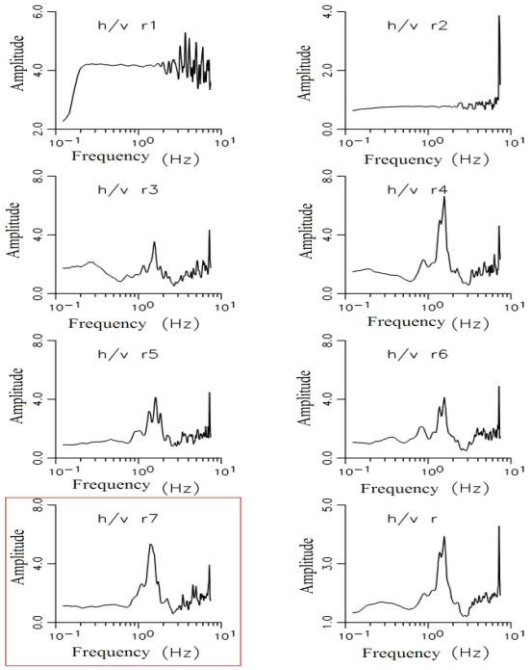

Point – 59. Parzen window with bandwidth of 19

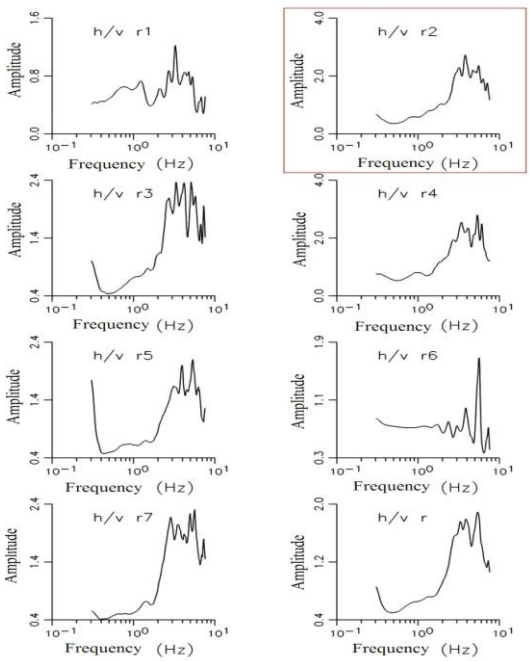

Point – 60. Parzen window with bandwidth of 49

Figure A.15. H/V spectra of points 56 - 60

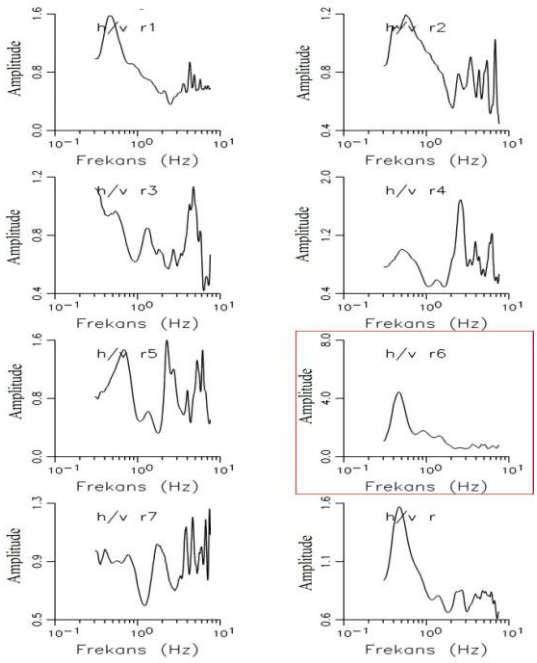

Point – 61. Parzen window with bandwidth of 49

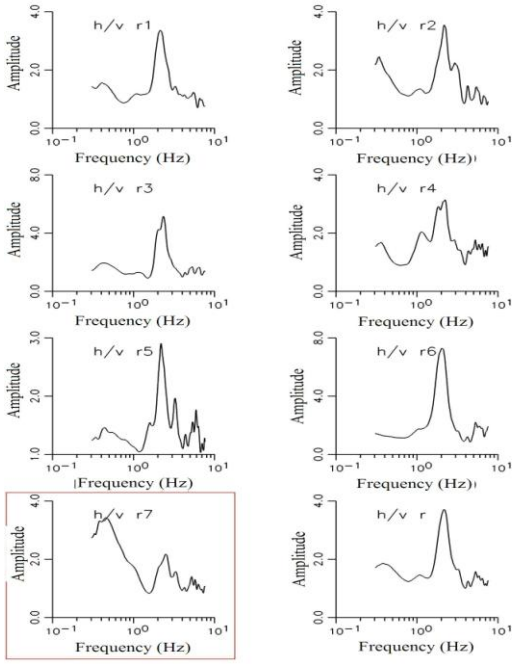

Point – 62. Parzen window with bandwidth of 49

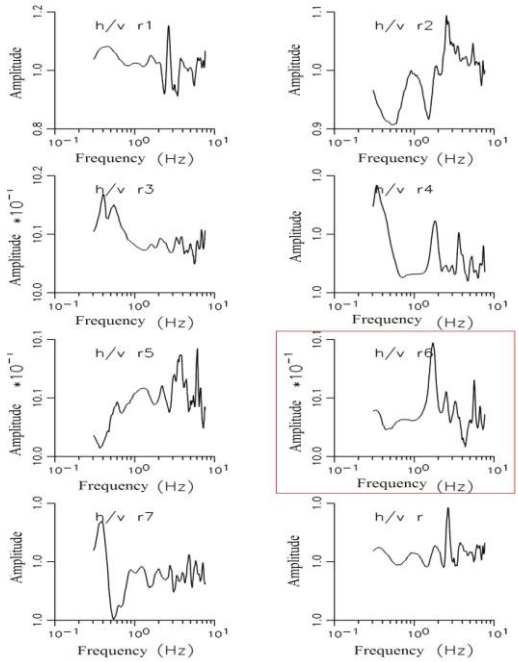

Point – 63. Parzen window with bandwidth of 49

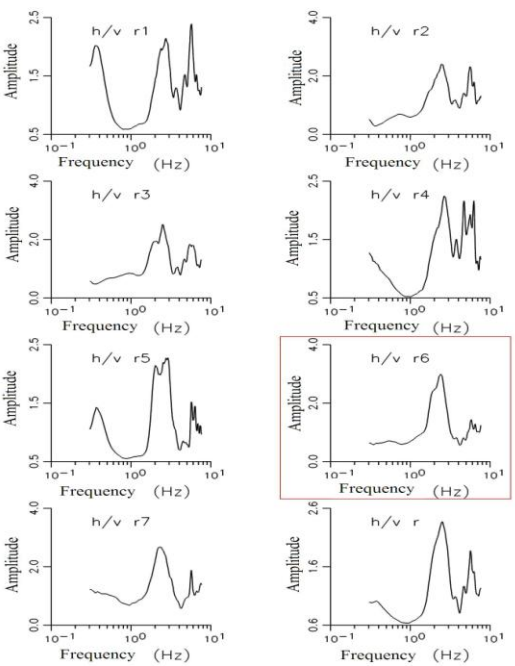

Point – 64. Parzen window with bandwidth of 49

Figure A.16. H/V spectra of points 61 - 64

REFERENCES

Aki, K. and P.G. Richards, 1980, "Quantitative Seismology", W.H. Freeman and Co., San Francisco, California, Vol. 1, pp. 137, ISBN 0-7167-1058-7.

Bard, P. Y. and M. Bouchon, 1985, "The Two-dimensional Resonance of Sediment-Filled Valleys", *Bulletin of the Seismological Society of America*, Vol.75, pp. 519-541.

Bard, P.Y., 1999, "Microtremor Measurements: A Tool for Site Effect Estimation? The Effects of Surface Geology on Seismic Motion", Vol. 3, pp. 1251-1279, Balkema.

Birgören G. and O. Özel, 2006, "Determination of Site Effects and Ground Motion Lengthening in İstanbul area derived from Small Earthquake Recordings", *Proceedings of 8th US National Conference on Earthquake Engineering*, San Francisco, 8NCEE-001908.

Birgören G., O. Özel, and B. Siyahi, 2008, "Bedrock Depth Mapping of the Coast South of İstanbul: Comparison of Analytical and Experimental Analyses", *Turkish Journal of Earth Sciences,* Vol. 18, pp. 315–329.

Erguvanlı K., 1949, "Hereke Pudingleriyle Gebze Taşlarının Inşaat Bakımından Etudu ve Civarlarının Jeolojisi", *Publication of Istanbul Technical University*, Istanbul, pp. 88.

Gutierrez, C. and S.K. Singh, 1992, "A Site Effect Study in Acapulco, Guerrero, Mexico : Comparison of Results from Strong Motion and Microtremor Data", *Bulletin of the Seismological Society of America*, Vol. 82, pp. 642 -659.

Haas, W., 1968, "Das Alt-Palaozoikum Von Bithynien Nordwest-Turkei*",* *Palaeontographica Abteilung*, Vol.131, No.2, pp.178-242.

Haas, W., 1968, “Trilobitenaus dem Silur und Devon von Bithynien”, *Palaeontographica Abteilung, Vol. 130,* pp. *60-207.*

Horike, M., B. Zhao, and H. Kawase, 2001, “Comparison of Site Response Characteristics Inferred from Microtremors and Earthquake Shear Waves”, *Bulletin of the Seismological Society of America,* Vol. 91, No.6, pp. 1526-1536.

Kanai, K. and T. Tanaka, 1954, “Measurement of the Microtremor”, *Bulletion of Earthquake Research Institute,* Tokyo University, Vol. 32, pp. 199-209.

\

Kanai, K., T. Tanaka and S. Yoshizava 1965, “On Microtremors IX.”, *Bulletin Earthquake Research Institute,* Vol. 43, pp. 577–588.

Kaneko, F., T. Kanemori, and K . Tonouchi, 1990, “Low Frequency Shear Wave Logging in Unconsolidated Formations for Geotechnical Applications: Geophysical Applications for Geotechnical Investigations”, Frederick L. Paillet and Wayne R. Saunders, (Eds), pp. 79-98.

Katz, L.J. and R. S. Bellon, 1978, “Microtremor Site Analysis Study at Beatty, Nevada”, *Bulletin of the Seismological Society of America*, Vol. 68, pp. 757-765.

Katz, L.J., 1976, “Microtremor Analysis of Local Geological Condition”, *Bulletin of the Seismological Society of America*, Vol. 66, No.1, pp. 45-60.

Kaya, O., 1973, “The Devonian and lower Carboniferous Stratigraphy of the Bostancı and Büyükada Subareas, O. Kaya (ed.), *Paleozoic of Istanbul, Publication of Ege University,* No. 40, pp. 1-143.

Ketin, I., 1959, “Tectonics of Region of Camlica”, *Bulletin of Geology of Turkey,* No.7, pp. 1-18 [in Turkish Language].

Kobayashi, H., K. Seo and S. Midorikawa , 1986, “Estimated Strong Ground Motions in the Mexico city due to the Michoacan, Mexico Earthquake of September 19, 1985 based on Characteristics of Microtremor”, “Part 2, Report on Seismic Microzoning Studies of the Mexico Earthquake of September 19, 1985”, *The Graduate School of Nagatsuta, Tokyo Institute of Technology*, Yokohama Japan.

Konno, K. and T. Ohmachi, 1998, “Ground-Motion Characteristics Estimated from Spectral Ratio between Horizontal and Vertical Components of Microtremor”, *Bulletin of the Seismological Society of America*, Vol. 88, No.1, pp. 228-241.

Kubotera, A. and M. Otsuka, 1970, “Nature of Nonvolcanic Microtremor Observed on the Aso-Caldera”, *Journal of Physics of the Earth*, Vol.18, pp. 115–124.

Kurtuluş, C., A. Bozkurt and C. H. Demirci , 2008, “Determination of Soil Characteristics Using Geological, Geophysical and Geotechnical Methods in Tuzla (Istanbul)”, *Journal of the Earth Sciences Application*,Vol.2, October, November.

Lachet, C. and P.Y. Bard, 1994, “Numerical and Theoretical Investigations on the Possibilities and Limitations of Nakamura‘s Technique”, *Journal of Physics of the Earth*, No.42, pp. 377-397.

Lermo, J. and F. J. Chavez-Garcia, 1994, “Are Microtremors Useful in Site Response Evaluation?”, *Bulletin of the Seismological Society of America*, Vol. 84, No. 5, pp. 1350-1364, October.

Lermo, J., C. Gutierrez, J. Morales, S. K. Singh, and R. Cabrera (1989), “Estudio del Periodo Dominante del Suelo en la Zona Urbana de Ciudad Guzman”, Jal., *in Memorias del VIII Congreso Nacional de Ingenieria Seismica*, SMIS, 1, Acapulco, Guerrero A87-A96 (in Spanish).

Louie, J, N., 2001, "Faster, Better: Shear-wave Velocity to 100 Meters Depth from Refraction Microtremor Arrays", *Bulletin of the Seismological Society of America*, Vol. 91, pp. 347-364.

Luna, R. and H. Jadi, 2000, "Determination of Dynamic Soil Properties using Geophysical Methods", Department of Civil Engineering, University of Missouri-Rolla.

McMechan, G. A., and M. J. Yedlin, 1981, "Analysis of Dispersive Waves by Wave Field Transformation: Geophysics", Vol. 46, pp. 869-874.

Mirzaoglu, M. and U. Dikmen, 2003, "Application of Microtremors to Seismic Microzoning Procedure", *Journal of the Balkan Geophysical Society*, Vol. 6, No. 3, pp. 143 – 156, August.

Nakamura, Y., 1989, "A method for Dynamic Characteristics Estimation of Subsurface using Microtremor on the Ground Surface.", *Quarterly Report of RTRI*, Vol.30, No.1.2, February.

Nakamura, Y., 2000, "Clear Identification of Fundamental Idea of Nakamura's Technique and Its Applications", *Proceeding of the 12WCEE*, Auckland-Australia.

Nakamura, Y., 2008, "On the H/V Spectrum", *Proceeding of the 14 World Conference on Earthquake Engineering*, October 12-17, Beijing, China.

Okada, H., 2003, "The Microtremor Survey Method", *Society of Exploration Geophysicists of Japan.*, Translated by Koya Suto, Geophysical Monograph Series No. 12, Society of Exploration Geophysicists.

Okay, A., C., 1947, "Geologishe und Petrographiche Untersuchung des Gebietes Zwischen Alemdağ, Karlıdağ und Kayısdağ in Kocaeli Bithynien, Turkei", Science Faculty of *Istanbul*, B, XII, No.4, pp. 269-288, (Geomar Kitaplığı).

Okay, A., C., 1948, " Geological Investigation of Sile, Mudarlı, Kartal and Riva", *Istanbul University Fen Fak. Mec,* B, XIII, No. 4, pp. 311-355 [in Turkish Language].

Onalan, M., 1981, "Sedimentary and Geological Characteristics about Pendik and Adalar", *Bulletin of Earthscience of Istanbul University Engineering Faculty*., pp. 193.

Özgül, N., 2009, "Palaeozoic to Lower Tertiary Stratigraphy of the Istanbul Region" *Conference about Geology of the Black Sea Region,* October.

Özgül, N., K. Üner, I. Akmeşe, I. Bilgin, R. Kokuz, I. Özcan, Z. Yıldız, U. Yıldırım, O. Akdag and M. Tekin., 2005, "General Geological Characteristics about Istanbul City", Department of Earthquake Risk Management and Urban Development, Istanbul Metropolitan Municipality, [in Turkish Language] .

Paeckelmann, W., 1925, "Beitrage zur Kenntnis des Devons am Bosporous, Insbesondere in Bithynien": *Abh. Preus. Geol. L.-A.,* No. 98, pp. 152, Berlin.

Paeckelmann, W., 1938, "Geologie von Konstantinopel", *Abh. Preus. Geol., L.-A.,* No. 168, Berlin.

Paeckelmann,W., 1938, "Neue Beitrage zur Kenntnis der Geologie, Paleontologie und Petrographie der Umgegend von Konstantinopel", *2. Geologie Thraziens, Bithyniens und der Prinzeninseln: Abh. Preus. Geol. L.-A.*, No. 186, pp. 202, Berlin.

Pullammanappallil, S., W. Honjas, and J. N. Louie, 2003, "Determination of 1-D shear Wave Velocities Using the Refraction Microtremor Method", *Proceedings of the Third International Conference on the Application of Geophysical Methodologies and NDT to Transportation and Infrastructure.*

Thorson, J. R., and J. F. Claerbout, 1985, "Velocity-stack and Slant-stack Stochastic Inversion", *Geophysics,* Vol. 50, pp. 2727-2741.

Udwadia, F. E. and M. D. Trifunac, 1973, "Comparison Earthquake and Microtremor Ground Motion in El Centro", *Bulletin of the Seismological Society of America*, Vol. 63, pp. 1227–1253.

Yalcinkaya, E., 2004, "Investigation of Parameters Affecting the Soil Amplification for One-dimensional Models", *Bulletin of Earthscience of Istanbul University Engineering Faculty,* Vol. 17, No.1, pp. 47-56.

Yılmaz, I., 1977, "Absolute Age and Genesis of the Sancaktepe Granite (Kocaeli Peninsula)", *Bulletin of the Geological Society of Turkey*, Vol. 20, pp.11-20, February.

Zülfikar C., Z.Cagnan, E. Durukal and M. Erdik, 2007, "Analysis of Earthquake Records of Istanbul Earthquake Early Warning Rapid Response System Stations", *Proceedings of the Sixth National Conference on Earthquake Engineering*, 16-20 October 2007, Istanbul,Turkey.

REFERENCES NOT CITED

"Active and Passive Surface Wave Techniques", *Geophysical Services a Division of Blackhawk GeoServices.*

Alcık, H., C. Gürbüz and B. Ucer, 1993, "Microzonation by Microtremor Measurement In Kadikoy and Uskudar Area", Geophysics 9, No.10, pp. 235-245.

"Urban Regeneration Project for Kartal Sub- Center & Kartal- Pendik Waterfront Design Brief",Istanbul Greater Municipality Metropolitan Planning&Urban Desing Center, *Bulletin of the Geological Society of Turkey*, Vol.20, No. 11-20, February.

Idriss, I. M. and Sun, Joseph I, 1992, "User's manual for SHAKE91: A Computer Program for Conducting Equivalent Linear Seismic Response Analyses of Horizontally Layered Soil Deposits" Center for Geotechnical Modeling, Department of Civil and Environmental Engineering, University of California, Davis (CA).

Kudo, K., T. Kanno, H., Okada, O. Özel, M. Erdik, T. Sasatani, S. Higashi, M. Takahashi and K. Yoshida, "Site Specific Issues for Strong Ground Motions during the Kocaeli, Turkey Earthquake of August 17, 1999, as Inferred from Array Observations of Microtremors and Aftershocks", *Bulletin of the Seismological Society of America*, Vol. 92, No. 1, pp. 448-465, February 2002.

Rudnicki. M, and T. H. Meyer, 2007, "Methods to Convert Local Sampling Coordinates into Geographic Information System/Global Positioning Systems (GIS/GPS) Compatible Coordinate Systems", *NRME Articles*, Department of Natural Resources Management and Engineering.

Schnabel, Per B., L., John, and S. H. Bolton, 1972, "SHAKE: a Computer Program for Earthquake Response Analysis of Horizontally Layered Sites" Earthquake Engineering Research Center, University of California, Berkeley, No.12, pp. 92.